Microbial Responses to the Biostimulation of Subarctic Hydrocarbon-Contaminated Soils under Seasonal Freeze-Thaw Conditions

By Sara Klemm

Department of Natural Resource Sciences

McGill University, Montreal

Submitted November, 2009

A thesis submitted to McGill University in partial fulfillment of the requirements of the degree of Master of Science, Microbiology

© Sara Klemm, 2009

Abstract

Nutrient-deficient, acidic soil from Resolution Island, Nunavut was contaminated with petroleum hydrocarbons during operations from 1954-1973 at a former radar station. Two mesocosm tanks containing ~200 kg hydrocarbon-contaminated Resolution Island soil each were exposed to a seasonal freezing profile designed to simulate *in situ* ground conditions after the summer landfarming season. Soil from one tank was treated with 100.0 mg N kg⁻¹ soil and 2.0 g CaCO₃ kg⁻¹ soil, while the second mesocosm remained untreated. Aliphatic nC10-nC16 hydrocarbon biodegradation was enhanced by soil treatments after an initial acclimation period, which corresponded to *Actinomycetales* and *Rhodanobacter* population growth from 2.4°C to -2.1°C. These *Actinomycetales* and hydrocarbon metabolite-utilizing r-strategists, respectively. Additionally, a novel indigenous archaeal community was related to *Thaumachaeota* ammonia oxidizers but not associated with hydrocarbon biodegradation. Two diazotrophic *Burkholderia* isolates from the soil also degraded ¹⁴C-naphthalene and/or ¹⁴C-phenanthrene at -5°C.

Résumé

Une terre acide pauvre en éléments nutritifs provenents de Resolution Island, Nunavut, a été contaminé par des hydrocarbures pétroliers durant les opérations d'une ancienne base de radar entre 1954 – 1973. Deux réservoirs mésocosmes contenant ~200 kg de terre de Resolution Island contaminée par des hydrocarbures ont été sujet à un profil saisonnier de gel et dégel conçu pour simuler les conditions du sol in situ après la saison estivale d'exploitation. La terre dans un réservoir a été traite avec 100.0 mg N kg⁻¹ de terre et 2.0 g CaCO₃ kg⁻¹ de terre, tandis que le deuxième réservoir n'a reçu aucun traitement. La biodégradation d'hydrocarbures aliphatiques (nC10 à nC16) a été stimulée par l'ajout d'éléments nutritifs après une période initiale d'acclimatisation, qui correspondait à une croissance des populations Actinomycetales et Rhodanobacter de 2.4°C à -2.1°C. Ces populations Actinomycetales et Rhodanobacter ont probablement représenté des K-stratégistes hydrocarbonoclastes et des r-stratégistes utilisant des métabolites d'hydrocarbures, respectivement. De plus, la communauté originale indigène d'archaea était apparentée aux oxydeurs d'ammoniac *Thaumachaeota*, mais n'était pas associée avec la biodégradation d'hydrocarbures. Deux isolats Burkholderia diazotrophiques de la terre ont aussi dégradé du ¹⁴C-naphtalène et/ou du ¹⁴Cphénanthrène à -5°C.

Acknowledgements

I would like to thank Dr. Lyle Whyte and Dr. Subhasis Ghoshal for their guidance in this project; WonJae Chang for geochemical and engineering contributions; Mike Dyen for providing methodology and prior results; Olga Onyshchenko and Keomany Ker for future contributions regarding the *Burkholderia* isolates; Kris Radke for correcting the abstract translation; Roli Wilhelm for assisting with the submission process. Thank you to Lou Spagnuolo from Indian and Northern Affairs Canada (INAC) Contaminated Sites Program and Philippe Simon from Qikiqtaaluk Environmental for funding this project.

Dr. Brian Driscoll and Dr. Don Niven offered valuable input during class and seminars. I was grateful to Dr. Don Niven and Dr. Gary Dunphy for teaching assistantship opportunities in Introduction to Microbiology and General Biology. I would like to thank Blaire Steven, Chin-Ying Lay, Kris Radke, Thomas Niederberger, Olga Onyshchenko, Ophelia Ferreira-Rodriguez, Roli Wilhelm and Sara Sheibani from the Whyte lab for their assistance in daily lab matters. Branislav Babic, Dave Meek, Michelle Poilly, Oli Trottier and Rateb Nabil Youseff from the Driscoll lab, and Ghitanjali Arya from the Niven lab also provided their assistance.

I wanted to thank people who made Happy Hour a weekly treat. I was grateful to Candice, Christina, Jen, people from Emerge, St. James Anglican and St. James United for support while in Montréal; Mom, Dad, Erika, Silver and family for their love; Chris, Dor, Jen, Jose, Nina and Phil for being there throughout the years.

Table of Contents

Abstracti
Résuméi
Acknowledge ments iv
Table of Contents
List of Figures
List of Tables x
Chapter 1: Background and Literature Review
Introduction.
1.1. Microbial Biodegradation in Hydrocarbon-Contaminated Environments
1.1.1. Hydrocarbons as Pollutants
1.1.2. Habitats and Metabolic Pathways of Hydrocarbon-Degrading Microbes2
1.2. The Bioremediation of Hydrocarbon-Contaminated Soils
1.2.1. Bioremediation Treatment Strategies in Hydrocarbon-
Contaminated Soils.
1.2.2. The Effect of Hydrocarbon Bioavailability on Microbial and Nucleic
Acid Sorption in Contaminated Soils
1.2.3. Nitrogen Fertilization Toxicity and Diazotrophy in Hydrocarbon-
Contaminated Soils10
1.3. Polar and Alpine Bioremediation of Hydrocarbon-Contaminated Soils
1.3.1. Biostimulation and Bioaugmentation in Polar and Alpine Soils12
1.3.2. The Effects of Freeze-Thaw Temperature Fluctuations on Soil
Microbial Communities
1.3.3. Microbial Communities in Polar and Alpine Soils
1.3.4. Nutrient Utilization by Microbial Communities from Arctic Soil10
1.3.5. Psychrotolerant Hydrocarbon Degraders from Polar and Alpine Soils16

1.3.6. Cold-Adapted Enzymes and Metabolic Processes in Psychrotolerant	
and Psychrophilic Bacteria	18
1.3.7. Microbial Community Characterization Techniques	19
Chapter 2: Project Objectives	
2.1. Resolution Island Site Background.	22
2.2. Specific Research Objectives.	23
Chapter 3: Methodology	
3.1. Seasonal Freeze-Thaw Conditions Simulated in Soil Mesocosms	25
3.2. Culture-Dependent Soil Microbial Community Characterization	
3.2.1. Heterotrophic and Hydrocarbon-Degrading Viable Plate Counts	27
3.2.2 ¹⁴ C-Hydrocarbon Mineralization Assay of Mesocosm Soils	27
3.3. Culture-Independent Soil Microbial Community Characterization	
3.3.1. Polymerase Chain Reaction (PCR) Amplification	
3.3.1.1. Soil DNA Extraction and PCR Reaction Conditions	28
3.3.1.2. DGGE PCR Amplification.	28
3.3.1.3. Clone Library PCR Amplification.	29
3.3.1.4. Catabolic Gene PCR Amplification.	29
3.3.2. Quantitative Real-Time PCR of Mesocosm Soils	29
3.3.3. Denaturing Gradient Gel Electrophoresis (DGGE) of Mesocosm Soils.	31
3.3.4. Clone Library Construction from Treated Mesocosm Soils	31
3.3.5. Phylogenetic Analyses of Clone Libraries.	32
3.4. Isolate Characterization	
3.4.1. Bacterial Isolation from Hydrocarbon-Contaminated Soil Enrichment	
Cultures and Isolate Characterization.	32
3.4.2. DNA Extraction and PCR Amplification of Isolates	33
3.4.3. Pure Culture ¹⁴ C-Hydrocarbon Mineralization Assay	34

Results and Discussion.	35
Chapter 4: Geochemical Characterization of Hydrocarbon-Contaminated Soils	in
Mesocosm Tanks during Simulated Seasonal Freezing	
4.1. Geochemical Properties of Hydrocarbon-Contaminated Soil from	
Resolution Island	36
4.2. The Effect of Seasonal Freeze-Thaw Fluctuations on Mesocosm	
Soils and Relevance to On-Site Conditions.	37
Chapter 5: n-Alkane Biodegradative Activity by Indigenous Bacterial Popula	ı tio ns
in Hydrocarbon-Contaminated Soils during Simulated Seasonal Freezing	
5.1. n-Alkane Biodegradation by the Soil Microbial Community during	
Simulated Seasonal Freezing	
5.1.1. Total Petroleum Hydrocarbon Concentrations.	38
5.1.2. ¹⁴ C-n-Alkane Mineralization by the Soil Microbial Community	38
5.2. Soil Bacterial Community Populations during Simulated Seasonal Freezing	
5.2.1. Heterotrophic and Bacterial 16S rDNA Population Sizes	40
5.2.2. Hydrocarbon-Degrading and <i>alkB</i> Population Sizes	41
5.3. Denaturing Gradient Gel Electrophoresis Profiling of the Bacterial	
Community Structure during Simulated Seasonal Freezing	42
5.4. n-Alkane Biodegradation by Psychrotolerant <i>Rhodococcus</i> Isolates from	
Hydrocarbon-Contaminated Soil	
5.4.1. Psychrotolerant <i>Rhodococcus</i> Strain Characterization	45
5.4.2. ¹⁴ C-n-Alkane Mineralization by Psychrotolerant <i>Rhodococcus</i> Strains.	47
5.5. Shifts in Bacterial Community Composition and Metabolic Activity	
during Simulated Seasonal Freezing.	48

Chapter 6: Characterization of Bacterial 16S rDNA Community from Treated
Mesocosm Soils during Simulated Seasonal Freezing
6.1. Compositional Analyses of Bacterial 16S rDNA Clone Libraries
6.2. Phylogenetic Analyses of Bacterial 16S rDNA Clone Libraries
6.3. An Evaluation of the Compositional and Metabolic Responses by the
Bacterial Community to Nutrient Availability and Soil pH during Simulated
Seasonal Freezing54
Chapter 7: Characterization of a Phylogenetically Novel Archaeal Community from Hydrocarbon-Contaminated Subarctic Soil
7.1. A Metabolic Assessment of the Archaeal Community in Treated Mesocosm
Soils during Simulated Seasonal Freezing
7.2. Compositional and Phylogenetic Analyses of a Novel Archaeal 16S rDNA Clone
Library from Hydrocarbon-Contaminated Subarctic Soil
Chapter 8: Polycyclic Aromatic Hydrocarbon Biodegradative Activity by Diazotrophic Isolates in Relation to Microbial Populations from Hydrocarbon Contaminated Subarctic Soils
8.1. Subzero Polycyclic Aromatic Hydrocarbon Biodegradation by Diazotrophic
Burkholderia Isolates from Hydrocarbon-Contaminated Soil
8.1.1. Psychrotolerant <i>Burkholderia</i> Strain Characterization
8.1.2. Subzero ¹⁴ C-Naphthalene and ¹⁴ C-Phenanthrene Mineralization
by Burkholderia Strains62
8.2. Polycyclic Aromatic Hydrocarbon Biodegradation by the Soil Microbial
Community during Simulated Seasonal Freezing
8.2.1. Identification of Polycyclic Aromatic Hydrocarbon-Degrading Genes65
8.2.2. ¹⁴ C-Naphthalene and ¹⁴ C-Phenanthrene Mineralization by the Soil
Microbial Community65

8.3. Diazotrophic Community Structure in Hydrocarbon-Contaminated Soils	
during Simulated Seasonal Freezing.	66
8.4. An Evaluation of Polycyclic Aromatic Hydrocarbon Biodegradation by	
Diazotrophic Burkholderia Strains Indigenous to Hydrocarbon-	
Contaminated Subarctic Soil	67
Chapter 9: Summary and Conclusions	70
References	72
Appendices	96

List of Figures

Figure 2.1. Map of Resolution Island (circled)	22
Figure 3.1. Soil mesocosm tank dimensions (100×65×35 cm) and layering (T: Top,	
M: Middle, B: Bottom)	25
Figure 3.2. Seasonal freezing and thawing profile with sampling timepoints	26
Figure 5.1. ¹⁴ C-Hexadecane mineralization of mesocosm soils at 5°C	39
Figure 5.2. Culturable heterotroph and bacterial 16S rDNA population levels	
during the freezing phase	40
Figure 5.3. Culturable hydrocarbon degrader and <i>alkB</i> population levels during the	
freezing phase compared to ¹⁴ C-hexadecane mineralization activity	41
Figure 5.4. Bacterial DGGE of freezing phase treated mesocosm soils	43
Figure 5.5. Bacterial DGGE of thawing phase treated mesocosm soils	44
Figure 5.6. ¹⁴ C-Hexadecane mineralization of <i>Rhodococcus</i> MD strains at 5°C	47
Figure 5.7. Subzero (-5°C) ¹⁴ C-hexadecane mineralization of <i>Rhodococcus</i>	
strain MD2	48
Figure 6.1. Bacterial 16S rDNA clone library composition from freezing phase	
treated mesocosm soils	51
Figure 6.2. Phylogenetic tree of bacterial 16S rDNA clone libraries and	
isolate sequences (depicted in bold).	53
Figure 7.1. Archaeal DGGE of freezing phase treated mesocosm soils	58
Figure 7.2. Archaeal 16S rDNA clone library composition from Day 0 treated	
mesocosm soil	59
Figure 7.3. Phylogenetic tree of archaeal 16S rDNA clone library sequences	
(depicted in bold)	60
Figure 8.1. Subzero (-5°C) ¹⁴ C-naphthalene mineralization of <i>Burkholderia</i>	
strains SK35.3 and SK4.2.	64
Figure 8.2. Subzero (-5°C) ¹⁴ C-phenanthrene mineralization of <i>Burkholderia</i>	
strain SK35.3.	64
Figure 8.3. ¹⁴ C-Naphthalene mineralization of top layer Day 39 mescosm soils at 5°C	65
Figure 8.4. ¹⁴ C-Phenanthrene mineralization of Day 39 mesocosm soils at 5°C	66
Figure 8.5. <i>nifH</i> DGGE of freezing phase untreated mesocosm soils	67

List of Tables

able 1. Ambient cold room and measured soil mesocosm temperatures	27
Table 2. Oligonucleotide primers utilized in this study.	30
Table 3. Characterization of psychrotolerant Rhodococcus soil isolates	46
Table 4. Statistical analyses of bacterial 16S rDNA clone libraries	52
Table 5. Characterization of psychrotolerant <i>Burkholderia</i> soil isolates	63

Chapter 1: Background and Literature Review

Introduction

Many subarctic and arctic sites contain petroleum hydrocarbon-contaminated soils (40). Contaminant sources include leaks and spills from fuel storage tanks and oil transportation pipes, illegal disposal of partially-filled fuel containers, and past practices at former military sites (40). Nutrient-deficient, coarse-textured soils typical of (sub)-arctic regions (3) are exposed to low temperatures ranging from 0°C to 10°C during two-month summers (40). Persistence of hydrocarbon pollutants in these soils has indicated that biodegradation rates are negligible (3, 13). As such, bioremediation treatments create more favorable growth conditions for enhanced hydrocarbon biodegradation (214). Cost-effective and non-disruptive strategies (40) such as landfarming are often applied to arctic sites (175, 236) that are far-removed from population centers (7).

1.1. Microbial Biodegradation in Hydrocarbon-Contaminated Environments 1.1.1. Hydrocarbons as Pollutants

Over 2 billion tons of petroleum is produced annually worldwide. According to the Environmental Protection Agency (EPA), over one million underground storage tanks primarily containing gasoline currently exist in the United States (215). In 2003, over 436,000 tanks confirmed releases into the environment (231). Such low level contamination events represent approximately 90% of anthropogenic hydrocarbons discharged into the environment (215).

Crude oil consists of more than 17,000 chemical components including aliphatic hydrocarbons, aromatic hydrocarbons, resins and asphaltenes (104). Nonpolar hydrocarbon molecules contain a carbon backbone where carbon (C) atoms are covalently bonded to each other or to hydrogen (H) atoms (161). Aliphatic hydrocarbons form straight, branched or cyclic structures and are classified by the number of carbon atoms (161). Saturated carbon chains only containing single bonds are called n-alkanes, while n-alkenes include one or more double bond(s) and n-alkynes include one or more triple bond(s) (161). Hexadecanes (nC16), for example, contain a saturated 16-carbon backbone

(161). Aromatic hydrocarbons contain one or more six-carbon ring(s) with alternating single and double bonds; delocalized electrons within these aromatic rings confer stability to the molecules (161). Polycyclic aromatic hydrocarbons (PAHs) consist of multiple fused aromatic rings; naphthalene and phenanthrene contain two and three rings, respectively (161).

The Canadian Council of Ministers for the Environment (CCME) Canada-wide standard for petroleum hydrocarbons - Soil Tier 1 Method categorizes total petroleum hydrocarbons (TPH) into four aliphatic fractions according to carbon backbone length (279). The F1 fraction ranges from nC6 to nC10, the F2 fraction from nC10 to nC16, the F3 fraction from nC16 to nC34 and the F4 fraction from nC34 to nC50 (279). Hexadecane (nC16) is categorized in the F2 fraction. Benzene, toluene, ethylbenzene and xylene (BTEX) and PAH components are also grouped into separate fractions (279).

The toxicity of contaminating hydrocarbons to a specific ecosystem is typically assessed using plant and earthworm survival tests (69, 264). Narcosis (non-specific disruption of cell membrane integrity, fluidity and activity) by such contaminants also poses a risk to a healthy microbial community (254), especially in low temperature and soil moisture habitats found in (sub)-antarctic regions. Because plants and earthworms are not viable in such regions, microbial population shifts have been investigated as an alternative. Since competing hydrocarbon interactions interfere with ammonia monooxygenase activity and limit nutrient availability (119, 132), microbial nitrification shifts have been studied as a useful indicator of hydrocarbon ecotoxicity. Microbial nitrifiers oxidize ammonium (NH₄⁺) into nitrate (NO₃⁻) (161). According to one comparative subantarctic study (240), nitrification was the most sensitive indicator with a 20% inhibitory concentration (IC20) at 190 mg diesel kg⁻¹ soil. A second study from Antarctica (241) found community composition (i.e., phospholipid fatty acid profiling) and nitrification to be sensitive indicators with 25% effective concentrations (EC25) at 800 mg petroleum hydrocarbons (PHC) kg⁻¹ soil and 2,000 mg PHC kg⁻¹ soil, respectively.

1.1.2. Habitats and Metabolic Pathways of Hydrocarbon-Degrading Microbes

Hydrocarbon-degrading microbes are ubiquitous throughout nature and have been isolated from soil, sand, salt- and freshwater habitats (228). According to a 2006 review

(104), 79 bacterial, 104 fungal, 14 algaeal and 9 cyanobacterial genera contain hydrocarbon degradative species. Specific bacterial isolates have demonstrated hydrocarbon-degradative activity under extreme conditions. *Rhodococcus* sp. strain Q15 metabolized n-alkanes (306) and *Thermus aquaticus* BTEX compounds (44) at 0°C and 70°C, respectively. Acidophilic heterotrophic isolates from acid mine drainage degraded n-alkanes at pH3 (87), while two *Rhodococcus erythropolis* strains utilized benzene at pH10 (74). At 10% (w/v) salinity, *Streptomyces albaxialis* metabolized crude oil (141), and *Rhodococcus erythropolis* and *Dietzia maris* degraded paraffins and turbine oil (150, 170, 323). A halophilic archaea isolate, strain EH4, degraded nC20 at 20.5% (w/v) salinity (22). Multiple *Halobacterium* spp. also demonstrated a high capacity for nC10–nC30 utilization at 30% (w/v) salinity (150, 170). n-Alkanes stimulated the growth of *Thermococcus sibiricus*, an archaea recently isolated from a pristine high temperature oil reservoir containing trace levels of proteinaceous compounds (164).

Hydrocarbonoclastic marine bacteria have been described as highly specialized microbes that utilize hydrocarbons as a sole carbon and energy source (315). Such bacteria are normally present at low numbers or not detectable, but drastically increase in number after hydrocarbon contamination (315). Terrestrial hydrocarbon degraders, in contrast, often utilize a variety of substrates and are readily detectable in pristine soils (315). Despite their metabolic versatility, *Rhodococcus* species found in soils typically prefer hydrocarbon pollutants over other substrates (19). Other hydrocarbonclastic soil bacteria have been isolated as well. The metabolic capacity of *Alkanindiges illinoisensis* is almost completely restricted to long-chain aliphatic hydrocarbons (21). *Thermoleophilum albans* and *Thermoleophilum minutum* exclusively degrade nC12-nC19 alkanes, cyclohexane, cycloheptane, nC12-nC18 alcohols and nC13-nC19 ketones (314).

As aliphatic hydrocarbons share structural similarities with cell membrane fatty acids and plant paraffin molecules, microbes readily metabolize such contaminants (161). Aromatic hydrocarbons including benzo[a]pyrene are degraded by white rot fungi lignin peroxidises (98). These aliphatic and aromatic hydrocarbons are degraded through various catabolic pathways (160, 161). Acetyl coenzyme A (CoA), succinyl CoA, fumarate, pyruvate and/or acetylaldehyde end products are then funneled into the Krebs

cycle for adenosine triphosphate (ATP), reduced nicotinamide adenine dinucleotide (NADH) and reduced flavin adenine dinucleotide (FADH₂) synthesis (160, 161).

Along with other pathway enzymes, oxygenases catalyze reactions involved in the initial stages of hydrocarbon degradation and are encoded on chromosomes and/or plasmids (215). Monooxygenases are involved in aliphatic hydrocarbon degradation and oxidize single bonds by incorporating one oxygen atom into the carbon chain (215). Dioxygenases break open aromatic ring structures by oxidizing double bonds and incorporating two oxygen atoms (215). Hydrocarbon-degradative genes located on plasmids in donor cells can be conjugatively transferred to recipient microbes through a pilus (64). For example, horizontal transfer of the toluene ortho-monooxygenase (TOM) plasmid, naphthalenesulfonate-degrading genes, carbazole-degrading genes have been observed in *Burkholderia cepacia* (251), *Sphingomonas* species (17) and *Pseudomonas* species (252), respectively. Alternative horizontal gene transfer mechanisms include transduction through bacteriophage infection and transformation of exogenous DNA from lysed microbes (64).

Integral membrane alkane monooxygenase (*alkB*) catabolizes nC5-nC16 alkane substrates (281, 284). Four distinct genotypes (*alkB1* and *alkB2* from *Rhodococcus* sp. strain Q15, *alkB* from *Pseudomonas putida* Gpo1 OCT plasmid, and *alkM* from *Acinetobacter* sp. strain ADP1) have been identified thus far (7, 281). The *alkBFGHJKL* and *alkST* operons from *P. putida* have been heavily characterized and encode all oxidation steps up to the β-oxidation cycle for energy utilization (282, 283). After oxidizing an NADH molecule, rubredoxin reductase (*alkT*) uses an intermediate soluble iron-containing rubredoxin (*alkF* and *alkG*) to transfer an electron to a membrane-bound monooxygenase (*alkB*), which oxidizes the n-alkane substrate into an alcohol (282, 283). This alcohol is further oxidized to an aldehyde by an alcohol dehydrogenase (*alkJ*) and then converted to a carboxylic acid by an aldehyde dehydrognase (*alkH*) (282, 283). An acyl-CoA synthetase (*alkK*) finally hydrolyzes the product into a fatty acid and attaches an acetyl-CoA for entry into the β-oxidation cycle (282, 283). Cytochrome P450 alkane hydroxylase, first identified in *Mycobacterium* sp. strain HXN-1500, utilizes a similar metabolic pathway to degrade C₅-C₁₆ (285).

The *Pseudomonas putida* mt-2 TOL plasmid is involved in methyl-modified aromatic ring catabolism (102). The upper pathway operon *xylCMABN* converts toluene/xylene to benzoate/toluate (102). The lower pathway operon *xylXYZLTEGFJQKIH* encodes catechol-2,3-oxygenase (*xylE*) which results in aromatic ring cleavage and yields pyruvate and acetylaldehyde as end products (102).

Naphthalene dioxygenase genes are unique to different *Proteobacteria* subphyla. y-Proteobacteria—specific genes were characterized from the Pseudomonas putida NAH7 plasmid, which contains *nahAaAbAcAd-BFCQED* upper-pathway and *nahGTHINLOMKJ* lower-pathway operons (97, 318). After oxidizing an NADH molecule, ferredoxin reductase (nahAa) uses an intermediate ferredoxin (nahAb) to transfer an electron to naphthalene dioxygenase (nahAc large and nahAd small subunits), which oxidizes the naphthalene to naphthalene cis-1,2,-dihydrodiol (97, 318). Subsequent oxidation steps involve naphthalene dihydrodiol dehydrogenase (nahB), dihydroxy-naphthalene dioxygenase (nahC), 2-hydroxychromene-2-carboxylic acid (HCCA) isomerase (nahD), trans-o-hydroxybenzlidene pyruvic acid (tHBPA) hydratase-aldolase (nahE), salicyladehyde dehydrogenase (nahF) and associated reaction products (97, 318). When lower-pathway operon genes are expressed, salicyclic acid is then converted to acetyl CoA and pyruvate through multiple catechol compounds, and funneled into the Krebs cycle for respiration (97, 318). β-Proteobacteria-specific genes were characterized using Ralstonia sp. strain U2. Upstream nagAaGHAbAcAdBFCQED (84) and downstream nagJIKLMN (321) operons are co-transcribed and encode steps initially similar to the nah pathway. Naphthalene is oxidized by a reduced naphthalene dioxygenase (nagAc large and nagAd small subunits) and converted to fumarate and pyruvate though a salicylate (2hydroxybenzoate) and gentisate (2,5-dihydroxy-benzoate) pathway for incorporation into the Krebs cycle (84, 321).

PAH dioxygenases are also unique to different taxonomic groups. A PAH dioxygenase encoded by the *nidDBA* gene region was characterized from *Mycobacterium vanbaalenii* PYR-1 and capable of pyrene, fluoranthene, biphenyl, phenanthrene, naphthalene, anthracene and benz[a]anthracene degradation (106, 133, 159, 184, 185). PAH substrates are oxidized into *cis*-3,4-dihydrodiols by the dioxygenase (*nidA* large and *nidB* small subunits) and converted to acetyl CoA and succinyl CoA end products through

a heavily characterized phthalate pathway (27, 135, 137, 268). Characterized from *Burkholderia* sp. strain RP007A, the *phnSFECDAcAdB* operon is transcribed in the presence of naphthalene and phenanthrene (149). Multiple *Burkholderia* species isolated from contaminated soil have been found to degrade phenanthrene as well (2, 15, 128, 248, 280). Although *phn* operon genes are divergent from *nah* gene sequences and are arranged differently, isofunctional gene products are nearly identical to the *nah* metabolic pathway (149). *phnB*, however, is more closely related to biphenylic catabolic pathway dehydrogenases, while *phnC* codes for PAH extradiol dioxygenase, and *PhnAa* and *phnAb* gene products are swapped (149). The *Burkholderia xenovorans* LB400 *bph* gene cluster involved in biphenyl and PCB degradation has been extensively characterized as well (71, 113, 114).

1.2. The Bioremediation of Hydrocarbon-Contaminated Soils

1.2.1. Bioremediation Treatment Strategies in Hydrocarbon-Contaminated Soils

Bioremediation is defined as the use of microorganisms to degrade xenobiotic substances such as diesel fuel at an environmental site (160). When completely degraded, petroleum hydrocarbons found in diesel fuel are mineralized into carbon dioxide (CO₂) and water (H₂O) (161). If the indigenous community lacks one or more required enzymes or cometabolism (i.e., non-specific enzymatic degradation of a similar molecule) occurs, contaminants may only partially degrade (39, 200, 276). Such incomplete oxidation can result in polymerization of the metabolic end products and generate a more stable, complex product (39, 200, 276).

Bioremediation strategies are classified according to treatment location. In contrast to *in situ* strategies where biodegradation of the contaminant occurs in place at the site, *ex situ* strategies involve removal of the contaminated region to another on-site or off-site location (7). Biostimulation and bioaugmentation are treatment options available at *in situ* and *ex situ* sites (7). Biostimulation of hydrocarbon-contaminated soil increases the metabolic activity of indigenous hydrocarbon-degrading microbes (214). By introducing nutrient amendments (e.g., nitrogen (N) and phosphorus (P)) to the soil and increasing oxygen through tilling, more favourable conditions are created for microbial metabolic activity (214). During bioaugmentation treatments, a microbial culture enriched

from indigenous hydrocarbon degraders is often added to the contaminated soil (214). Alternative bioaugmentation options include the introduction of non-indigenous hydrocarbon degraders, genetically engineered microbes and/or DNA for microbial uptake (161, 214). Compared to soil-adsorbed indigenous microbes with stable access to nutrient sources, (re)-introduced microbes have difficulty creating a niche in the new environment and maintaining populations over an extended period of time (52). Irreversible attachment (35) develops over a long period of time, when extracellular polymeric substances (EPS) (8, 277, 289) or cell surface structures (e.g., pili, fimbriae) have cemented the cell to the soil particle and formed soil aggregates (109, 172, 204, 286). Natural attenuation (a.k.a., intrinsic bioremediation), in contrast, does not involve a treatment strategy (111). If biodegradation rates are determined to be at appropriate levels, the indigenous microbial community is simply left to degrade the pollutant (111).

Cost-effective and simple ex situ bioremediation strategies such as biopiles (182) and landfarming (175, 236) have been widely utilized in arctic regions far removed from population centers (7). The oil industry has an established history of using landfarming to treat upstream drilling and downstream refinery waste materials (187, 214). Biopiles are excavated piles of soil ranging from sub-cubic meters to 10,000m³ for full-scale operations (139). Nutrient amendments are mixed into the soil before shaping the biopile on a solid surface to best distribute oxygen levels (139, 214, 292). Often lined and covered to prevent leaching, biopiles are aerated with vehicle-assisted plowing and irrigated if necessary (139, 214, 292). If organic material is added to increase microbial metabolic activity, the ex situ strategy is called windrow composting (247). Although similar in concept to biopile strategies, landfarming involves a much larger and shallower soil treatment area at a fixed facility (214). Soil depths range between 12-18 inches, or roughly 30-45 cm (70), while variable surface areas have included 1 acre and 4 hectacres (214). Optimal water levels are maintained using sprinkler irrigation, perimeter dikes to prevent runoff and a lined drainage layer underneath (214). In addition to stimulating hydrocarbon biodegradation, the landfarming surface area is likely to enhance hydrocarbon volatilization into the atmosphere (187).

1.2.2. The Effect of Hydrocarbon Bioavailability on Microbial and Nucleic Acid Sorption in Contaminated Soils

Bioavailable hydrocarbon contaminants are accessible by a viable microbial population with the genetic capacity for biodegradation (154, 229). Such hydrocarbon-degrading microbes require adequate nutrient levels to remain metabolically active (187). The 200:1 to 9:1 C:N (187) and 100:1 to 20:1 C:P (181, 273) ratios necessary for sustainable activity are skewed by hydrocarbon contamination (187). As the sudden influx of carbon increases microbial respiration, nitrogen and phosphorus molecules are rapidly consumed and the contaminated soil becomes nutrient-deficient (187). Hydrocarbon biodegradation is optimal when 50-80% of pore space is filled with water and soil microbes have access to both oxygen and water (187). Accumulated hydrocarbon metabolites including carboxylic acids (Section 1.1.2.) slightly lower the soil pH (7), potentially beyond the optimum pH 6.5-8.0 range (187). Temperature and salinity also affect microbial activity and associated biodegradation rates (151).

Soils containing a mixture of clay, silt and sand maintain optimal air/water flow levels for viable microbial populations (161) which are usually attached to soil particles. According to a review by Ranjard and Richaume (223), over 80% of microbes are attached to soil aggregates in 2µm to 6µm pore spaces. Coarse-textured soils contain large quantities of gravel (>2 mm diameter) and sand (0.05 mm to 2 mm diameter) particles, while fine-textured soils predominantly contain silt (0.002 mm to 0.05 mm diameter) and clay (<0.002 mm diameter) particles, as classified by Morgan and Watkinson (187). In comparison to a sand particle (0.0003 m² g⁻¹ soil), the approximate surface area of a fine clay particle (30 m² g⁻¹ soil) is up to five orders of magnitude larger (161). Soil particle surface area directly correlates with the negative surface charge from ionized hydroxyl groups (161), as indicated by cation exchange capacity (CEC) (43). Both relatively homogenous soils (75) and soils with widely-varying mineral content (213) have yielded coefficient of determination (R²) values of 0.90 and 0.66, respectively. Reduced surface charge causes coarse-textured sandy soils to have a lower pH buffering capacity (7). In one study, $>0.45 \mu m$ soil particle quantities decreased linearly ($R^2 =$ 0.993) with buffering capacity (126). Limited CEC (213) and large pore spaces (313) in sandy soils also cause low moisture content and increased leaching. Soil aggregates,

however, are surrounded by adsorbed films of water due to surface charge (63), with increased microbial adhesion at the air-water interface (239).

Microbial uptake is another key component of hydrocarbon bioavailability (161, 229). Low aqueous solubility limits microbial access to such hydrophobic molecules (229), especially as hydrocarbons increase in molecular volume (118). Equilibriumrelated perturbations in neighbouring soil, air and non-aqueous phase liquid (NAPL) phases also affect concentrations present in water (215). Hydrocarbon contaminants adsorbed to soil aggregates are accessible by microbes due to a variety of hydrophobic interactions (229). Bacterial strain *Rhodococcus* sp. Q15 made direct contact with adsorbed hydrocarbons and suspended droplets through biosurfactant production (307). Biosurfactants increase cell surface hydrophobicity (9, 253, 320) and aqueous hydrocarbon solubility by forming 500-1,500 Da micelles (148, 190). Antarctic bacterium Halomonas sp. ANT-3b produced glycolipid emulsifiers yielding nanodroplets at the hexadecane-water interface (212). Hydrocarbon adhesion by Acinetobacter calcoaceticus RAG-1 is mediated by thin, hydrophobic fimbriae (230). A. calcoaceticus RAG-1 also produces an anionic bioemulsan with hydrophobic fatty acid side chains that adhere to oil droplets (229). As bacteria multiply at the hydrocarbon-water interface, a monomolecular bioemulsan film accumulates around the depleted droplet, preventing reattachment of the capsule-deficient hydrophobic RAG-1 cells (229).

Hydrocarbon metabolite-related pH changes have the potential to interfere with microbial adhesion in contaminated soils. Microbial transport towards a soil particle is primarily due to bulk water flow, although diffusion and cell motility (e.g., flagellar chemotactic response) also have an affect (287). Cell and soil particle surfaces are both negatively charged and form an electrical double layer during adhesion (287). Cations surrounding soil and microbial surfaces repel each other (287). Adhesion occurs when the repulsion is low enough for van der Waals forces and hydrophobic interactions to weakly bind the two surfaces (287). A smaller, more compressed double layer is less repulsive and promotes cellular adhesion. Greater ionic strength (i.e., the concentration of cations and anions in solution) increases the similarity between the cation-dense layer and bulk solution concentrations (322). Consequently, cations are more likely to diffuse away from

cell or particle surfaces, compressing the double layer and increasing adhesion levels (322).

Changes in soil pH also affect exogenous nucleic acid adsorption, potentially impacting results from DNA- and RNA-based methodologies. Because DNA carries a negative charge in neutral and alkaline soils (above pH5.0), adsorption is minimal and confined to external clay surfaces (93). In acidic soils (below pH5.0), positively-charged DNA adsorbs more readily to negative clay particles, with greater concentrations on internal clay surfaces (93). Compared to larger sizes (23 kb), small DNA fragments (2.69 kb) sorb more strongly to soil particles (199). Higher divalent cation (Ca²⁺ and Mg²⁺) concentrations also increase nucleic acid binding due to changes in ionic strength; 25% total DNA and 30% total RNA were desorbed from clay particles after soil neutralization (93).

Colloid-bound nucleic acids are primarily protected from biodegradation due to nuclease adsorption rather than associated adsorption affinity (36). When bound to sand particles, DNA is one-hundred times more resistant to DNase I degradation (227); because clay has a greater surface area and cation exchange capacity than sand, DNA adsorption is likely to be even stronger. Proximal microbes, however, can cause uniform structural collapse of soil colloids and free DNA to be degraded (94). No studies regarding the effect of temperature on nucleic acid adsorption were found. Soil aggregate disruptions from seasonal freezing and thawing (206), however, are likely to increase nucleic acid degradation rates.

1.2.3. Nitrogen Fertilization Toxicity and Diazotrophy in Hydrocarbon-Contaminated Soils

Nitrogen-phosphorus fertilizers are typically used to promote hydrocarbon biodegradation in contaminated soils. Since degradation rates in coarse-textured, low moisture soils are limited by osmotic stress from excess soluble fertilizer salts (23, 79, 293, 295), nutrient concentrations must be optimized prior to field-scale application. According to Walworth et al. (295), maximum hydrocarbon degradation in sandy soil occurred at low nitrogen fertilizer levels, while optimum nutrient concentrations were 18-fold greater in loamy silt soils. Reduced water-holding capacity and increased salinity levels also correlated with decreased microbial oxygen consumption (295). A comparison

of different nitrogen fertilizer concentrations in diesel-contaminated loam soil suggested an inhibitory osmotic effect from excess nitrogen (293). Greatest at the lowest nitrogen concentration, microbial respiration and gross nitrification rates were also inversely proportional to water potential measurements (293). Hydrocarbon-contaminated antarctic soils amended with 1,000-1,600 mg N kg⁻¹ soil water mineralized optimal levels of ¹⁴C-octadecane (79) using calculations from Walworth et al. (295). Slow-releasing fertilizers such as cod bone meal have the potential to prevent nitrogen fertilizer toxicity without impacting biodegradation rates (296). In alpine soil, cod bone meal and diammonium phosphate amendments both enhanced hydrocarbon removal to the same extent (296).

Nitrogen inputs by diazotrophic soil microbes provide an alternative to fertilizer treatments (218). Nitrogen fixation, the microbial reduction of nitrogen (N₂) gas to ammonia (NH₃) or ammonium (NH₄⁺), is mediated by an oxygen-sensitive enzyme complex (310). An iron-molybdenum (FeMo) nitrogenase component (containing an active site for N₂ triple bond cleavage) pairs with an iron-sulfur (FeS) nitrogen reductase for hydrogenation, dissociating after each catalytic cycle (99). Corresponding nifD and nifH genes (245) are down-regulated by NH₄⁺ and oxygen (O₂) (66), and used to identify diazotrophic microbes in hydrocarbon-contaminated environments. Elevated biodegradation rates correlated with increased nitrogen fixation in nutrient-deficient sandy soils (275). Particulate organic carbon (POC) amendments enhanced hydrocarbon degradation in diesel fuel-amended coastal water samples, which was preceded by a spike in nitrogen fixation from indigenous diazotrophic bacteria (218). Five bacterial isolates enriched from fuel-contaminated antarctic soils fixed nitrogen heterotrophically and nonsymbiotically in the dark (67). Nutrient-deficient conditions from hydrocarbon contamination probably conferred a selective advantage to such diazotrophs (67). Two of these isolates, identified as *Pseudomonas* species, utilized jet fuel vapors as a sole carbon and energy source when provided with NH₄⁺ (67). Nitrogen-fixing isolates could be associated with non-diazotrophic hydrocarbon degraders, which provide reduced oxygen levels and organic metabolic byproducts (67).

1.3. Polar and Alpine Bioremediation of Hydrocarbon-Contaminated Soils1.3.1. Biostimulation and Bioaugmentation in Polar and Alpine Soils

Polar and alpine regions are characterized by extremely cold temperatures and nutrient-deficient, coarse-textured soils with a low water-holding capacity (3). Maximum soil temperatures range from below 0 to 20°C at the snow-free soil surface (16) for only one to two months of the year (270). When soil albedo decreases after hydrocarbon contamination, the darker soils absorb more solar energy and soil aggregate temperatures increase slightly (16). The persistence of contaminating hydrocarbons, however, indicates that biodegradation rates are low in these soils (3, 13). Although microbial activity has been detected at -15°C in arctic permafrost (267), biodegradation is limited by slower metabolic processing and limited microbial uptake at freezing temperatures (16). Microbial activity measured in saline films of seawater from -2°C to -20°C (122) suggest that hydrocarbons attached to soil aggregates could be metabolized at subzero temperatures. Decreased temperatures also result in greater hydrocarbon viscosity, decreased volatilization of toxic low molecular weight compounds and reduced bioavailability of long-chain n-alkanes (187, 306).

Biostimulation treatments have consistently increased ¹⁴C-alkane and/or ¹⁴C-naphthalene mineralization in polar and alpine soils (5, 23, 183, 304, 305) and resulted in significant TPH losses (5, 23, 24, 50, 51, 59, 72, 125, 168, 169, 171, 175, 182, 208, 233, 236, 263, 273, 304). Both nitrogen and phosphorus amendments are required for optimal hydrocarbon biodegradation in contaminated arctic soils (23, 183). ¹⁴C-Hexadecane and ¹⁴C-naphthalene mineralizations were greatest at 100:45 N:P mg kg⁻¹ soil, the lowest N:P concentration (23). Metabolic activity as determined by bacterial 16S ribosomal RNA: ribosomal DNA (rRNA: rDNA) ratios and CO₂ production indicated that enhanced TPH removal in fertilized arctic soil was due to biotic processes (72, 125). Fertilized soils exhibited greater hydrocarbon degradation at an alpine glacier site for three consecutive summers, but slowed over time despite repeated nutrient amendments (171). Oxygen depletion in contaminated Norwegian arctic soils suggested metabolic activity at subzero temperatures starting at -6°C before seasonal thawing (224). Fertilized diesel- or oil-contaminated (sub)-antarctic soil impacted desert and mineral soil to a greater extent than vegetal cover or organic soil (59, 60), and significantly enhanced n-alkane degradation

over PAH degradation (50, 51). Biostimulation increased naphthalene-degrading gene populations and aromatic hydrocarbon degradation in soil from an antarctic field trial (291). Nutrient fertilization lowered the pH from 7.4 to 6.8 in a sandy petroleum hydrocarbon-contaminated soil from the Norwegian Arctic (24). Approximately 50% aliphatic hydrocarbons were degraded biotically in surface and subsurface soils, while approximately 50% aromatic hydrocarbons were biotic and abiotic (i.e. soil adsorption, transformation and evaporation) losses (24). Natural attenuation was sufficient at former alpine tank farm, where hydrocarbon degradation levels were similar in fertilized and unfertilized soils (169).

Ambiguous results across multiple studies have indicated bioaugmentation is far less effective than biostimulation (167, 168, 273). Although inoculation with indigenous hydrocarbon-degradative enrichment cultures further stimulated ¹⁴C-dodecane mineralization and/or TPH removal in contaminated arctic soils and biopiles (182, 183), hydrocarbon degradation was not enhanced in other studies (167, 233, 273). Bioaugmentation with a diesel-degrading *Actinomycetes* species temporarily enhanced TPH reductions in contaminated alpine soil (168). A marine gas oil-degrading *Pseudomonas* species increased degradation rates in a recently contaminated antarctic soil (263).

1.3.2. The Effects of Freeze-Thaw Temperature Fluctuations on Soil Microbial Communities

As reviewed by Henry (108), freeze-thaw studies have been inconsistent due to a lack of standard methodology and have not necessarily reflected *in situ* conditions. Temperatures during soil collection have not corresponded to simulated freezing-thawing profiles (108). Experimental freeze-thaw cycles varying in length from one day to over a week have typically been fewer than five in number (108). *In situ* conditions, however, involve the cumulative effects of numerous freeze-thaw cycles over a cold season (108). Microcosm and mesocosm soils were exposed to ambient air temperatures on the sides and bottom, and have involved 0.05-5.39 L volumes and 1.0-60.0 g masses (108). Because low soil quantities equilibrate rapidly with air temperatures, soils from freeze-thaw studies have been exposed to amplitudes and ranges which are unreasonably harmful to microbes (108, 148, 156, 259, 316). Diurnal temperature fluctuations are

highly muted in ground soils, even at a 5 cm depth (108). Unless air temperatures are sustained over a long period of time, *in situ* soils under a thick snowpack do not reach -20°C, a commonly-used minimum temperature (108). Decreased albedo from hydrocarbon contamination further delays soil freezing (16). Consequently, hydrocarbon-contaminated polar and alpine soils might not be frozen at subzero air temperatures (108).

Despite methodology-related challenges, such temperature fluctuations impact the soil environment. Carbon and nutrient losses during the winter have been attributed to freeze-thaw cycling (112, 243), with moderate freeze-thaw cycles having less of an effect (96). Freeze-thaw cycles have resulted in greater soluble organic matter losses (297). Levels of dissolved phosphorus increased after freeze-thaw cycling under controlled conditions (290). Although two studies did not detect changes in soluble phosphorus (209, 262), soluble phosphorus lost during thawing may be derived from plant tissue (18). Reductions in snowpack thickness led to increased aggregate disruption and phosphorus leaching from soil freezing (82). Due to the expansion of ice crystals in pore spaces (257), freeze-thaw cycling has exacerbated disruption in soils with high moisture levels (205, 257). Such disruption has been more pronounced in macroaggregate soil particles than in microaggregates (257). Smaller ice crystals formed during rapid freezing could potentially reduce soil aggregate disruption (108).

Soil microbial community structures shift in response to freeze-thaw cycles (148, 250, 294). During seasonal freezing, predominant bacterial populations shift to fungal populations in the winter (238). No consensus has been reached in regards to microbial damage from cyclic freeze-thaw patterns (108). The effects of soil freezing and thawing have been significant in some studies (269, 297), but relatively subtle in others (96, 258). While decreased microbial viability and microbial biomass have been associated with initial and later freeze-thaw cycles, respectively (294, 311), alpine and arctic tundra studies have indicated an indigenous microbial community adapted to these selective pressures (96, 154, 156).

Soil respiratory bursts measured by denitrification and carbon mineralization have been associated with spring thaw across a wide range of systems, including temperate peatland, tundra, alpine meadow, forest and agricultural soils (32, 130, 180, 221, 259). These denitrification bursts are partially explained by the availability of dissolved organic

carbon (246). Successive free-thaw cycles have also been associated with decreasing and continued pulses of released CO₂ (44) and nitrous oxide (N₂O) (46, 157). Heterotrophic activity has typically been higher under thick snow cover, where insulated soil temperatures remain near 0°C (29, 30). Although microbes could remain metabolically active at -10°C, soil respiration rates typically exhibit an abrupt decline near 0°C, suggesting a shift in respiration-related processes at subzero temperatures (130, 180, 258).

1.3.3. Microbial Communities in Polar and Alpine Soils

Polar and alpine microbial communities consist of psychrophilic and psychrotolerant species adapted to the harsh climate; psychrophiles grow optimally <15°C but not above 20°C, while psychrotolerant microbes are metabolically active at 0°C with optimal growth between 20-40°C (107). Alpine, Canadian arctic and Finnish arctic soils primarily contain *Proteobacteria* species, with substantial proportions of *Actinobacteria*, Acidobactericeae and Bacteroidetes (143, 155, 163, 197). The Finnish bacterial community remained consistent during freeze-thaw fluctuations from spring to late summer (162). Simulated fall/winter freeze-thaw cycles, however, resulted in decreased β-Proteobacteria populations (163). Acidobacteriaceae species from the same region are particularly dominant in low pH (4.6–5.2) soils, proportionally decreasing above pH 5.5 (163). y-Proteobacteria are more predominant in Canadian soils and δ -Proteobacteria in Siberian soils (195). Soils from both regions, however, contained significantly lower amounts of Verrucomicrobia and decreased quantities of Acidobacteriaceae than alpine soil (195). Bacteria from subarctic soils almost solely utilized starch as a carbon source, while subarctic fungi utilized other sources of carbon (225). Arctic and alpine fungal populations were greater during cold seasons than in warm seasons (155, 162).

Arctic soils also contain an acid-tolerant, nitrogen-fixing community of methanotrophic bacteria. *Methylocystis rosea* was isolated from arctic wetland soil (299), *Methylocella tundrea* from acidic tundra soil (57), and *Methylocapsa acidiphila* and *Methylocella palustris* from acidic sphagnum boreal bogs (58). In addition, methanogenic archaea *Methanomicrobiales*, *Methanobacteriaceae*, *Methanosaetaceae* and *Methanosarcinaceae* have consistently been found in arctic and subarctic soils (86, 115, 116, 177, 226).

1.3.4. Nutrient Utilization by Microbial Communities from Arctic Soil

Originally an ecological model, r/K-selection theory relates how microbial communities adapt to nutrient availability in stable or unstable environments (217). Copiotrophic r-strategists have high nutritional requirements and prefer labile organic carbon sources, but are adapted to unstable environments; they alternate between periods of dormancy and maximum growth during nutritional abundance (81, 178, 271). Characterized by slower metabolic rates and lower nutritional requirements, oligotrophic K-strategists outcompete copiotrophs in stable nutrient-deficient environments and remain at constant levels near the carrying capacity (81, 178, 271).

r-Strategists are likely to be prevalent in soils with large quantities of organic carbon (e.g., hydrocarbon contaminants). β -Proteobacteria and Bacteroidetes were most abundant in North American soils with high carbon availability, including arctic and subarctic regions (81). These taxons also exhibited the highest levels of carbon mineralization (81). Abundant β -Proteobacteria populations in Finnish arctic soil were most active prior to cyclic freeze-thaw patterns, as indicated by a high rRNA:rDNA ratio (163). A significant reduction in ribosomal content after freeze-thaw cycling suggests that copiotrophic metabolism is no longer favoured and the microbes have become dormant (163).

K-Strategists, in contrast, predominate in soils with low available carbon content (81). *Acidobacteria* were most abundant in North American soils with very low resource availability (81). Soils amended with high concentrations of organic carbon, however, exhibited a decrease in relative abundance and carbon mineralization (81). Consistently low rRNA:rDNA ratios indicated that Finnish arctic soil *Acidobacteria* populations are oligotrophic (156).

1.3.5. Psychrotolerant Hydrocarbon Degraders from Polar and Alpine Soils

In Antarctica, culturable hydrocarbon degrader and yeast populations are negligible in pristine soils and typically measure over $1x10^5$ CFU g⁻¹ soil in hydrocarbon-contaminated soils (3). Culturable heterotrophs measure one to two orders of magnitude higher in contaminated Antarctic soils than in pristine soils (3). Since polar fungi prefer to utilize fatty acids, only psychrotolerant bacteria have been isolated as hydrocarbon-degraders in polar and alpine soils (3). *Rhodococcus, Acinetobacter* and *Pseudomonas*

isolates have been involved in n-alkane biodegradation, and *Sphingomonas* and *Pseudomonas* isolates in PAH degradation (7). n-Alkane utilization is mediated by biosurfactant production in some *Rhodococci* (31, 47, 191, 210, 211, 216, 278, 307).

Increased Acinetobacter and Pseudomonas putida hydrocarbon-degradative gene proportions significantly correlated (P < 0.001) to TPH concentrations in contaminated and pristine alpine soils (166), while *Rhodococcus* and *Pseudomonas* alkane-degradative and Pseudomanas PAH-degradative genes were detected in hydrocarbon-contaminated antarctic soils (158). Although *Proteobacteria* 16S rDNA proportions were similar in hydrocarbon-contaminated (56%) and pristine (46%) alpine soils, pristine soils only contained α -Proteobacteria (143). Contaminated soils, however, contained decreased α -*Proteobacteria* (24%) and increased β -Proteobacteria (8%) and γ -Proteobacteria (24%) proportions (143). Acinetobacter populations remained at similar (18-20%) levels in both soils (143). Copiotrophic y-Proteobacteria populations (e.g. Pseudomonas and Acinetobacter spp.) from alpine soil increased in response to hydrocarbon contamination, while oligotrophic Actinobacteria (e.g. Rhodococcus and Mycobacteria spp.) maintain sizeable levels (165). Hydrocarbon-polluted antarctic coastal soils are predominated by Pseudomonas, Sphingomonas, and Variovorax species and are lower in diversity than pristine soils, which contain Cytophaga/Flavobacterium/Bacteroides, Deinococcus/Thermus and Fibrobacter/ Acidobacterium (3). Geotrichim and Chrysosporium are abundant fungal species in pristine soil, while Phialophora is present at high levels in contaminated soil (3).

Microbial community structures from temperate hydrocarbon-contaminated soils contain genera known to degrade hydrocarbons in cold-region soils and may provide insights into metabolic preferences. In a compost biofilter used to treat toluene vapors, *Pseudonocardia* and *Rhodococcus* were thirty-four times more numerous than other genera, including r-strategists *Pseudomonas* and *Acinetobacter*, which are adapted to fast growth in a resource-abundant and uncrowded environment (124). This microbial community is adapted to a K-environment with slow-releasing nutrient sources (e.g., humic compounds) (124). In general, *Rhodococci* are considered K-strategists that persist in starvation conditions, preferring to catabolize (hydrocarbon) pollutants over easily-degradable carbon sources (19). *R. erythropolis* N9T-4, for example, is an extremely

oligotrophic strain (isolated from crude oil stockpiles in Japan) that fixes carbon dioxide and grows on solidified minimal salt medium without any additional carbon source (201).

1.3.6. Cold-Adapted Enzymes and Metabolic Processes in Psychrotolerant and Psychrophilic Bacteria

Cold-adapted enzymes demonstrate tenfold greater activity at temperatures below 20-30°C than their mesophilic counterparts (76, 77). Although O₂ consumption and CO₂ production rates in contaminated arctic soil have suggested subzero hydrocarbon biodegradation (224), no hydrocarbon-degradative enzymes are known to be cold-adapted. A biphenyl dioxygenase from psychrotolerant bacterium *Pseudomonas* sp. strain Cam-1 demonstrated activity at 4°C, but did not exhibit cold-adapted enzyme characteristics (174). As reviewed by Feller and Gerday (76), enzymatic structures with lower stability and greater flexibility yield greater activity levels to compensate for cold-induced inhibition (48, 53, 80). A larger catalytic cavity is more accessible to ligands, accommodating substrate at low energy cost, and facilitating release of end products (1, 234). Either residues in loops bordering the active site are deleted, or bulky side chains at the active site entrance are replaced with smaller groups (136, 261). Structural adjustments also enhance electrostatic potential near the active site, attracting oppositely-charged ligands and channelling the substrate towards the catalytic cavity (25, 136).

At low temperatures, stronger structural interactions between nucleic acid strands impair DNA replication, messenger RNA (mRNA) transcription and translation processes (76). Psychrophilic and psychrotolerant microbes utilize cold-adapted proteins to bind nucleic acids and compensate for these temperature-imposed limitations (37, 179, 272). To increase structural flexibility and instability found in cold-adapted proteins (88), amino acid residues involved in secondary, tertiary and quaternary binding are reduced. Such residues include proline and arginine, which restrict backbone rotations and can form multiple hydrogen bonds and salt bridges (234, 261). Clusters of glycine residues increase localized chain mobility (234, 261). Exposing a greater proportion of non-polar side groups to the surrounding aqueous medium further enhances structural instability (234, 261).

Under particularly harsh conditions, even psychrophilic and psychrotolerant bacteria become dormant and are no longer immediately culturable (132). Dormant

microbes maintain an extended state of low metabolic activity where gene expression ceases or remains minimal. Under more favorable conditions, genes are reactivated during an acclimation period and cells return to a vegetative state (129). Comprising over 80% total RNA (300), cellular rRNA levels only decrease when utilized as a nutrient source under starvation conditions (61). Because replication, transcription and translation processes are inhibited during cold temperature-induced dormancy (76), cellular rRNA is no longer degradable and microbial rRNA levels would remain steady.

1.3.7. Microbial Community Characterization Techniques

Microbial ecology research examines how microbes interact with each other and their environment (160). A variety of culture-dependent and -independent techniques have been used to assess population size, microbial activity and biodiversity in hydrocarbon-contaminated soils (161). The techniques described below compare multiple environmental samples and were relevant to this thesis. Methodology-related references are cited in Chapter 3 as appropriate.

Since dormant cells are not readily culturable, viable plate counts provide an estimate of vegetative cell populations (Section 1.3.3.). Viable heterotroph populations are cultured on R2A agar, a low-nutrient medium that provides a competitive advantage to slow-growing soil bacteria (Section 3.2.1.). Viable hydrocarbon-degrader populations are cultured on a minimal salts medium (MSM) using arctic diesel as a sole carbon source (Section 3.2.1.). Whyte et al. (304) cultured cold-adapted heterotrophs and hydrocarbon degraders from contaminated Canadian high arctic soil to determine the population sizes in response to three treatment regimes.

To compare hydrocarbon biodegradation rates and cumulative mineralization levels from different (sub)-arctic soil samples (266), radiolabeled carbon substrates are spiked into small-scale microcosms and incubated at a constant temperature (153). Respired ¹⁴CO₂ is trapped as a carbonate salt in an alkaline hydroxide solution and the radioactivity measured using a liquid scintillation counter (153, 266). Hydrocarbon biodegradation levels are relative to volatilized ¹⁴CO₂ levels indicated by sterile negative controls (266). Steven et al. (267) utilized ¹⁴C-acetic acid and ¹⁴C-glucose mineralizations to demonstrate microbial activity in Canadian arctic permafrost near ambient

temperatures (-15°C). Carbon substrates utilized in this study include ¹⁴C-hexadecane, ¹⁴C-naphthalene and ¹⁴C- phenanthrene (Section 3.2.2.).

Microbial communities or individual isolates are screened for the capacity to degrade specific hydrocarbons or utilize related nutrient sources by amplifying catabolic genes with polymerase chain reaction (PCR) (190). Margesin et al. (166) amplified nalkane, aromatic hydrocarbon and PAH-degradative genes to determine the prevalence of seven genotypes in eight pristine and twelve oil-contaminated alpine soils. Hydrocarbon-degradative *alkB*, P450, *ndoB* (*nahAc* homolog), *nagAc*, *nidA*, *xylE* and *phnAc* genes (Section 1.2.2.), and nitrogen-fixing *nifH* and *nodC* genes (Section 1.3.3.) were targeted in this study.

To detect and compare gene copy numbers from different soil samples, quantitative real-time PCR (qPCR) measures the cycle at which amplified fluorescence from a dye (e.g., SYBR-Green) passes through a threshold baseline (105). SYBR-Green exhibits over a hundredfold increase in fluorescence when intercalated into double-stranded DNA (188). Because fluorescence is directly proportional to amplified gene numbers, the cycle threshold (Ct) value of plasmid standard dilutions and the corresponding number of gene copies are used to calculate a linear standard curve (105). Powell et al. (220) quantified n-alkane degrader population sizes with *alkB* qPCR during a bioremediation field trial of hydrocarbon-contaminated antarctic soil. Both *alkB* and archaeal 16S rDNA populations were compared to bacterial 16S rDNA populations here (Section 3.3.1.5.). Further comparisons to viable plate counts reflected changes in dormant cell populations (Section 1.3.3.).

To approximate compositional shifts in the microbial community of comparative soil samples, denaturing gradient gel electrophoresis (DGGE) fingerprinting separates different sequences from an amplified gene based on relative stability while passing through a chemical denaturant gradient (193). By sequencing strong bands from the DGGE profile, significant members of the microbial community are identified (192). Labbé et al. (143) profiled the bacterial 16S rDNA communities from five pristine and nine hydrocarbon-contaminated alpine soils with DGGE. Bacterial and archaeal 16S rDNA community structures profiled in this study were compared to hydrocarbon

degradation levels, while PAH-degrading and diazotrophic community structures were fingerprinted using *phnAc* and *nifH* genes (Section 3.3.3.).

The microbial community composition in a soil sample is more thoroughly characterized using a clone library. After the gene target region is cloned into a vector and a statistically significant number of clones sequenced, phylotypes are identified and corresponding taxon proportions quantified (202, 206). Biodiversity analyses include richness estimates and diversity indices, which determine the number and distribution of species within the microbial community (Section 3.3.5.). Bottos et al. (22) compared the diversity of bacterial and archaeal mat communities from two Canadian high arctic ice shelves using associated 16S rDNA clone libraries. The composition of bacterial and archaeal 16S rDNA clone libraries from this study were compared to hydrocarbon degradation levels (Section 3.3.4.).

Chapter 2: Project Objectives

2.1. Resolution Island Site Background

A former United States Air Force radar base on Resolution Island, Nunavut has been a site of environmental restoration by Indian & Northern Affairs Canada (INAC) and Qikiqtaaluk Environmental. Resolution Island is located off the southeastern tip of Baffin Island approximately 310 km from Iqaluit at the mouth of Frobisher Bay (Fig. 2.1) (208). Situated above the treeline but below the Arctic Circle (66°33′N), the subarctic site (61°36′N) (203) is characterized by short two-month summers (July and August) where mean daily temperatures cycle from 1 to 10°C (40). Temperatures decline during mid-September to October seasonal freezing (91). Winter temperatures range from -10 to -30°C in December and January (68), remaining at subzero levels until spring thawing from mid-May to June (91).

Opened in November 1954 on a small island just south of Resolution Island (Radio Island), the station (BAF-5) was operated by the 920th Aircraft Control and Warning Squadron as a part of the Pinetree Line (203). Although the base was

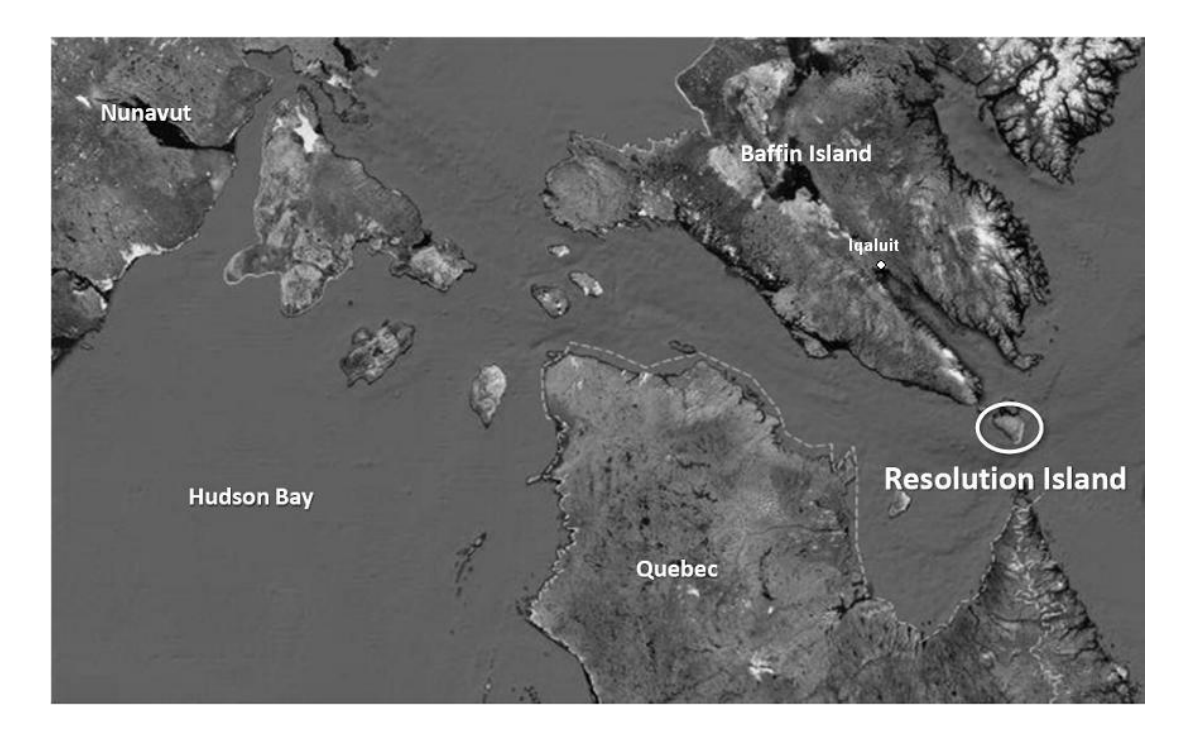


Figure 2.1. Map of Resolution Island (circled).

used to detect incoming aircraft and missiles in a troposcatter communications network, it primarily served as a navigational aid and weather station until operations ceased in November 1961 (203). In March 1962, the station was relocated to the northeastern corner of Resolution Island as a part of the Pole Vault Line and was operated under the Canadian Department of Transport (203). The site came under Indian and Northern Affairs Canada (INAC) jurisdiction in 1974 and was completely vacated by August 1975 (203). After being upgraded and merged with new stations in the North Warning System, the unmanned base was reopened as a short range radar station in 1993 (203).

Site investigations between 1987 and 1990 revealed that area soils were heavily contaminated with polychlorinated biphenyls (PCBs) from radar equipment insulating fluids, petroleum hydrocarbons from fuel storage/oil pipeline leaks and illegal waste disposal practices, asbestos from building/electrical insulation, and heavy metals (120). Between 1993 and 1994, an environmental site assessment of the area was completed and temporary barriers were placed across drainage paths (120). In partnership with Qikiqtaaluk Environmental, site remediation of PCB-contaminated soils began in 1997 and was completed in 2007 (120). Landfarming of petroleum hydrocarbon-contaminated soil remains ongoing at the site.

2.2. Specific Research Objectives

This thesis details microbiology work completed between September 2007 and August 2009, and focuses on seasonal freezing conditions after a two-month summer landfarming period. Seasonal thawing conditions were examined briefly. Soil mesocosm treatments were already optimized from earlier results (40) and compared to untreated mesocosm soils. The following objectives are specific to this study:

 To assess the impact of soil treatments on the bacterial community during simulated seasonal freezing by comparing population growth and compositional shifts to nalkane mineralization levels.

- 2. To identify key bacterial phylotypes present in the soil during simulated seasonal freezing and evaluate the metabolic capacity for hydrocarbon biodegradation at subzero tempratures.
- 3. To determine the effect of freezing temperatures on the metabolic activity of hydrocarbon-degrading and non-hydrocarbon-degrading bacteria in the soil.
- 4. To examine the composition of the indigenous archaeal community compared to its nearest phylogenetic neighbors and determine a potential biogeochemical role.
- To isolate diazotrophic hydrocarbon degraders adapted to subzero temperatures, assess their nitrogen input into the soil and compare to the soil diazotrophic community.

Chapter 3: Methodology

3.1. Seasonal Freeze-Thaw Conditions Simulated in Soil Mesocosms

Resolution Island soil obtained by INAC and Qikiqtaaluk Environmental was received by the McGill Department of Civil Engineering and Applied Mechanics (CEAM) in October, 2005. Soil was stored at approximately -4.0°C and adjusted to 1.0°C ambient temperature in a computer-regulated cold room prior to the experiment. Soils sampled in sterile Whirl-pak bags were transported to the McGill Department of Natural Resource Sciences (NRS) in a cooler with ice and stored at –20°C. WonJae Chang (CEAM) was responsible for mesocosm experimental design (91) and total petroleum hydrocarbon (TPH) analyses (279).

Seasonal temperature shifts on Resolution Island were simulated in two $100\times65\times35$ cm stainless steel tanks containing 200 kg hydrocarbon-contaminated soil (Fig. 3.1). One mesocosm tank contained treated soil with nutrient amendments (100 mg N g⁻¹ soil; 20:20:20 PlantProd fertilizer, containing 20% total nitrogen, 20% available phosphate and 20% potash) and pH neutralization from liming (2.0g CaCO₃ g⁻¹ soil), while a second tank was left untreated. Both mesocosms were initially tilled.

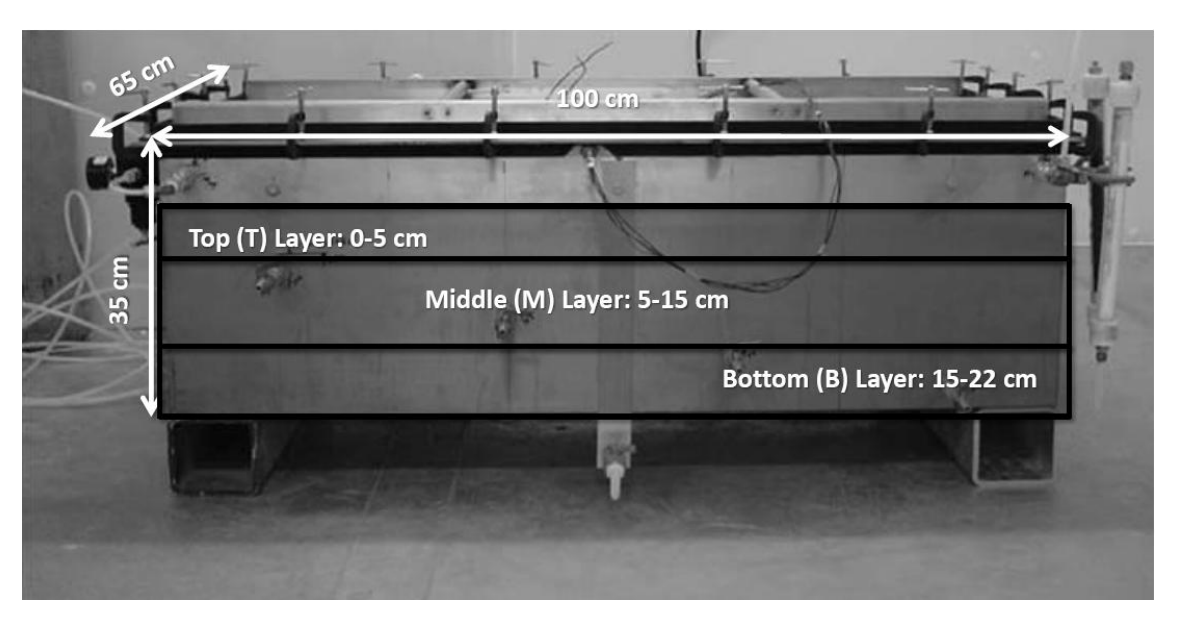


Figure 3.1. Soil mesocosm tank dimensions (100×65×35 cm) and layering (T: Top, M: Middle, B: Bottom).

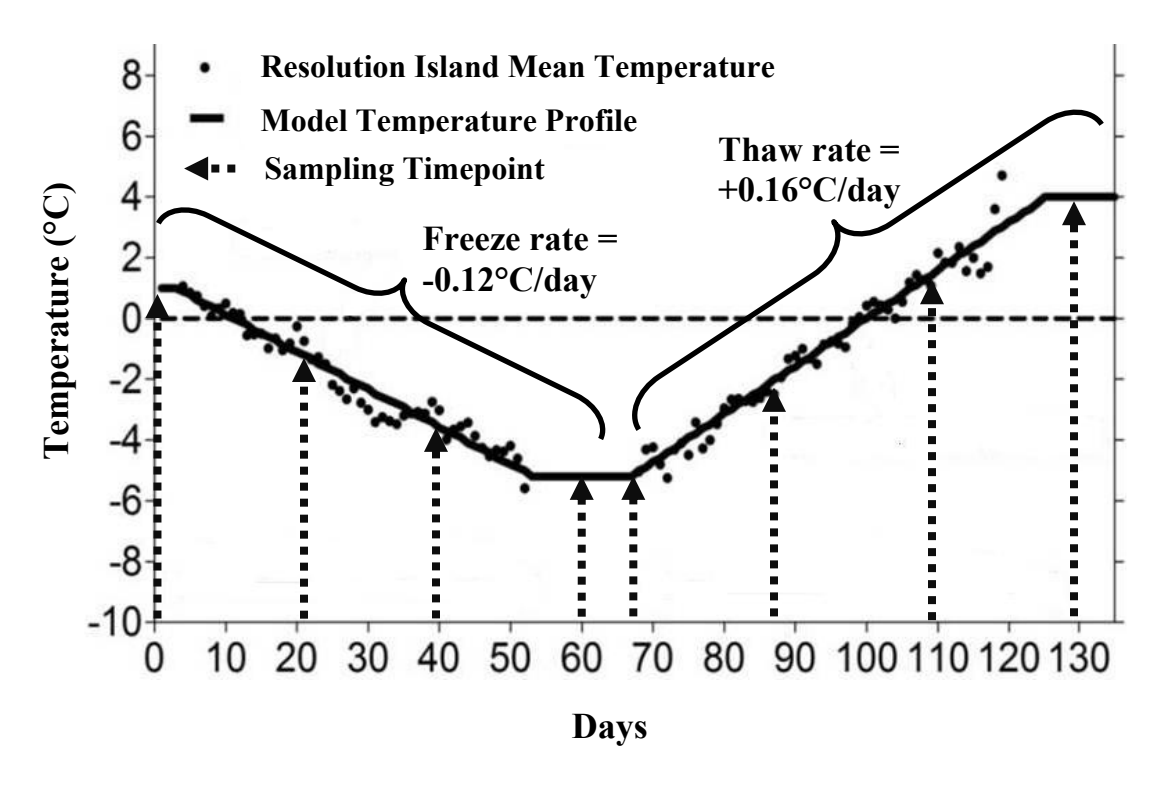


Figure 3.2. Seasonal freezing and thawing profile with sampling timepoints. Mean temperatures from the freezing phase and thawing phase reflected on-site conditions from mid-September to October and mid-May to June, respectively.

The soil mesocosms were aseptically sampled at 20-day intervals during consecutive 60-day freezing and thawing periods (Fig. 3.2; Table 1). For each sample, five to ten evenly distributed cores were mixed to form a soil composite. Initial Day 0 composites were sampled prior to soil treatments and included cores from multiple depths. For all other timepoints, each core was consecutively sampled at three different layers (top (T), middle (M) and bottom (B) at 0-5 cm, 5-15 cm and 15-22 cm, respectively) into corresponding composites. With a total of ten samples from the freezing phase and thirteen samples from the thawing phase, soil collected was stored at -20°C. All sample temperatures represented in this study were direct soil mesocosm measurements (Table 1).

C-21 C1 (D)	Freezing Phase				Thawing Phase			
Soil Sampling (Days)	0	21	39	60	67	87	109	129
Ambient Temperature (°C)	1.0	-1.0	-3.5	-5.0	-5.0	-2.0	1.5	4.0
Soil Temperature (°C)	2.4	-0.3	-2.1	-4.4	-5.0	-1.2	2.3	4.0

Table 1. Ambient cold room and measured soil mesocosm temperatures.

3.2. Culture-Dependent Soil Microbial Community Characterization

3.2.1. Heterotrophic and Hydrocarbon-Degrading Viable Plate Counts

To determine culturable heterotroph and hydrocarbon degrader population sizes, 1.0 g soil was vortexed for 30 seconds in a screw-top test tube containing 2.5 g sterile 3 mm glass beads and 9.0 ml minimal salts medium (MSM) broth (95). 100 μl aliquots of 10⁰, 10⁻¹, 10⁻², 10⁻³ and 10⁻⁴ serial dilutions with 0.1% Na₂PO₇ were spread onto triplicate R2A agar plates (Becton, Dickson and Company, Sparks, MD) and incubated at 5°C for four weeks. 0.1% Na₂PO₇ aliquots were used for triplicate negative controls. This procedure was repeated using MSM agar plates amended with 150 μl arctic diesel (Shell Oil) as the sole carbon source. The arctic diesel was pipetted onto 2.5 cm² piece of filter paper on the inner Petri dish lid.

3.2.2. ¹⁴C-Hydrocarbon Mineralization Assay of Mesocosm Soils

Hydrocarbon degradation activities of freezing phase soils were measured using triplicate microcosms as described previously (266). Each microcosm contained 10.0 g soil spiked with 50,000 disintegrations per minute (dpm) ¹⁴C-hexadecane to 100 ppm in cold hexadecane, 50,000 dpm ¹⁴C-naphthalene to 10 ppm in cold methanol-dissolved naphthalene or 50,000 dpm ¹⁴C-phenanthrene to 10 ppm in cold methanol-dissolved phenanthrene. Microcosm CO₂ traps contained 1 M potassium hydroxide (KOH) and 10% v/v ethylene glycol as a freezing depressant, previously shown to have the lowest signal quenching (266). Triplicate sterile negative controls were autoclaved for 45 minutes and incubated at room temperature for 48 hours. Microcosms were incubated at 5°C in Fisherbrand Isotemp Refrigerated Incubators (Fisher Scientific). Microcosm CO₂ traps were sampled regularly for ten weeks; microcosms were chilled on ice during sampling.

Evolved ¹⁴CO₂ was detected using a LS6500 multipurpose scintillation counter and supplied software (Beckman Coulter, Fullerton, CA).

3.3. Culture-Independent Soil Microbial Community Characterization

3.3.1. Polymerase Chain Reaction (PCR) Amplification

3.3.1.1. Soil DNA Extraction and PCR Reaction Conditions

Total soil DNA was extracted from 1.0 g soil sample using the UltraClean Soil DNA Isolation kit maximal yields protocol (MO BIO Laboratories, Solana Beach, CA). Standard PCR reaction conditions included 5 μ l 10x PCR buffer, 3.5 mM MgCl₂, 0.2 mM deoxynucleotide triphosphates (dNTPs), 0.4 μ g/ μ l bovine serum albumin (BSA), 1U native Taq polymerase (Invitrogen), 0.2 μ M FWD primer, 0.2 μ M REV primer, 5 μ l template DNA and MilliQ water to 50 μ l. An alternate set of reaction conditions included 2.5 μ l 10x PCR buffer, 2.5 mM MgCl₂, 0.2 mM dNTPs, 0.2 μ g/ μ l BSA, 1U native Taq polymerase, 0.10 μ M FWD primer, 0.10 μ M REV primer, 3.5 μ l template DNA and MilliQ water to 25 μ l. All primer sequences are listed in Table 2.

3.3.1.2. DGGE PCR Amplification

3.3.1.3. Clone Library PCR Amplification

Primers 27F and 1492R were used to amplify bacterial 16S rRNA genes used in clone libraries and identify isolates. Thermocycler conditions included an initial 3 minute denaturation; 30 cycles of 95°C denaturation for 30 sec, 57°C annealing for 55 sec, 74°C extension for 45 sec, and a final 5 minute elongation. Archaeal 16S rRNA and *nifH* genes were amplified as described previously (Section 3.3.1.2.).

3.3.1.4. Catabolic Gene PCR Amplification

Standard reaction conditions were used to amplify catabolic *alkB*, *nidA* and *nagAc* genes, as well as the *nifH* gene. A 549 bp *alkB* fragment was amplified with primers H1F and H3R. Thermocycler conditions included touchdown annealing for 1 min 10 sec, 72°C extension for 1 min 10 sec; followed by 20 cycles of 94°C for 1 min, 55°C for 1 min 10 sec, 72°C for 1 min 10 sec, and a final 10 minute elongation. 141 bp *nid A* and 107 bp *nagAc* fragments were amplified with nidA F/nidA R (56) and nagAc-like-F/nagAc-like-R (62) as described previously. *nifH* was amplified as described previously (Section 3.3.1.2.).

Alternate reaction conditions were used to amplify catabolic P450, *ndoB*, *xyE* and *phnAc* genes. A339 bp P450 fragment with primers P450fw1 and P450rv3 was amplified as previously described (285). 642 bp *ndoB* (equivalent to *nahAc*) and 834bp *xylE* fragments were amplified with primers ndoB F/ndoBR and xylE F/xylE R using identical thermocycler conditions (305). A 462 bp *phnAc* fragment was amplified with primers phnAc F and phnAcR. Thermocycler conditions included an initial 5 minute denaturation; 35 cycles of 94°C denaturation for 30 sec, 52°C annealing for 30 sec, 72°C extension for 1 min, and a final 10 minute elongation.

3.3.1.5. Quantitative Real-Time PCR of Mesocosm Soils

Bacterial, archaeal and n-alkane degrader population sizes were determined using the iQ Real-Time PCR Detection System (Bio-Rad Laboratories, Hercules, CA). Plasmid standards used to generate a standard curve were constructed by cloning the PCR-amplified target region into a pGEM-T Easy vector (Promega Corporation, Madison, WI). Target regions included bacterial 16S rRNA and *alkB* genes from *Rhodococcus* sp. strain Q15 and archaeal 16S rRNA genes from Day 0 soil. Cloned plasmids were isolated using the QIAprep Spin Miniprep kit (Qiagen) and the T7/Sp6-amplified insert

Primer	Sequence (5' to 3')	Target Gene	Reference
341F	CCT ACG GGA GGC AGC AG		194
758R	CTA CCA GGG TAT CTA ATC C		152, 312
27F	AGA GTT TGA TCC TGG CTC AG	Destablished apply	146
1492R	GGT TAC CTT GTT ACG ACT T	Bacterial 16S rRNA	146
338F	ACT CCT ACG GGA GGC AGC AG		146
518R	ATT ACC GCG GCT GCT GG		193
A109F	ACK GCT CAG TAA CAC GT		302
A571F	GCY TAA AGS RIC CGT AGC	Archaeal 168 rRNA	14
915R	GTG CTC CCC CGC CAA TTC CT		54
alkB H1F	CIG IIC ACG AII TIG GIC ACA AGA AGG		45
alkB H3R	IGC ITG ITG ITG ATC III GTG ICG CTG IAG	All	45
alkBFd	AAC TAC MTC GAR CAY TAC GG	Alkane monooxygenase	220
alkBRd	TGA MGA TGT GGT YRC TGT TCC		220
P450fw1	GTS GGC GGC AAC GAC ACS AC	Cytochrome P450	285
P450rv3	GCA SCG GTG GAT GCC GAA GCC RAA	alkane hydroxylase	285
ndoB F	CAC TCA TGA TAG CCT GAT TCC TGC CCC CGG CG	Naphthalene diooxygenase	305
ndoB R	CCG TCC CAC AAC ACA CCC ATG CCG CTG CCG	(γ-Proteobacteria)	305
nidA F	TTC CCG AGT ACG AGG GAT AC	(Musehastaria)	56
nidA R	TCA CGT TGA TGA ACG ACA AA	(Mycobacteria)	56
nagAc-like-F	GGC TGT TTT GAT GCA GA	(β-Proteobacteria)	62
nagAc-like-R	GGG CCT ACA AGT TCC A	(р-гтонеовисиети)	62
xylE F	GTG CAG CTG CGT GTA CTG GAC ATG AGC AAG	Control Page 1	305
xylE R	GCC CAG CTG GTC GGT GGT CCA GGT CAC CGG	Catechol-2,3-diooxygenase	305
phnAc F	ACA AAA TTC TCT GAC GGC GC	Phenanthrene diooxygenase	149
phnAc R	CAA TTA CGG TGA TTT CGT GAC C	(Burkholderia)	149
nifH(forA)	GCI WTI TAY GGN AAR GGN GG		308
nifH(forB)	GGI TGT GAY CCN AAV GCN GA	Dinitrogen reductase	308
nifH(rev)	GCR TAI ABN GCC ATC ATY TC		308
nodCfor540	TGA TYG AYA TGG ART AYT GGC T	Nod factor N-acetylglucos-	237
nodCrev1160	CGY GAC ARC CAR TCG CTR TTG	aminyltransferase	237

Table 2. Oligonucleotide primers utilized in this study.

sequenced. Plasmid copy numbers were determined using calculated molecular weights and optical density readings from a NanoDrop 2000 spectrophotometer (NanoDrop, Wilmington, DE). Triplicate $1x10^7$, $1x10^5$ and $1x10^3$ copy plasmid standard dilutions were aliquoted into corresponding wells. Each reaction well contained 12.5 μ l 2x iQ SYBR-Green Supermix, 0.5 μ l DMSO, 1 μ g/ μ l BSA, 0.2 μ M FWD, 0.2 μ M REV, 5 μ l template DNA and MilliQ water to 25 μ l.

A 181 bp fragment of the bacterial 16S rRNA gene was amplified from hundredfold dilutions of soil DNA using primers 338F and 518R as previously described (207). Fluorescence was measured during a 10 sec 80°C primer dimer removal step at the end of each cycle; a final melt curve from 55°C to 99°C determined whether primer dimers were present. A 345 bp fragment of the archaeal 16S rRNA gene was quantitatively amplified with primers A571F and 915R. Thermocycler conditions included an initial 5 minute denaturation step; 40 cycles of 94°C denaturation for 1 min, minimum ramping speed to 48°C annealing for 30 sec, 72°C elongation for 1 min 30 sec, 80°C primer dimer removal and signal acquisition for 10 sec; a melt curve from 48°C to 99°C. Originally amplified with previously described primers alkBFd and alkBRd (220), the *alkB* gene was quantitatively amplified with primers H1F and H3R to generate a 549 bp product. Thermocycler conditions included an initial 5 minute denaturation step; 40 cycles of 95°C denaturation for 30 sec, annealing at 53°C for 10 sec followed by 55°C for 40 sec, 72°C extension for 40 sec, 80°C primer dimer removal and signal acquisition for 10 sec; a melt curve from 55°C to 99°C.

3.3.3. Denaturing Gradient Gel Electrophoresis of Mesocosm Soils

Approximately 500 ng of bacterial 16S ribosomal rRNA, archaeal 16S rRNA, phnAc or nifH gene PCR products (Section 3.3.1.2.) were loaded onto an 8% polyacrylamide gel with a 35%-65% denaturing gradient as described in the DCode Universal Mutation Detection System manual (Bio-Rad, Hercules, CA). Samples were run for 16 hours at 80 V in 60°C 1x TAE. The gel was stained in 0.6 μg ethidium bromide ml⁻¹ 1xTAE for 30 minutes, destained in 1xTAE for 5 minutes and visualized using the ChemiGenius Bioimaging system (Cambridge, UK). Intense bands were excised and DNA eluted in 50 μl MilliQ water at 4°C overnight. DNA was re-amplified for sequencing using primers without a GC clamp.

3.3.4. Clone Library Construction from Treated Mesocosm Soils

Bacterial clone libraries were constructed from Day 0 and Day 60 (middle layer) soils, and an archaeal clone library from Day 0 soil. Bacterial and archaeal 16S rRNA genes were PCR-amplified (Section 3.3.1.3.) and cloned into the pGEM-T-Easy vector (Promega Corporation, Madison, WI). After transformation into chemically competent

Escherichia coli DH5α using a standard protocol (235), clones were selected by blue/white screening on Luria-Bertani (LB) agar plates containing 150 µg/ml ampicillin (FisherBiotech) and 0.5 mg 5-bromo-4-chloro-3-indolyl-β-D-galactopyranoside (X-gal; FisherBiotech). Plasmid DNA was extracted by boiling lysis (235) and the insert PCR-amplified with pGEM-T Easy-targeted T7 and SP6 primers. Clones containing identical inserts were identified using amplified ribosomal DNA restriction analysis (ARDRA) with RsaI and HhaI as previously described (265) and unique banding patterns sequenced with the primer 27F.

3.3.5. Phylogenetic Analyses of Clone Libraries

Sequences were identified using the classifier from Ribosomal Database Project (RDP) Release 10 (298) and compared to Basic Local Alignment Search Tool - Nucleotide (BLASTN) (10) matches from the NCBI database. Potential chimeras were detected (99.9%) using Mallard version 1.02 (11) and analyzed using Pintail version 1.1 (11). CLUSTALX was used to align clone library sequences and the DNADIST component of PHYLIP program version 3.65 (78) was used to construct distance matrices with the Jukes Cantor correction. The matrices were then input into the DOTUR program (234) for statistical analyses, which included Chao1 (41) and ACE (42) richness estimators, and Shannon (249) and the reciprocal of Simpson (255) species diversity indices. Statistical differences between the bacterial libraries were compared using WEBLIBSHUFF version 0.96 (256) and library coverage (92) was calculated for all libraries. Phylogenetic trees were constructed from CLUSTALW alignments using the program MACVECTOR 7.0. Rooted neighbor-joining best trees were constructed with Jukes Cantor correction and branch reliability determined from bootstrap analysis of 1,000 replicates.

3.4. Isolate Characterization

3.4.1. Bacterial Isolation from Hydrocarbon-Contaminated Soil Enrichment Cultures and Isolate Characterization

Hydrocarbon-degrading microorganisms were enumerated in 50 ml MSM enrichment cultures containing 4.0 g Day 39 treated soil and 800µl arctic diesel (21). Using an Accumet basic AB15 pH meter (Fisher Scientific), MSM + arctic diesel

enrichment cultures were adjusted to pH 3.5 and pH 4.0 with hydrochloric acid (HCl). After shaking at 20-25°C for one week, 1.0 ml culture was transferred to fresh medium and incubated for a second week at 20-25°C; 100 µl or 200 µl aliquots were then spread onto R2A agar plates and incubated at 5°C for 4 weeks. Selected isolates were streaked for pure culture, 15% sterile glycerol stocks were prepared in MSM+YTS (95) and stored at -80°C. SK (Sara Klemm) strains were isolated from the low pH enrichment cultures described above. MD isolates (Michael Dyen) were already available in pure culture (65).

To determine growth characteristics, isolates were cultured for four weeks at 5°C under varying NaCl concentrations, pH values and aerobic/anaerobic conditions; isolates were also cultured at various temperatures. Salt tolerance was determined with R2A agar plates containing 2.5%, 5.0%, 7.5%, 10% or 12.5% NaCl. Prior to autoclaving, pH values for R2A agar were adjusted using HCl or KOH; final pH measurements were determined by melting solidified medium from an unused plate. A washed agarose-R2A medium was used below pH 5.5, where agar solidification begins to cease (121). Anaerobic growth was determined with R2A agar plates incubated in a sealed jar with a BBL GasPak100 pouch. Isolates were grown on R2A agar plates at 5°C, 25°C, 28°C and 37°C for three days or four weeks of incubation. Freezing depressants were added to R2A plates for subzero incubations: -5°C plates were amended with 5% ethylene glycol + 1.35 M NaCl or 5% ethylene glycol + 7% sucrose and -10°C plates amended with 10% ethylene glycol + 10% sucrose or 5% ethylene glycol + 1.35 M NaCl + 7% sucrose. Growth on subzero plates was checked after four weeks, and rechecked after an additional month.

3.4.2. DNA Extraction and PCR Amplification of Isolates

To determine the genetic capacity for hydrocarbon degradation and nitrogen fixation, isolate DNA was extracted using boiling lysis. 16S rDNA, *alkB*, P450, *ndoB*, *nidA*, *nagAc*, *phnAc*, *xylE* and *nifH* genes were then PCR-amplified and sequenced (Sections 3.3.1.3. and 3.3.1.4.). To further characterize the isolates' capacity to fix nitrogen, 641bp region of the nod factor *N*-acetylglucosaminyl-transferase (*nodC*) gene was amplified with primers NodCfor540 and NodCrev1160 using previously described conditions (237).

3.4.3. Pure Culture ¹⁴C-Hydrocarbon Mineralization Assay

MD isolate ¹⁴C-hexadecane microcosms and SK isolate ¹⁴C naphthalene and ¹⁴C-phenanthrene microcosms were set-up and monitored as described previously (Section 3.2.2.), with the following exceptions. Soil was substituted with 20ml MSM + 25 ppm yeast extract broth (YE) inoculated with MD or SK isolates. Subzero microcosms contained MSM + YE media amended with 1.35 M NaCl + 5% ethylene glycol freezing depressants and incubated at -5°C on a shaker. Evolved ¹⁴CO₂ was trapped in a 1 M KOH + 20% ethylene glycol collection solution and measured during biweekly samplings as described previously.

Results and Discussion

Chapter 4: Geochemical Characterization of Hydrocarbon-Contaminated Soils in Mesocosm Tanks during Simulated Seasonal Freezing

4.1. Geochemical Properties of Hydrocarbon-Contaminated Soil from Resolution Island

Geochemical results presented in this section were obtained previously by WonJae Chang (CEAM). Hydrocarbon-contaminated soil from the site contained TPH concentrations ranging from 700 to 2,456 mg kg⁻¹ soil (90). Contamination primarily consisted of F2 (nC10-nC16) and F3 (nC16-nC34) n-alkane fractions, measuring at 800-1400 mg kg⁻¹ soil and 650-840 mg kg⁻¹ soil, respectively (65). The F4 (nC34-nC40) alkane fraction measured at 12-43 mg kg⁻¹ soil and polycyclic aromatic hydrocarbons (PAHs) were less than 0.1 mg kg⁻¹ soil (65). Volatile F1 alkanes (nC6-nC10) were not detected (65).

Typical of nutrient-deficient arctic soils, Resolution Island soil contained minimal amounts of organic matter, with only traces of nitrogen (NO₃⁻, NO₂⁻ and NH₃ not detected) and phosphorus (200-210 mg P kg⁻¹ contaminated soil) (90). Sodium and chloride levels were measured at 125-180 mg Na and 5.1-15 mg Cl kg⁻¹ contaminated soil (90). When compared to optimal soil moisture levels (10-25%), the low level here (10-11% gravimetric water contents in contaminated soil) limits water-soluble nutrient bioavailability (90). Mineral content of contaminated soils included 62% quartz, 14% plagioclase feldspar, 10% potassium feldspar and 3% kaolinite (90). Although the coarse soil texture (24% gravel, 75% sand, 1.6% combined clay and silt) could promote biodegradation due to aeration, it does not buffer the acidic soil (pH4.3) or hinder excess water drainage (65, 90).

4.2. The Effect of Seasonal Freeze-Thaw Fluctuations on Mesocosm Soils and Relevance to On-Site Conditions

Inconsistencies in previous freeze-thaw studies as described by Henry (108) were considered in this research. Soil obtained from Resolution Island in September/October 2005 should contain a microbial community relevant to the simulated seasonal freezing profile, which was constructed using mean daily temperatures found on-site from mid-September to October (68). As in other polar and alpine studies, soil microbes from Resolution Island are adapted to on-site air temperature fluctuations (96, 108, 154, 156) including diurnal freeze-thaw cycles, which are muted in ground soils (108). Meso- and microcosm soils exposed to air temperatures from multiple sides, especially at low quantities, are unrealistically affected by temperature fluctuations (108). Because excessively harsh freeze-thaw cycles not reflective of on-site conditions are harmful to soil microbes (108, 148, 156, 259, 316), diurnal freeze-thaw cycles were not included in this study. Mesocosm tanks also contained significantly larger quantities of soil than in other studies with maximum 5.39 L and 40.0-60.0 g volumes and masses (108). To simulate on-site ground soil conditions more closely, mesocosms here contained approximately 200.0 kg soil, roughly equivalent to 143.00 L soil.

Chapter 5: n-Alkane Biodegradative Activity by Indigenous Bacterial Populations in Hydrocarbon-Contaminated Soils during Simulated Seasonal Freezing

5.1. n-Alkane Biodegradation by the Soil Microbial Community during Simulated Seasonal Freezing

5.1.1. Total Petroleum Hydrocarbon Concentrations

As provided by Dr. WonJae Chang (91), TPH concentrations in treated soil exhibited an 8.5% reduction from approximately 1250 mg kg⁻¹ soil during seasonal freezing from 2.4°C to –4.4°C. This decline was due to a 13.1% reduction from approximately 580 mg kg⁻¹ soil in the F2 fraction (nC10-nC16) (91). As depicted in Appendix A, F2 fraction concentrations decreased significantly from 550 to 480 mg kg⁻¹ soil between -0.3°C and -2.1°C (91). Untreated soils demonstrated negligible reduction levels (91).

5.1.2. ¹⁴C-n-Alkane Mineralization by the Soil Microbial Community

Catabolic gene screening indicated that alkane monooxygenase (*alkB*) and cytochrome P450 alkane hydroxylase genes were present in treated and untreated soils. ¹⁴C-hexadecane (n¹⁴C16) mineralizations measured physiological expression of these genes. As observed in TPH F2 fraction reductions (Section 5.1.1.), treated soils degraded significantly greater amounts of ¹⁴C-hexadecane than untreated soils (2.6±0.1%) during seasonal freezing (Fig. 5.1). Mineralization in initial (2.4°C) samples was negligible (0.8±<0.1%) (Fig. 5.1). ¹⁴C-Hexadecane degradation reached maximum levels (26.0±1.0%) thirty-nine days after soil treatments (-2.1°C), followed by a slight decrease (24.1±0.6%) on Day 60 (-4.4°C) (Fig. 5.1). Day 21 (-0.3°C) samples exhibited mineralization activity one week later than subsequent timepoints and degraded lower quantities (19.1±0.5%) of ¹⁴C-hexadecane (Fig. 5.1).

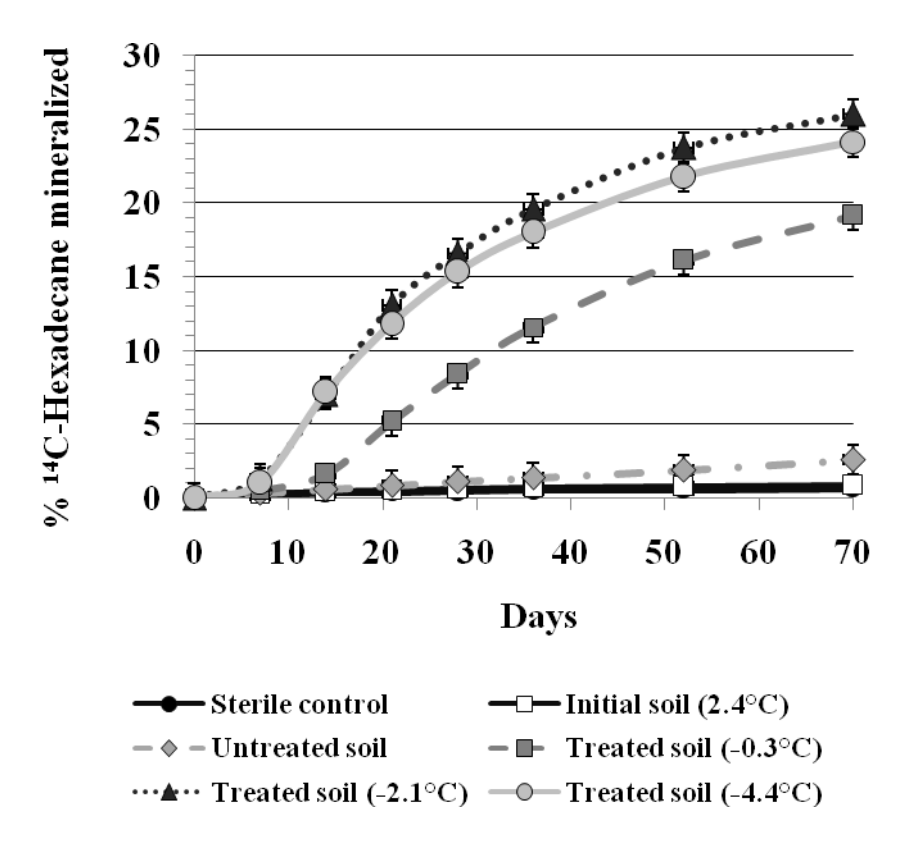


Figure 5.1. ¹⁴C-Hexadecane mineralization of mesocosm soils at 5°C.

Mineralization assay microcosms contained low soil quantities (10.0 g) and were not well-insulated from 5°C incubation temperatures, as described by Henry (108). In addition, aged n-alkane contamination trapped in Resolution Island soil only diffuses out of soil micropores at an extremely slow rate. Because ¹⁴C-hexadecane amendments remain bioavailable to soil microbes, mineralization levels do not accurately measure degradation rates observed in TPH and F2 fraction reductions. Although soil microcosms do not realistically simulate on-site conditions, mineralization results remain valuable as a comparative measurement of microbial biodegradation potential from different soil samples.

5.2. Soil Bacterial Community Populations during Simulated Seasonal Freezing

5.2.1. Heterotrophic and Bacterial 16S rDNA Population Sizes

Culturable heterotrophic populations from treated soils increased during seasonal freezing. Although populations did not increase twenty-one days after initial soil treatments, heterotrophic counts increased nearly one hundredfold from $1.0 \times 10^5 \pm < 0.1$ to $7.9 \times 10^6 \pm 2.9 \times 10^6$ CFU g⁻¹ soil by Day 39 followed by a tenfold decrease to $7.7 \times 10^5 \pm 2.7 \times 10^5$ CFU g⁻¹ soil on Day 60 (Fig. 5.2). Except for a tenfold increase to $9.9 \times 10^5 \pm 2.5 \times 10^5$ on Day 39, untreated soils remained near initial levels ($8.9 \times 10^4 \pm 13.0$ CFU g⁻¹ soil) throughout the freezing phase (Fig. 5.2).

According to calculations from a statistically reliable standard curve (y = -3.45x + 40.198; $R^2 = 0.998$), total bacterial 16S rDNA populations were slightly higher in treated

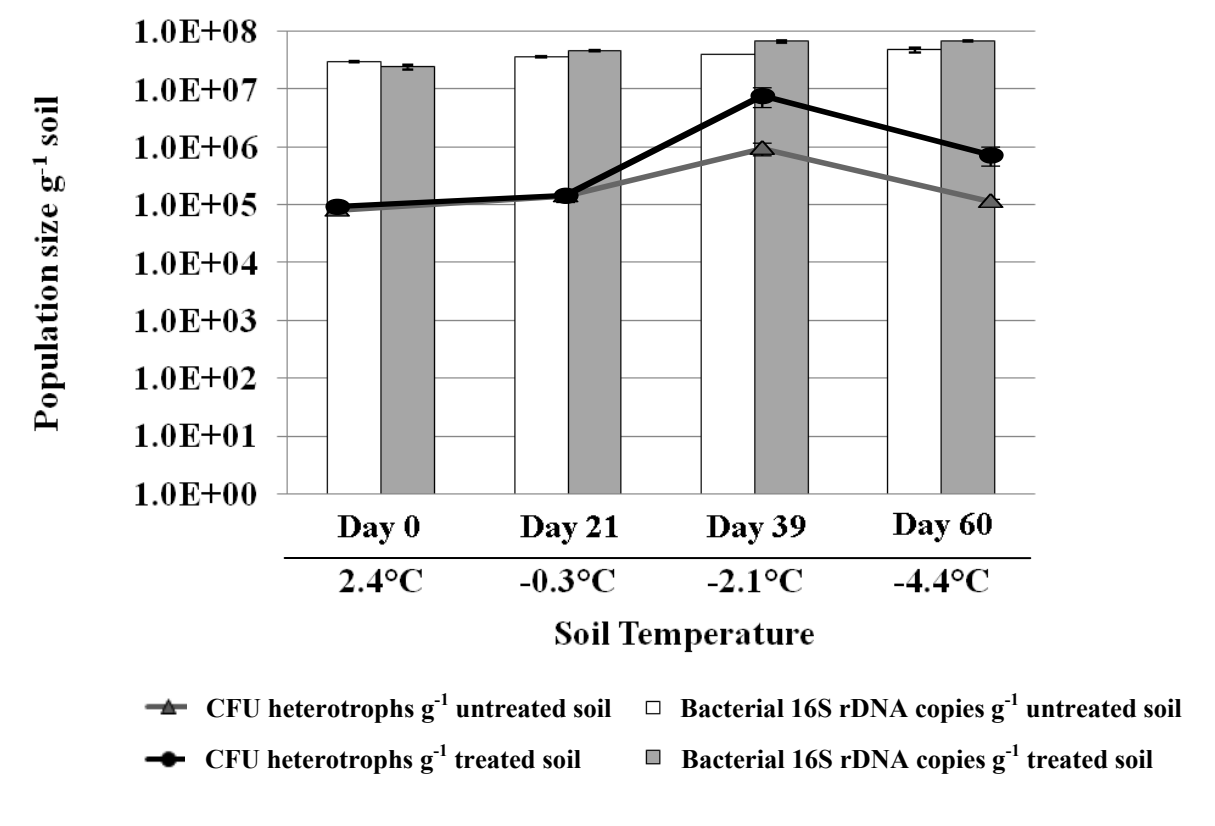


Figure 5.2. Culturable heterotroph and bacterial 16S rDNA population levels during the freezing phase.

than untreated soils (Fig. 5.2). Bacterial populations in treated soil increased from $2.5 \times 10^7 \pm 2.5 \times 10^6$ to $4.5 \times 10^7 \pm 1.1 \times 10^6$ copies 16S rDNA g^{-1} soil twenty-one days after initial soil treatments, increasing further to $6.7 \times 10^7 \pm 2.5 \times 10^6$ copies 16S rDNA g^{-1} soil by Day 39 and remaining steady at $6.8 \times 10^7 \pm 2.7 \times 10^6$ copies 16S rDNA g^{-1} soil though Day 60 (Fig. 5.2). Corresponding populations in untreated soil increased from $3.0 \times 10^7 \pm 9.1 \times 10^5$ to $3.7 \times 10^7 \pm 1.2 \times 10^6$ copies 16S rDNA g^{-1} soil, followed by increases to $4.0 \times 10^7 \pm \text{ND}$ copies 16S rDNA g^{-1} soil and $4.8 \times 10^7 \pm 4.2 \times 10^6$ copies 16S rDNA g^{-1} soil (Fig. 5.2). During the first twenty-one days of soil treatments, culturable heterotrophs comprised approximately 0.1% of total bacterial 16 S rDNA populations in treated and untreated soils. Treated soil proportions increased one hundredfold to 10.0% by Day 39, followed by a tenfold decrease on Day 60. Untreated soil proportions exhibited a tenfold increase to 1.0% on Day 39 and returned to 0.1% by Day 60.

5.2.2. Hydrocarbon-Degrading and alkB Population Sizes

Culturable hydrocarbon degrader levels were similar in freezing phase treated and untreated soils. Hydrocarbon degrader populations exhibited consecutive tenfold increases from $3.3 \times 10^3 \pm < 0.1$ to $2.8 \times 10^4 \pm 1.4 \times 10^3$ CFU g⁻¹ soil by Day 21 and a further increase to $3.1 \times 10^5 \pm 7.4 \times 10^4$ CFU g⁻¹ soil by Day 39, with a final decrease to $1.2 \times 10^4 \pm 3.4 \times 10^3$ CFU g⁻¹ soil on Day 60 (Fig. 5.3). Hydrocarbon degrader populations were ten- to one hundredfold lower than culturable heterotroph counts (Section 5.2.1.).

According to calculations from a statistically reliable standard curve (y = -3.968x + 44.472; $R^2 = 0.998$), n-alkane degrader population levels increased from $2.1x10^4$ $\pm 7.7x10^2$ copies alkB g⁻¹ soil to $5.9x10^4\pm 1.4x10^3$ twenty-one days after initial soil treatments, increasing further to $8.9x10^4\pm 5.9x10^3$ copies alkB g⁻¹ soil by Day 39 and $1.0x10^5\pm 6.8x10^3$ copies alkB g⁻¹ soil by Day 60 (Fig. 5.3). In contrast to hydrocarbon-degradative and heterotrophic counts, alkB copy numbers from treated mesocosm soils were 10^3 to 10^4 times lower than bacterial 16S rDNA populations (Section 5.2.1.). ¹⁴C-Hexadecane mineralization levels (Section 5.1.2.) increased proportionally to n-alkane

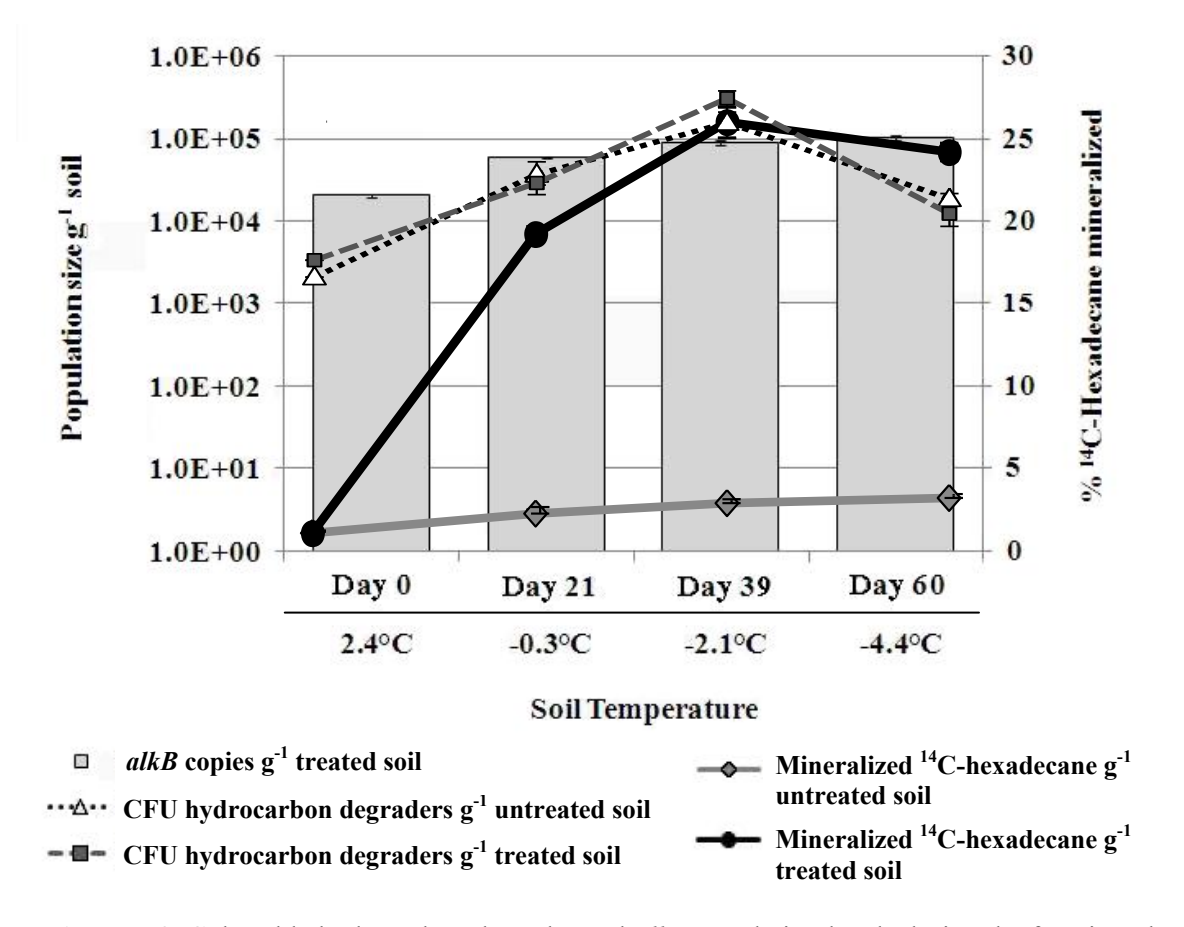


Figure 5.3. Culturable hydrocarbon degrader and *alkB* population levels during the freezing phase compared to ¹⁴C-hexadecane mineralization activity.

degrader populations during the first thirty-nine days of soil treatments, with a contrasting decrease for the remaining twenty-one days. Due to limited reagents, n-alkane degrader population levels were not measured in untreated mesocosm soils.

5.3. Denaturing Gradient Gel Electrophoresis Profiling of the Bacterial Community Structure during Simulated Seasonal Freezing

Bacterial DGGE fingerprints from freezing and thawing phases revealed a shift in community composition in treated soils (Figs. 5.4, 5.5) and a constant community structure in untreated soils (Appxs. B, C). A cold room malfunction resulted in an overnight temperature spike to nearly 25°C immediately after the freezing phase. Consequently, mesocosm soils were incubated at -5°C for an additional two weeks prior to the thawing phase. Since the thawing phase Day 0 banding profile did not match the

freezing phase Day 60 profile, further analysis of thawing phase data was disregarded (Appxs. B, C).

Three *Xanthomonadaceae* bands RDP-classified as *Rhodanobacter* (91-96% confidence level) and two unclassified bacteria bands were present in all treated (Figs. 5.4, 5.5) and untreated (Appxs. B, C) soils. BLASTN matches *Rhodanobacter terrae* strain GP18-1 (301) and *Rhodanobacter spathiphylli* (55) were most closely related to the *Rhodanobacter* bands (99-100% coverage/93-94% identity). Freezing phase DGGE profile patterns revealed two new bands after soil treatments (Fig. 5.4). One *Actinomycetales* band identified as *Corynebacterineae* (91% confidence level), appeared

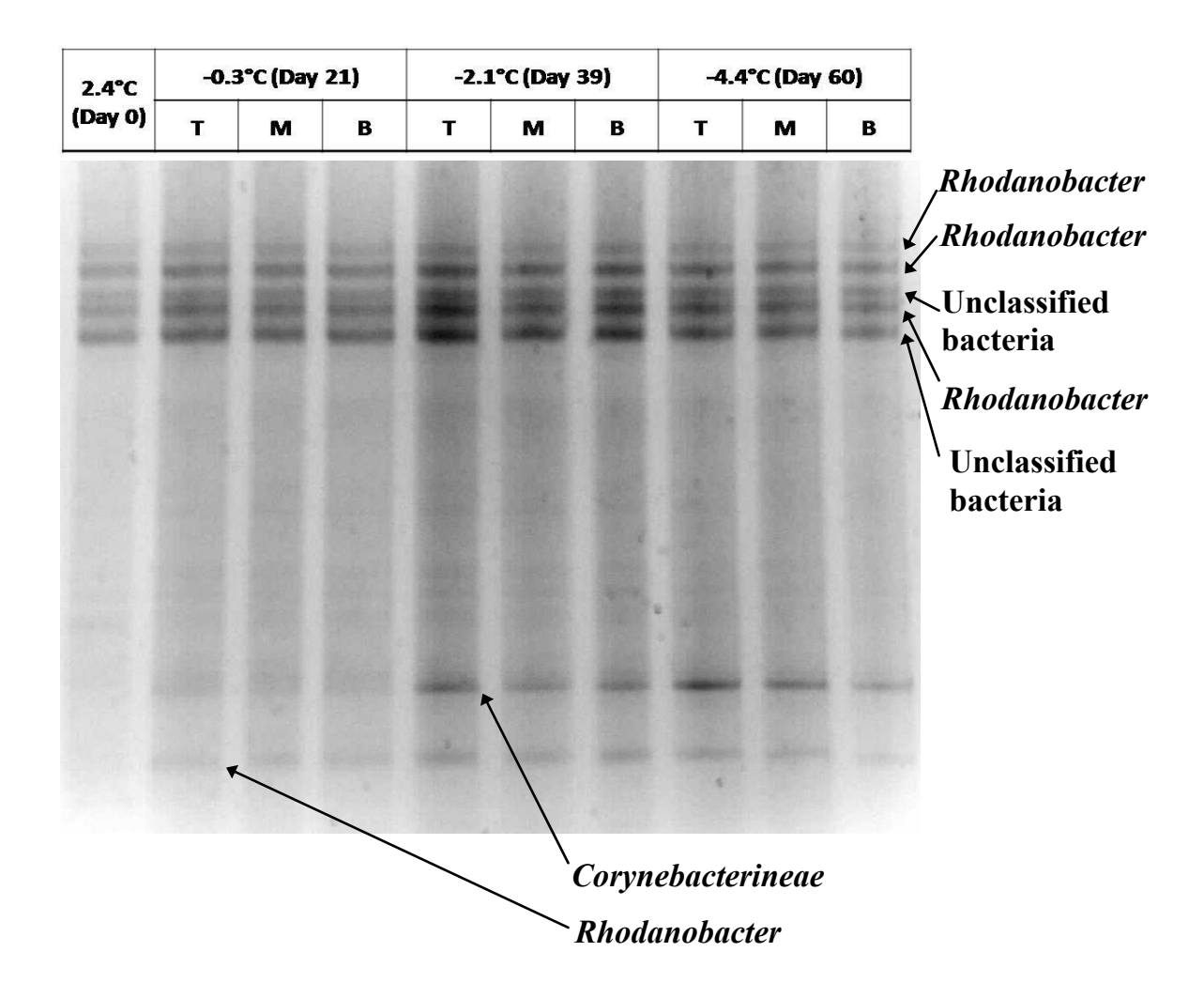


Figure 5.4. Bacterial DGGE of freezing phase treated mesocosm soils.

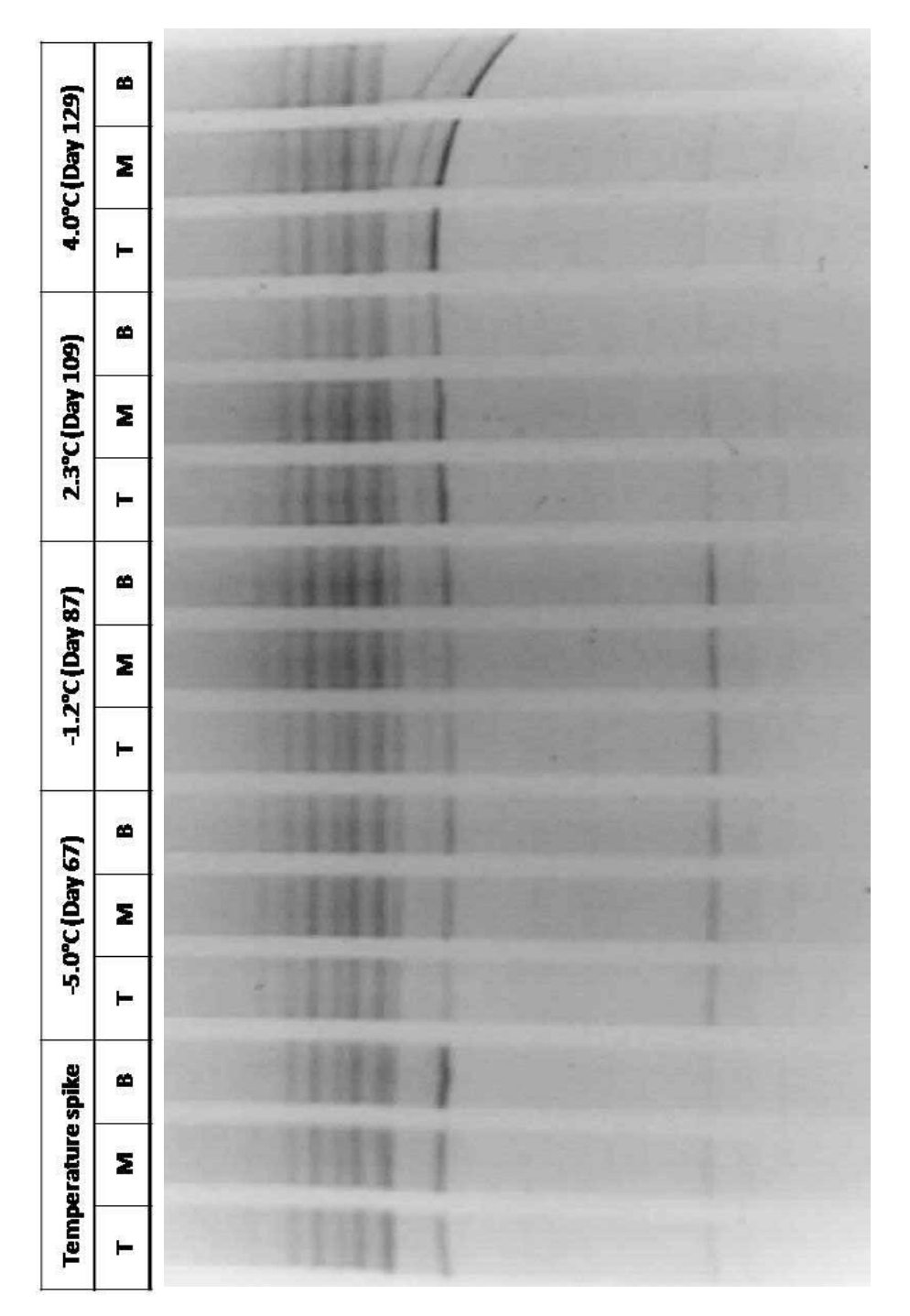


Figure 5.5. Bacterial DGGE of thawing phase treated mesocosm soils.

on Day 39 (-2.1°C) and remained present throughout all subsequent freezing phase soils. Highest scoring BLASTN match *Rhodococcus sp. KAR69* (98% coverage/100% identity), a Norwegian arctic permafrost isolate (101), was RDP-classified as *Corynebacterineae* (87% confidence level). BLASTN matches also included *Rhodococcus*, *Nocardia* and *Tsukamurella* species in the *Corynebacterineae* family (98% coverage/95-96% identity). A second *Xanthomonadaceae* band identified as *Rhodanobacter* (90% confidence level), appeared by Day 21 (-0.3°C) and remained present on Day 60 (-4.4°C). *R. terrae* strain GP18-1 (78% coverage/95% identity) (55) was again retrieved as the highest scoring BLASTN match.

5.4. n-Alkane Biodegradation by Psychrotolerant *Rhodococcus* Isolates from Hydrocarbon-Contaminated Soil

5.4.1. Psychrotolerant Rhodococcus Strain Characterization

Five psychrotolerant *Rhodococcus* strains MD1, MD2, MD3, MD4 and MD9 (RDP classification, 100% confidence level) were isolated from enrichment cultures of hydrocarbon-contaminated Resolution Island soil (65). Highest scoring BLASTN matches with ≥99% identity indicated that MD1 and MD2 were *R. erythropolis* strains (222), MD3 was a *R. fascians* strain (138), and MD4 was a *Rhodococcus* sp. OS-11 strain (176) (Table 3). Strain MD9 was most closely related to BLASTN match *R. erythropolis* at 100% coverage/96% identity (222). As is typical of *Rhodococcus* species (19), these aerobic isolates were Gram-positive, catalase-positive, oxidase-negative cocci. These strains tolerated saline conditions up to 5.0-10.0% (w/v) NaCl and moderately acidic conditions as low as pH 3.2-4.8. Strain MD2 exhibited subzero hydrocarbon degradation after two weeks of growth at -5°C on MSM + arctic diesel. The other strains did not exhibit growth under identical conditions until over one month later. *R. erythropolis* strains produced mucoid colonies with abundant EPS.

	MD1	MD2	MD3	MD4*	MD9
Colony morphology	White,	White/pale pink, mucoid	Yellow,	Pink, smooth	White, mucoid
Cell morphology	Cocci; pairs/tetrads	Cocci; pairs	Cocci; chains	Cocci; pairs/chains	Cocci; clusters
Gram stain	+	+	+	+	+
Catalase	+	+	+	+	+
Oxidase	-	-	-	-	-
Motility	-	-	-	-	-
RDP classification	Rhodococcus	Rhodococcus	Rhodococcus	Rhodococcus	Rhodococcus
Highest scoring	Rhodococcus	Rhodococcus	Rhodococus	Rhodococcus	Rhodococcus
BLAST match;	erythropolis;	erythropolis;	fascians;	sp. OS-11;	erythropolis;
(coverage/identity)	(100%/99%)	(100%/99%)	(100%/99%)	(99%/100%)*	(100%/96%)
alkB	+	+	-	+	+
P450	+	+	+	+	+
ndoB	-	-	-	-	-
nidA	-	-	-	-	-
nagAc	-	-	-	-	-
phnAc	-	-	-	-	-
xylE	-	-	-	-	-
Temperature range**	-5 to 28°C	-5 to 28°C**	-5 to 28°C	-5 to 28°C	-5 to 28°C
pH range	3.2 to 10.1	3.2 to 10.1	4.6 to 10.1	4.8 to 8.6	4.2 to 10.1
NaCl (w/v) tolerance	7.5%	7.5%	10.0%	7.5%	5.0%
O ₂ growth conditions	Aerobic	Aerobic	Aerobic	Aerobic	Aerobic

Table 3. Characterization of psychrotolerant *Rhodococcus* isolates. *The bacterial phylogenetic tree (Fig. 4.7) indicated strain MD4 was most closely related to *Rhodococcus coryne-bacteroides*. **Strain MD2 exhibited growth after two weeks of incubation at –5°C on MSM + arctic diesel, while strains MD1, MD3, MD4 and MD9 exhibited growth over one month later.

5.4.2. ¹⁴C-n-Alkane Mineralization by Psychrotolerant *Rhodococcus* Strains

n-Alkane-degradative *alkB* and P450 genes were detected in *Rhodococcus* strains MD1, MD2, MD9 and MD4, but only P450 was detected in *Rhodococcus* MD3 (Table 3). ¹⁴C-Hexadecane mineralizations were used to confirm physiological expression of these genes. *Rhodococcus* MD1 degraded 41.3±1.7% ¹⁴C-hexadecane after 8 weeks of 5°C incubation, while *Rhodococcus* MD2, MD4 and MD9 mineralized 55.2±1.1%, 50.0±ND% and 18.3±1.8% ¹⁴C-hexadecane, respectively (Fig. 5.6). *Rhodococcus* MD3 did not degrade ¹⁴C-hexadecane (data not shown). These results provided a rationale for *alkB* qPCR design. Since *Rhodococcus* MD4 was the only isolate detected using previously published *alkB* primers (220), degenerate primers targeting a large 549 bp *alkB* region were utilized instead (45).

Rhodococcus strain MD2 degraded $4.6\pm0.1\%^{14}$ C-hexadecane at a linear rate (y = 0.0803x-0.161) after eight weeks of subzero incubation at -5°C (Fig. 5.7). Sterile controls

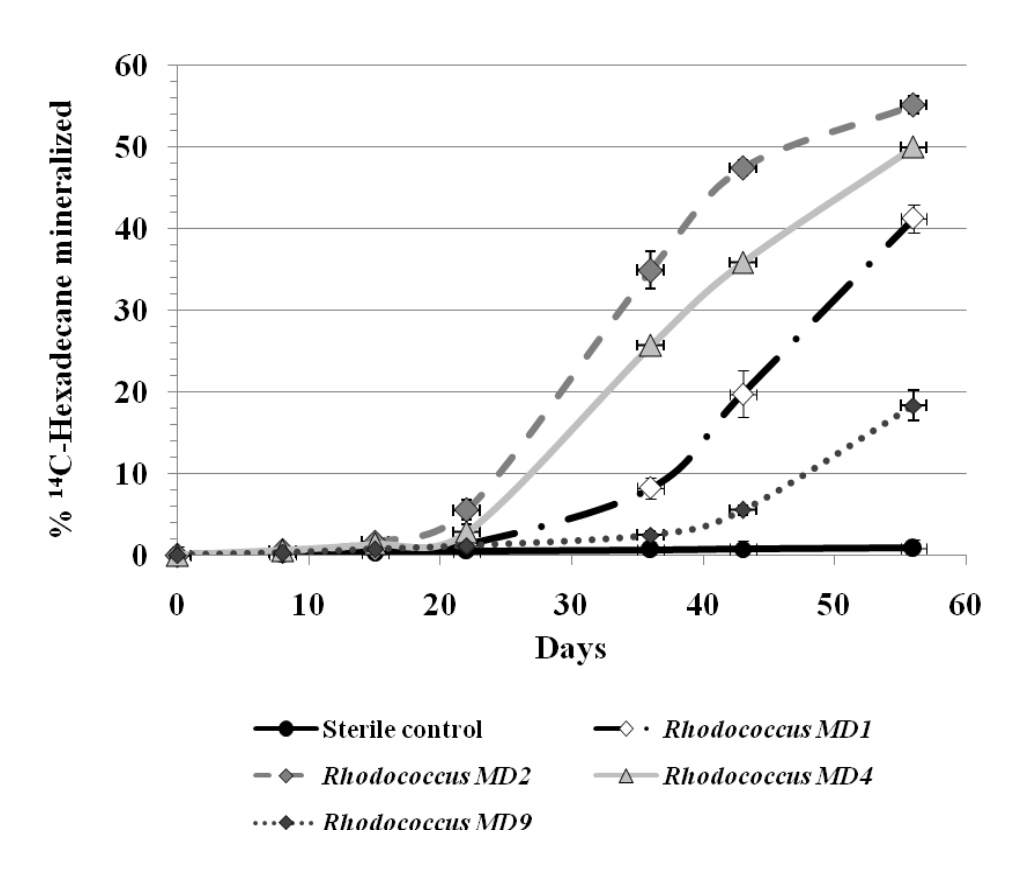


Figure 5.6. ¹⁴C-Hexadecane mineralization of *Rhodococcus* MD strains at 5°C.

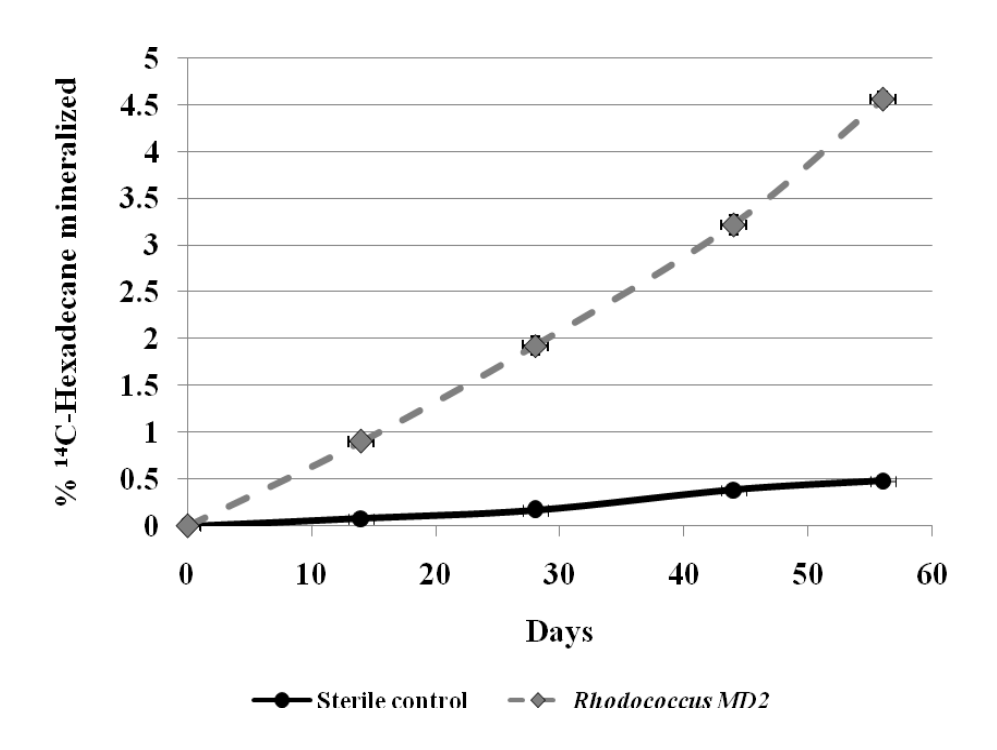


Figure 5.7. Subzero (-5°C) ¹⁴C-hexadecane mineralization of *Rhodococcus* strain MD2.

mineralized 0.5±<0.1% ¹⁴C-hexadecane under identical conditions (Fig. 5.7). These *Rhodococcus* sequences were compared to the *Corynebacterineae* band found in the freezing phase treated soil DGGE (Section 5.3.). Strain MD4 shared a 94% identity to the band sequence, while MD1, MD2, MD3 and MD9 strains shared a 93% identity.

5.5. Shifts in Bacterial Community Composition and Metabolic Activity during Simulated Seasonal Freezing

Nutrient amendments and soil neutralization significantly enhanced the degradation of F2 fraction hydrocarbons in contaminated Resolution Island soil prior to simulated seasonal freezing, which concurred with previous polar and alpine biostimulation studies (5, 23, 24, 50, 51, 59, 72, 125, 168, 169, 171, 175, 182, 183, 208, 233, 236, 263, 273, 304, 305). Bacterial community profile shifts in treated mesocosm soils correlated with significantly higher ¹⁴C-hexadecane mineralization levels, while a constant community structure in untreated soils was associated with minimal biodegradation. Negligible mineralization levels in sterile negative controls confirmed

that ¹⁴C-hexadecane degradation was due to metabolic utilization rather than volatilization.

Two DGGE bands represented species that grew in response to soil treatments and are likely responsible for increased hydrocarbon biodegradation. A *Corynebacterineae* species appeared by Day 21 (-0.3°C), indicating enhanced growth in response to nutrient amendments and pH neutralization. Appearance of a *Rhodanobacter* species by Day 39 (-2.1°C) implied a longer adjustment period and/or initial changes required in the microbial community. Enhanced growth suggested the two species have a selective advantage and are metabolically active at -0.3°C and -2.1°C. Both bands were detected through Day 60 (-4.4°C).

Culturable heterotrophs and bacterial 16S rDNA populations remained near initial levels twenty-one days after soil treatments. Relative proportions indicated no increase in heterotrophic vegetative cell levels. Because F2 and F3 fractions in contaminated Resolution Island soil are the predominant carbon source, culturable hydrocarbon degraders and aliphatic nC5 to nC16 degrading *alkB* populations (281, 284) grew more rapidly in response to a balanced C:N:P ratio and optimized pH. Compared to *alkB* populations, a tenfold increase in culturable hydrocarbon degraders indicated vegetative cell growth in response to more favorable conditions. A one week delay in ¹⁴C-hexadecane mineralization further suggested an acclimation period by previously dormant cells (132). Acclimation was probably slower at lower temperatures due to metabolic processes involved in gene reactivation. Since viable cells were not yet fully functional, TPH and F2 fraction reductions were not observed. The bacterial community in untreated soil did not exhibit increased metabolic activity.

Hundred- and tenfold increases in culturable heterotroph and hydrocarbon-degrader populations eighteen days later indicated metabolic activity at –2.1°C by fully acclimated cells in treated soils. At 10⁶-10⁷ heterotrophic CFU g⁻¹ soil and 10⁵ hydrocarbon degradative CFU g⁻¹ soil, population sizes corresponded to estimates from previous antarctic bioremediation studies (3). Having reached maximum population levels during simulated seasonal freezing, vegetative cells represented approximately 10.0% of bacterial 16S rDNA populations in treated soil and approximately 1.0% in untreated soil. Because increased vegetative populations in untreated soil suggest sample contamination

and/or improper storage, vegetative cell levels in Day 39 treated soil could be excessively high. Culturable hydrocarbon degrader levels in treated and untreated soils were equivalent to *alkB* population sizes, also suggesting that population increases were due to initial tilling. ¹⁴C-Hexadecane mineralization levels and F2 fraction reductions indicated that hydrocarbon-degrading microbes were metabolically active thirty-nine days after soil treatments. When compared to bacterial population sizes, increased hydrocarbon biodegradation was due population growth.

Compared to a slight increase in bacterial 16S rDNA and *alkB* populations, a tenfold decrease in culturable heterotroph and hydrocarbon degradative populations indicated vegetative cell levels had reduced substantially by Day 60. Bacterial genes detected by qPCR and DGGE probably represented dormant microbes. Steady F2 fraction concentrations revealed that metabolic activity ceased by –4.4°C, despite biostimulation treatments and the genetic capacity of the bacterial community. ¹⁴C-Hexadecane mineralization, however, was not delayed and remained closest to Day 39 levels. Since hydrocarbon-degrading soil bacteria retained some metabolic activity and did not require an acclimation period, they were not fully dormant. Overall, application of soil treatments immediately before seasonal freezing will enhance petroleum hydrocarbon biodegradation on the field scale.

A soil isolate *Rhodococcus erythropolis* MD2 mineralized 14 C-hexadecane at -5.0°C, indicating that indigenous soil microbes degrade contaminating F2 fractions at -4.4°C soil temperatures from Day 60. Saline water films capable of supporting metabolic bacterial activity (122) are likely associated with frozen soil aggregates and potentially contain the metabolically active isolate at $\leq 7.5\%$ (w/v) salinity. Since covered mesocosms were stored in a dark cold room, aggregate temperatures remain unaffected by decreased soil albedo (16). Due to low metabolic rates found at cold temperatures (76) and limited hydrocarbon bioavailability in frozen soil, TPH and F2 fraction reductions were not observed below -2.1°C. Compared to other psychrotolerant hydrocarbon degraders which mineralize n-alkanes at temperatures as low as 0°C (306), this thesis is the first report of subzero hydrocarbon degradation.

Chapter 6: Characterization of Bacterial 16S rDNA Community from Treated Mesocosm Soils during Simulated Seasonal Freezing

6.1. Compositional Analyses of Bacterial 16S rDNA Clone Libraries

Two bacterial 16S rDNA clone libraries (70 and 68 total clones) were created from initial Day 0 (2.4°C) and treated Day 60 (-4.4°C) soils, respectively. Phylogeny was determined using RDP classification with an 80% confidence threshold. Total *Acidobacteriaceae* remained at similar levels (slight decrease from 40.0% to 38.2%) despite soil treatments, with genus *Gp1* exhibiting a decrease from 32.9% to 26.5% (Fig. 6.1). By Day 60, total *Xanthomonadaceae* proportions increased substantially from 18.6% to 33.8%; *Rhodanobacter* species increased from 17.1% to 22.1% and unclassified

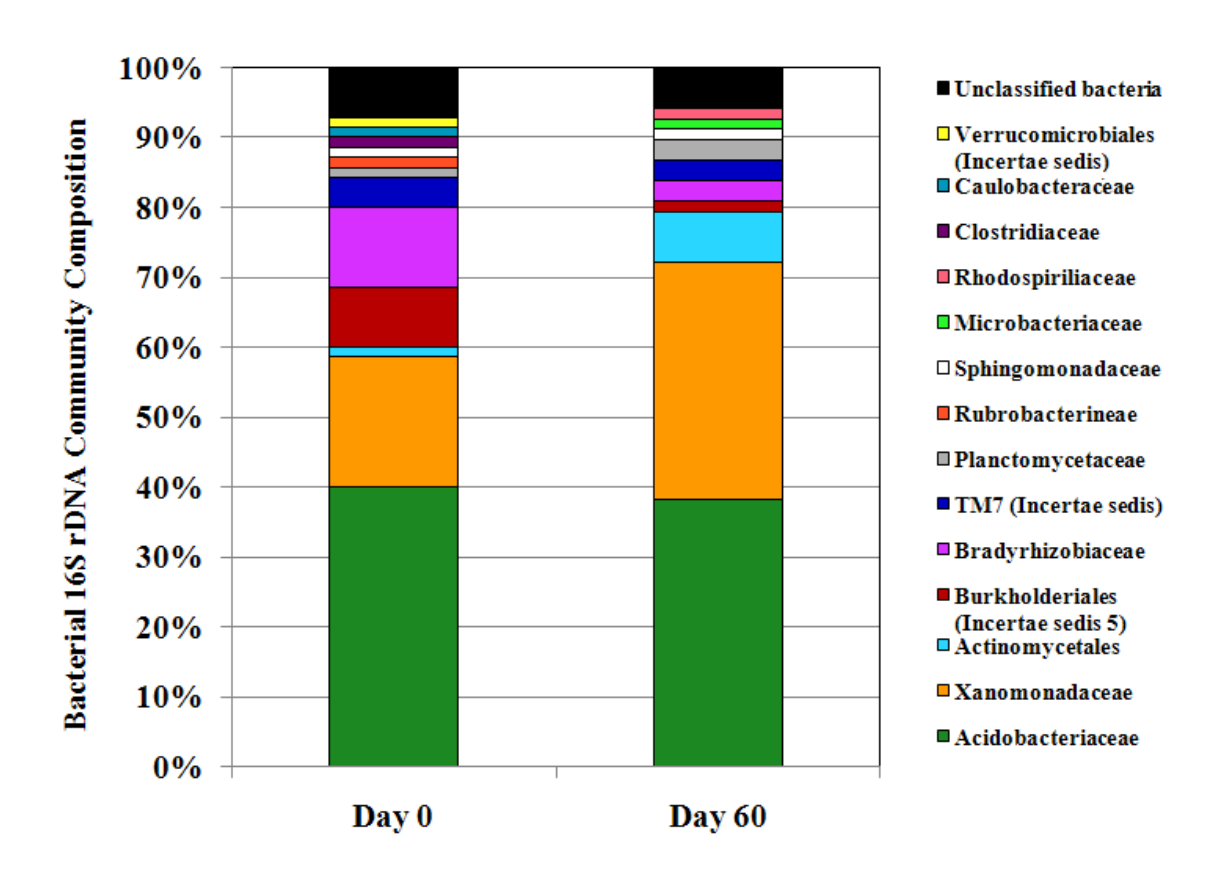


Figure 6.1. Bacterial 16S rDNA clone library compositions from freezing phase treated mesocosm soils.

Xanthomonadaceae increased nearly tenfold from 1.4% to 11.8% (Fig. 6.1). All Xanthomonadaceae clones shared 95-96% identity to Rhodanobacter DGGE band sequences (Section 5.3.). A non-hydrocarbon-degrading Rhodanobacter strain SK35.1 (RDP classification, 83% confidence level) isolated in association with Burkholderia (Section 8.1.) shared 91-92% identity to Rhodanobacter DGGE band sequences (Section 5.3.) and 99% identity to corresponding clone library sequences. Actinomycetales proportions also increased from 1.4% to 7.4% during the freezing phase (Fig. 6.1). Associated clone sequences shared 85-99% identity with the Actinomycetales DGGE band (Section 5.3.) and 88-89% identity to Rhodococcus isolates (Section 5.4.). Burkholderiales and Bradyrhizobiaceae proportions decreased from 8.6% to 1.5% and 11.4% to 2.9%, respectively (Fig. 6.1).

6.2. Phylogenetic Analyses of Bacterial 16S rDNA Clone Libraries

Bacterial 16S rDNA clone libraries were determined to be statistically different (*P*=0.001) using WebLIBSHUFF. As shown in Table 4, species richness estimates halved while Shannon diversity indices remained at consistently high levels, indicating a decrease in low level phylotypes during seasonal freezing. Relative to the number of operational taxonomic units (OTUs) in each library, increased Simpson diversity values revealed a decrease in evenness of the most abundant phylotypes.

	Day 0	Day 60
Clones analyzed	70	67
Operational taxonomic units	42	39
Library coverage (%)	67.74%	73.58%
Chao1 richness estimate	182.25	71.50
ACE richness estimate	248.94	118.00
Shannon's diversity index (H')	3.36	3.38
Simpson's diversity index (1/D)	22.78	27.99

Table 4. Statistical analyses of bacterial 16S rDNA clone libraries. Sequence groupings for operational taxonomic units and statistical analyses based on a 0.02% difference from DOTUR.

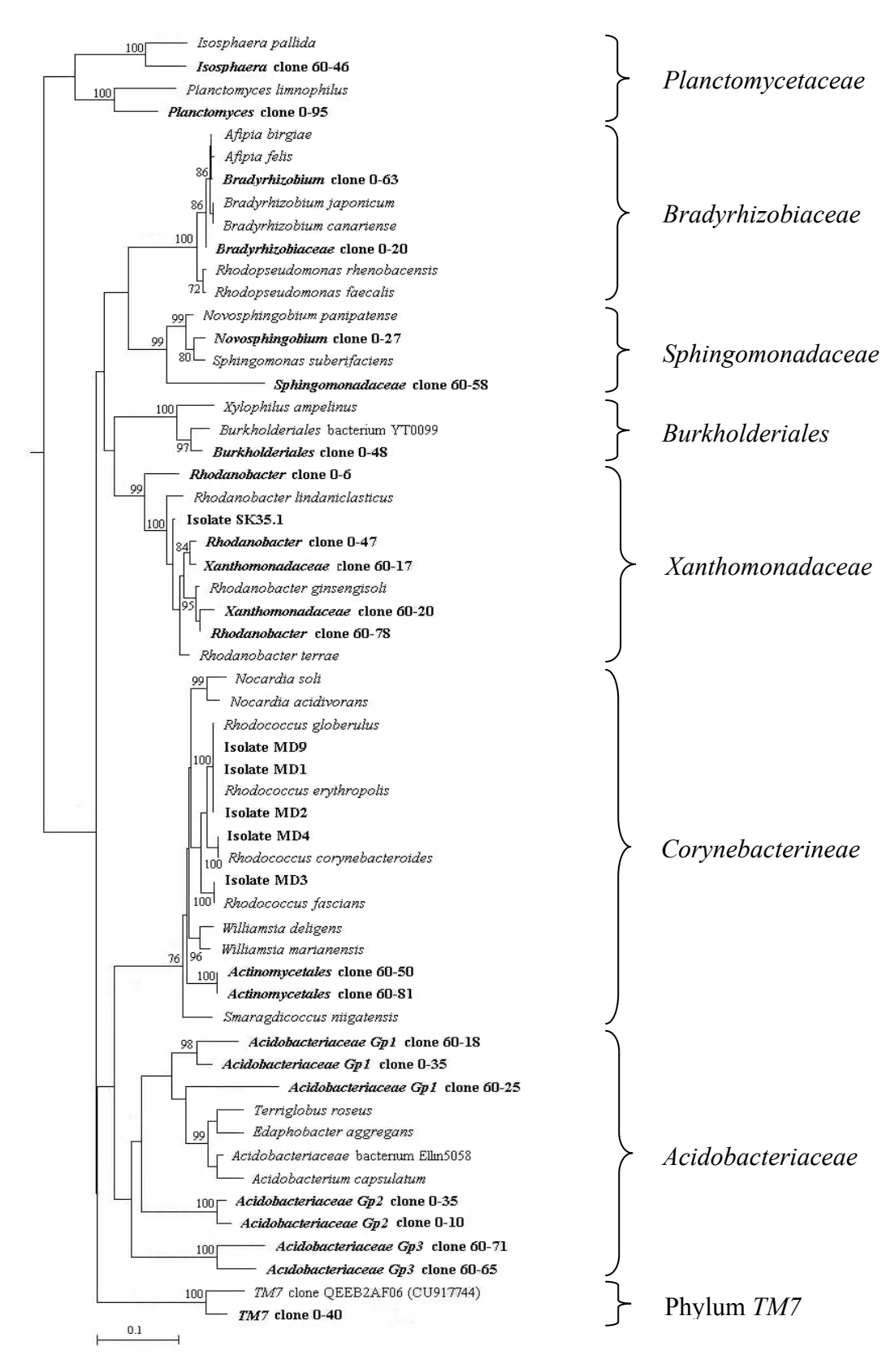


Figure 6.2. Phylogenetic tree of bacterial 16S rDNA clone libraries and isolate sequences (depicted in bold). The tree was rooted using the 16S rDNA sequence from *Acidianus ambivalens*.

As depicted in the bacterial 16S rDNA phylogenetic tree (Fig. 6.2), *Acidobacteriaceae Gp1* clones were more closely related to cultured *Acidobacteriaceae* species than *Gp2* and *Gp3* clones. *Acidobacteriaceae* BLASTN matches were predominated by clone library representatives, including sequences from boreal forest (317) and alpine tundra (196) soils. Both *Rhodanobacter* and unclassified *Xanthomonadaceae* clone sequences clustered with cultured *Rhodanobacter* species (Fig. 6.2). Highest scoring BLASTN matches for both phylotypes included *R. ginsengisoli* GR17-7 (84-98% coverage/98-99% identity) and *R. terrae* strain GP18-1 (98-100% coverage/95-97% identity) (301). *Actinomycetales* clones could not be classified to the genus level. *Rhodococcus* sp. KAR69 (90-94% coverage/94-99% identity) (101) was again retrieved as the highest scoring BLASTN match.

6.3. An Evaluation of the Compositional and Metabolic Responses by the Bacterial Community to Nutrient Availability and Soil pH during Simulated Seasonal Freezing

Increased *Actinomycetales* populations represented in bacterial clone libraries during simulated seasonal freezing corresponded to the appearance of *Corynebacterineae* DGGE bands twenty-one days after soil treatments. *Actinomycetales* sequences exhibited strong homology to an RDP-classified *Corynebacterineae* species from Norwegian permafrost (101), but were phylogenetically distinct from *Rhodococcus* isolates. Such *Actinobacteria* species are frequently found in polar and alpine soils (6, 143, 155, 163, 197) including hydrocarbon-contaminated sites (6, 7, 165). Substantial *Rhodanobacter* populations in both libraries correlated with three bands detected in all mesocosm soils, while increased proportions during simulated seasonal freezing corresponded to the appearance of a *Rhodanobacter* DGGE band thirty-nine days after soil treatments. Such *γ-Proteobacteria* are often predominant in polar and alpine soils (143, 155, 163, 195, 197) with increased populations after hydrocarbon contamination (143, 165). Abundant *Acidobacteriaceae* populations remained at constant levels, possibly corresponding to unclassified bacteria DGGE bands present in all mesocosm soils.

16S rDNA clone libraries used here do not distinguish between vegetative and dormant populations. Consequently, 16S rRNA libraries have been used to determine the

composition of active microbial communities (73, 125, 163). Since exogenous DNA remnants do not adsorb to soil particles more readily than RNA molecules (93), intact microbes are equally represented in both library types. Soil-bound nucleic acids are significantly more resistant to degradation when exposed to acidic conditions below pH5.0 (93, 228). As such, numerous low-level phylotypes found in the Day 0 bacterial clone library are explained by the pH4.3 soil prior to treatments. Nucleic acid degradation is also limited by decreased metabolic activity at low temperatures. The Day 60 clone library, however, was constructed from neutral soil and more accurately represents phylotype distributions in the bacterial community. Large ice crystal formations from gradual freezing (108) could also enhance nucleic acid degradation by disrupting soil aggregates (37, 94). The increased ionic strength (322) found in subzero water films (122), however, promotes nucleic acid-soil adhesion from a more compressed double layer (94, 323).

Total RNA levels are greater in metabolically active vegetative cells than in dormant ones due to gene reactivation (129). Dormant at low nutrient concentrations, r-strategists maximize rRNA transcription and other metabolic processes during periods of high nutrient availability (163). K-strategists maintain consistently low transcription levels despite varying nutrient concentrations (163). Consequently, rRNA clone libraries are biased toward copiotrophic r-strategists and against oligotrophic K-strategists (163). Since rRNA copy numbers are variable and one copy rDNA is present in each cell, rDNA libraries quantify microbial community structure and must be used for comparison when determining microbial activity (72, 125) in a compositional framework (163).

Starvation- and temperature-induced dormancy impact metabolic processes associated with 16S rRNA and ribosomal content differently (129). Because nutrient deficient, acidic Day 0 soils contained an unfavorable C:N:P ratio from hydrocarbon contamination, dormancy was probably induced by rRNA utilization as a nutrient source (61). Accordingly, bacterial clone library phylotypes represented K-strategists and dormant r-strategists not associated with ¹⁴C-hexadecane biodegradation and TPH reductions. Since Day 60 treated soils are not nutrient deficient, the observed shift towards dormancy was caused by inhibited metabolism associated with cold temperatures decreasing beyond -2.1°C (76). The corresponding bacterial clone library contained K-

strategists and semi-vegetative r-strategists associated with enhanced ¹⁴C-hexadecane mineralization and TPH reductions. 16S rRNA levels likely remain consistent at cold temperatures which inhibit starvation-induced ribosome degradation (76). Consequently, microbial activity determined by rRNA clone libraries would be limited and rDNA clone libraries are most relevant here.

Associated with enhanced hydrocarbon biodegradation and increased growth by hydrocarbon degrading populations, *Actinomycetales/Corynebacterineae* populations increased twenty-one days after soil treatments and appeared to be r-strategists responding to favorable growth conditions from a balanced C:N:P ratio and/or soil neutralization. Actinobacteria species from hydrocarbon-contaminated polar and alpine soils, however, have been characterized as oligotrophic K-strategists (7, 19, 165). A biofilter study (124) also demonstrated that oligotrophic Pseudonocardia and Rhodococcus species were thirty-four times more numerous than r-strategists when exposed to toluene vapor. Consequently, *Actinomycetales* detected here potentially represent a psychrotolerant, hydrocarbonoclastic K-strategist (315) that grows optimally at a neutral pH and preferentially metabolizes F2 fractions prevalent in the soil. A preference for other available carbon sources would also be enhanced by nitrogen and phosphorus inputs. Coarse-textured polar soil, however, is characterized by low organic content (3, 5, 270) and utilization of alternative carbon sources are likely to be severely limited. Naturally occurring sources include starch (225), proteins, cellulose and fatty acids from decomposing microbial organic matter (165). No autotrophic Actinomycetales species capable of utilizing atmospheric CO₂ were found. Although lime soil treatments result in greater CO₃ concentrations, heterotrophic microbes are unlikely to metabolize a fully oxidized compound that could function as an anaerobic electron acceptor.

Increased *Xanthomonadcaeae /Rhodanobacter* populations were also associated with enhanced hydrocarbon biodegradation and increased heterotrophic growth thirtynine days after soil treatments. Alpine studies describing copiotrophic *γ-Proteobacteria* in hydrocarbon-contaminated soil (143, 165) established *Rhodanobacter* species here as likely psychrotolerant r-strategists. The late appearance of the *Rhodanobacter* DGGE band suggests utilization of hydrocarbon metabolites (7) from enhanced hydrocarbon-degrader growth. *Rhodanobacter* strain SK35.1 was isolated in association with PAH-

degrading *Burkholderia* strains SK. 35.3 and 4.2, but did not contain any hydrocarbon-degrading genes. This association suggests a symbiotic relationship in which *Rhodanobacter* utilizes metabolic byproducts from PAH degradation. Another study found that concomitant growth of *Rhodanobacter* sp. strain BPC1 within a bacterial consortium was associated with stimulated benzo[a]pyrene mineralization (127). The strain, however, did not grow on benzo[a]pyrene, simple hydrocarbons or diesel fuel in pure culture (127). The authors hypothesized that *Rhodanobacter* sp. strain BPC1 grows on metabolites produced by fellow members and/or contributes to benzo[a]pyrene mineralization by increasing bioavailability of the compound (127).

Substantial *Xanthomonadaceae/Rhodanobacter* and *Acidobacteriaceae* populations in untreated soils were not associated with enhanced hydrocarbon biodegradation. These *Rhodanobacter* species are most likely dormant r-strategists which may or may not have returned to a vegetative state after soil treatments. Inactive cells could have limited access to utilizable carbon sources. Alternatively, sizeable *Rhodanobacter* populations could have been present prior to starvation-induced dormancy. Constant *Acidobacteriaceae* populations correspond to previous studies (81, 143, 155, 163, 197) indicating these microbes are K-strategists. Although prevalent in arctic and acidic soils, of this family is undercharacterized because cultured representatives are extremely limited (81, 163).

Chapter 7: Characterization of a Phylogenetically Novel Archaeal Community from Hydrocarbon-Contaminated Subarctic Soil

7.1. A Metabolic Assessment of the Archaeal Community in Treated Mesocosm Soils during Simulated Seasonal Freezing

qPCR Ct values for archaeal 16S rDNA indicated that Day 0 soil samples contained $4.36 \times 10^6 \pm 9.46 \times 10^5$ copies g⁻¹ soil (y = -3.812x + 42.020 standard curve; R² = 0.999). When compared to initial bacterial 16S rDNA populations (Section 5.2.1.), indigenous soil archaea only comprise 0.16% of non-eukaryotic microbes. The low population size suggests that metabolic activity by the archaeal community is negligible, even in the presence of dormant bacterial populations (Section 5.5.).

The archaeal DGGE community structure remained constant despite soil treatments and was not associated with enhanced hydrocarbon biodegradation during simulated seasonal freezing. Since increased nitrogen levels (e.g., NH₄⁺ and NH₃) from fertilizer treatments did not induce a compositional shift in the archaeal community, these archaea are likely dead, oligotrophic or dormant cells. Dormancy could be due to cold

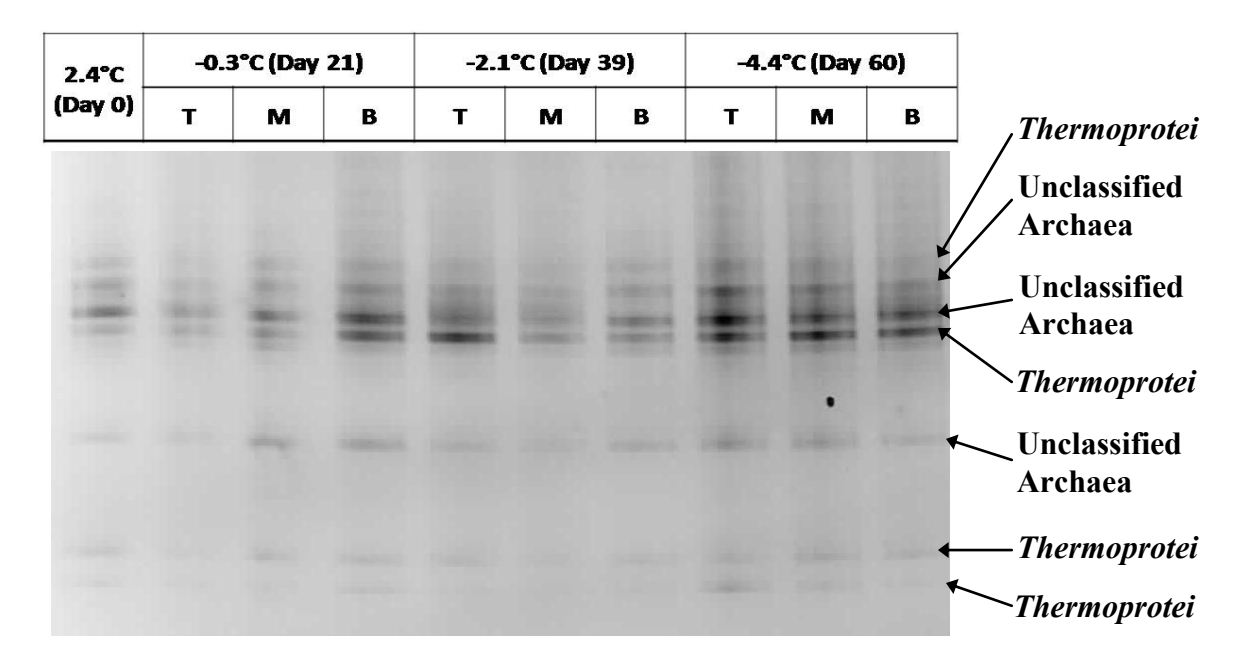


Figure 7.1. Archaeal DGGE of freezing phase treated mesocosm soils.

temperatures, lack of utilizable carbon and/or low soil moisture content. The DGGE banding profile included four *Crenarchaeota* (91-98% confidence level, *Thermoprotei* class) and three unclassified archaea species (Fig. 7.1). Low-scoring BLASTN matches indicated that the DGGE band sequences were not closely related to any cultured archaea.

7.2. Compositional and Phylogenetic Analyses of a Novel Archaeal 16S rDNA Clone Library from Hydrocarbon-Contaminated Subarctic Soil

To further clarify ambiguous phylogenetic relationships, an archaeal 16S rDNA clone library (83 total clones) was constructed from initial treated mesocosm soil (2.4°C) and twelve phylotypes (designated ResIs) were identified using amplified rDNA restriction analysis (ARDRA). These representative clone phylotypes formed two clades which were distinct from *Crenarchaeota*, *Euryarchaeota*, *Nanoarchaeota* and *Korarchaeota* species represented in the archaeal phylogenetic tree (Fig. 7.3). Clade I phylotype clusters were subdivided into Clade Ia, Clade Ib and Clade Ic. Clade II phylotypes constituted one distinct cluster.

ResIs phylotypes constituting Clade Ia were closely related to shale-based soil (100), alpine glacier (196) and boreal peatland (123) clones. Comprising 71.1% of the archaeal community (Fig. 7.2), Clade Ia contained four taxonomic clusters, each with

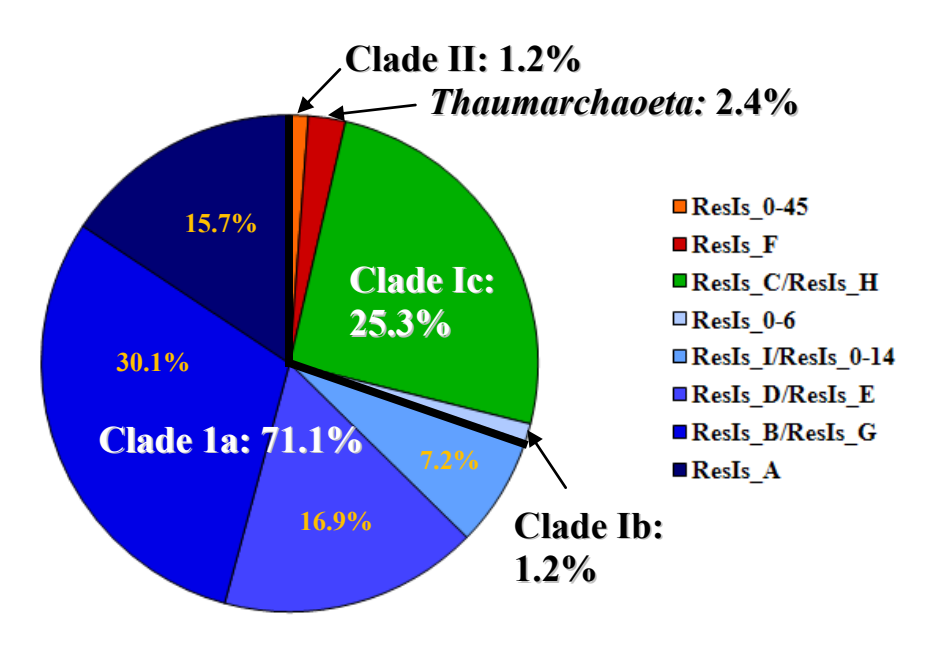


Figure 7.2. Archaeal 16S rDNA clone library composition from Day 0 treated mesocosm soil. ResIs designations refer to sequenced ARDRA banding patterns.

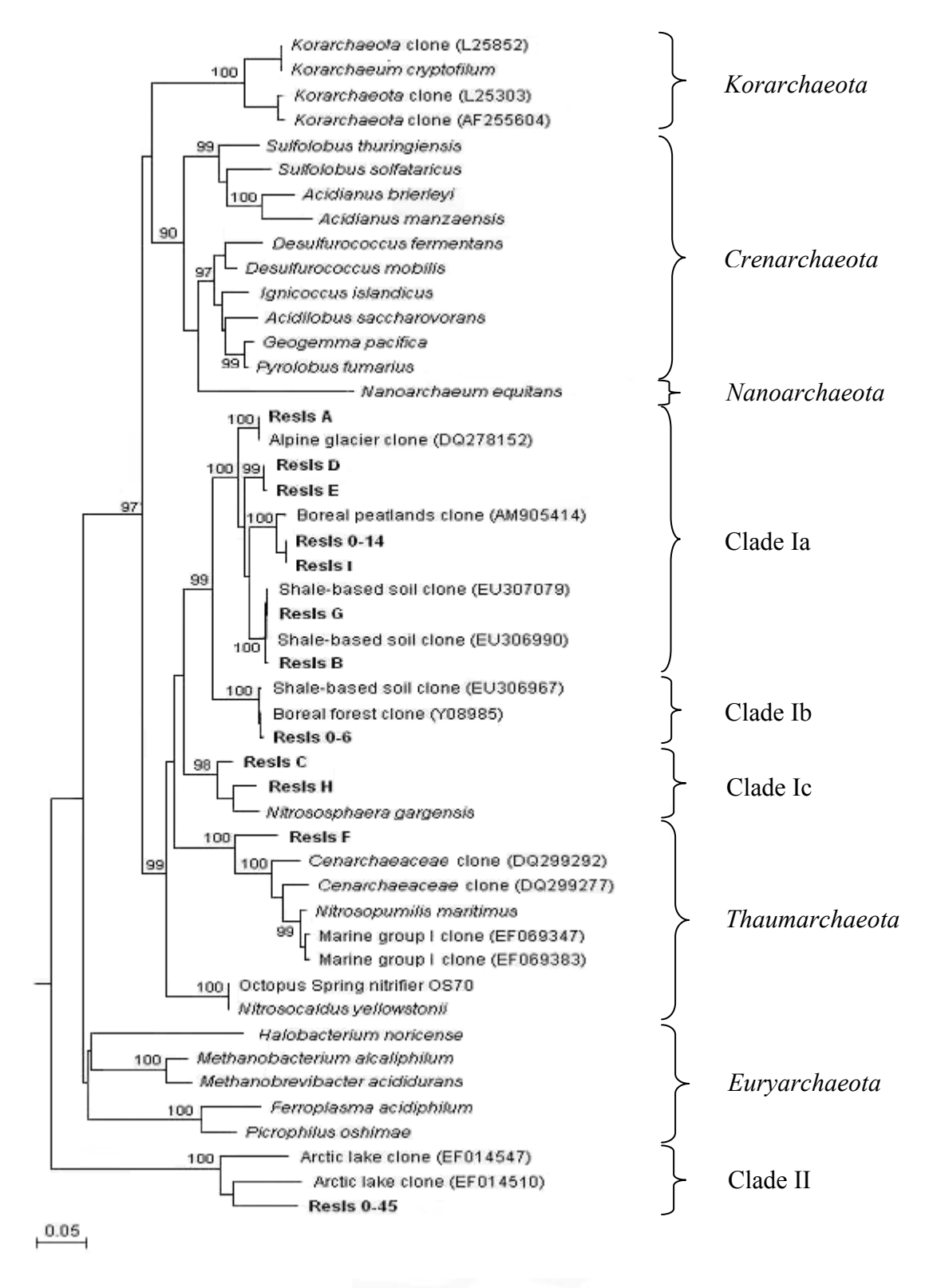


Figure 7.3. Phylogenetic tree of archaeal 16S rDNA clone library sequences (depicted in bold). The tree was rooted using the 16S rDNA sequence from *Pseudomonas putida* GPo1.

96-99% identity and sharing 90-94% identity to one another (Fig. 7.3). Clade Ib included ResIs 0-6, shale-based soil and boreal forest clones, which exhibited 96% identity to each other and shared 89-91% identity to Clade Ia sequences (Fig. 7.3). ResIs phylotypes classified within Clade Ic comprised 25.3% of the archaeal community (7.2) and were related to *Nitrosphaera gargensis* (103). Clade Ic sequences shared 92-95% identity to each other and 86-89% identity to other Clade I sequences (Fig. 7.3). Clone ResIs F was most closely related to *Nitrosopumilus maritimus* (140), marine *Cenarchaeaceae* (117) and marine group I (26) clones (87-88% identity), which constitute a novel phylum *Thaumarchaeota* (28) (Fig. 7.3). These sequences shared 82-85% identity with Clade Ia, 87% identity with Clade Ib and 86-89% identity with Clade Ic.

Distance-based tree structure and sequence alignments indicated that Clade I sequences potentially represented *Thaumarchaeota* species. This novel phylum contains sequences previously classified as *Crenarchaeota* (28). The only cultured representative, *Nitrosopumilus maritimus* is an ammonia-oxidizing nonthermophilic chemolithoautotroph (140). Still considered an unclassified *Crenarchaeote*, *Nitrososphaera gargensis* is a moderately thermophilic ammonia oxidizer more closely related to *Thaumarchaeota* (103). Both species are related to archaeal clones from low temperature marine environments (26, 117) which have also been associated with ammonia oxidation (144, 219, 232, 319). As such, Clade I sequences may be associated with nitrification in oil-based and/or acidic soils from temperate and cold regions.

A distinct cluster with 71-73% identity to all other phylogenetic tree sequences formed Clade II (Fig. 7.3). Clade II sequences included ResIs 0-45 and arctic lake clones (85) which shared 86% identity to one another (Fig 7.3). Sequence alignments of represented *Crenarchaeota* and *Euryarchaeota* species shared 83% and 75% identity, respectively (Fig. 7.3). Sequence alignments yielded approximately 80% identity between the two phyla. Although a sequence-based taxonomic cutoff could not be established, alignments suggest Clade II constitutes a novel phylum. Clade II sequences, in contrast, diverged from the evolutionary root before other phyla began to diverge from one other. Exhibiting low 71-73% identity to all other archaea represented in the phylogenetic tree, Clade II could represent a novel phylum associated with arctic lakes and similar bodies of water.

Chapter 8: Polycyclic Aromatic Hydrocarbon Biodegradative Activity by Diazotrophic Isolates in Relation to Microbial Populations from Hydrocarbon-Contaminated Subarctic Soils

8.1. Subzero Polycyclic Aromatic Hydrocarbon Biodegradation by Diazotrophic *Burkholderia* Isolates from Hydrocarbon-Contaminated Soil

8.1.1. Psychrotolerant Burkholderia Strain Characterization

Two psychrotolerant *Burkholderia* strains SK35.3 and SK4.2 (RDP classification, 100% confidence level) were isolated from low pH enrichment cultures of hydrocarbon-contaminated Resolution Island soil. Highest scoring BLASTN matches indicated that isolate SK4.2 was a *Burkholderia xenovorans* strain (100% coverage/99% identity) (35), while strain SK35.3 was most closely related to *Burkholderia bryophila* at 100% coverage/98% identity (288) (Table 5). As is typical of *Burkholderia* species, these Gramnegative, catalase-positive, oxidase-positive rods were motile diazotrophs. These strains tolerated moderately acidic conditions as low as pH 3.5 and exhibited subzero hydrocarbon degradation after two weeks of growth at -5°C on MSM + arctic diesel.

8.1.2. Subzero ¹⁴C-Naphthalene and ¹⁴C-Phenanthrene Mineralization by *Burkholderia* Strains

Both *Burkholderia* strains contained *phnAc* genes (Table 5) which were most closely related to BLASTN matches *Burkholderia phenazinium* and *Burkholderia glathei nahAc* (100% coverage/99% identity) (300). Strains SK35.3 and SK4.2 degraded $3.7\pm<0.1\%$ and $2.9\pm<0.1\%$ ¹⁴C-naphthalene at linear rates (SK35.3: y=0.06629x+0.156; SK4.2: y=0.05212x+0.06867) after eight weeks of subzero incubation at -5.0°C (Fig. 8.1). Strain SK35.3 also mineralized $3.107\pm0.259\%$ ¹⁴C-phenanthrene at a linear rate (y=0.05726x+0.018) (Fig. 8.2). By comparison, sterile controls only mineralized $0.7\pm<0.1\%$ ¹⁴C-naphthalene (Fig. 8.1) and $0.8\pm0.1\%$ ¹⁴C-phenanthrene (Fig. 8.2).

	Burkholderia bryophila	SK35.3	Burkholderia xenovorans	SK4.2
Cell morphology	Rods	rods	rods	rods
Gram stain	-	-	-	-
Catalase	+	+	+	+
Oxidase	+	+	+	+
Motility	+/-	+	+	+
RDP classification	Burkholderia	Burkholderia	Burkholderia	Burkholderia
Highest scoring BLAST match(es); (coverage/identity)	B. bryophila (100%/100%)	B. bryophila (100%/98%)	B. xenovorans Tco-26 (100%/100%)	B. xenovorans Tco-26 (100%/99%)
nifH	ND	+	+	+
phnAc*	ND	+	ND	+
bph	ND	ND	+	ND
Temperature conditions; (growth range)	mesophilic (ND)	psychrotolerant (-5 to 28°C)	mesophilic (ND)	psychrotolerant (-5 to 28°C)
pH conditions; (growth range)	ND**	acid-tolerant (pH3.5 to 8.2)	neutrophilic (ND)	acid-tolerant (pH3.5 to 8.2)
NaCl (w/v) tolerance	<3.0%	<2.5%	<1.5%	<2.5%
O ₂ requirements	Aerobic	Aerobic	Aerobic	Aerobic

Table 5. Characterization of psychrotolerant *Burkholderia* isolates. *BLASTN search retrieved *nahAc* matches. ** Isolated from acidic sphagnum bogs, but cultured at pH6.8. ND: Not determined

Both *Burkholderia* strains contained *nifH* genes and exhibited growth on nitrogen-deficient MSM agar with arctic diesel as the sole carbon source. According to BLASTN, the *nifH* genes from *Burkholderia xenovorans* strains CAC124 (173) and LB400 (38) (95% coverage/97% identity) were most closely related to the *nifH* gene from *Burkholderia* strain SK4.2. Highest scoring BLASTN hits for *Burkholderia* strain SK35.3 included *nifH* clones from Québec rhizosphere soil (97% coverage/76% identity) (145).

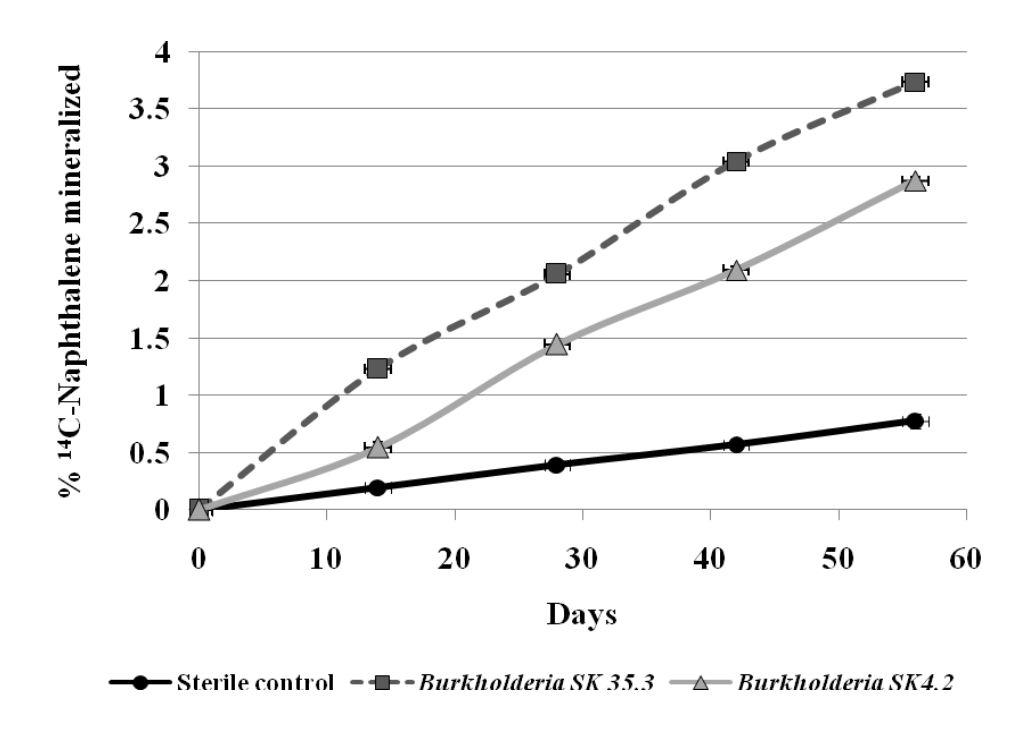


Figure 8.1. Subzero (-5°C) ¹⁴C-naphthalene mineralization of *Burkholderia* strains SK35.3 and SK4.2.

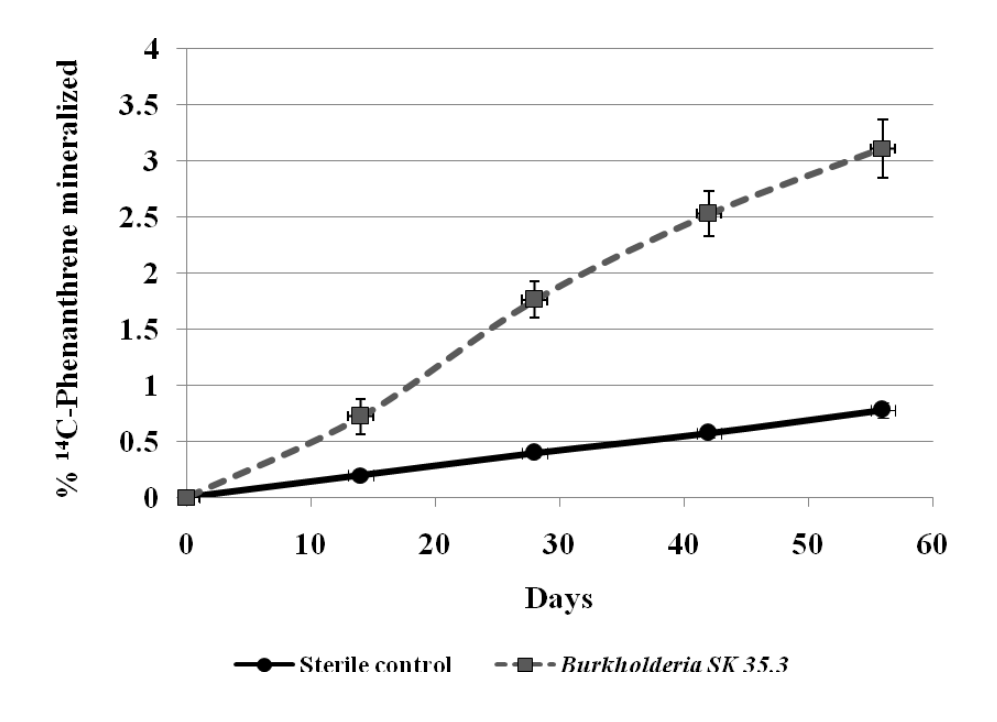


Figure 8.2. Subzero (-5°C) ¹⁴C-phenanthrene mineralization of *Burkholderia* strain SK35.3.

8.2. Polycyclic Aromatic Hydrocarbon Biodegradation by the Soil Microbial Community

8.2.1. Hydrocarbon-Degradative Gene Identification of Contaminated Soil

Catabolic gene screening indicated that *nagAc* and *phnAc* genes were present in all treated and untreated soils; *ndoB* (a *nahAc* homolog), *nidA* and *xylE* were not detected. DGGE fingerprinting of treated soil *phnAc* genes revealed a single phylotype throughout the freezing phase (Appx. D). BLASTN hits *Burkholderia glathei* and *Burkholderia phenazinium nahAc* genes (100% coverage/100% identity) matched the phylotype sequence exactly (309). These genes shared 97-98% similarity and retrieved identical matches to *Burkholderia* isolate *phnAc* hits (Section 8.1.).

8.2.2. ¹⁴C- Polycyclic Aromatic Hydrocarbon Mineralization by the Soil Microbial Community

Polycyclic aromatic hydrocarbon (PAH) mineralization activity was measured using soil samples from Day 39. Due to limited substrate availability, soils sampled at

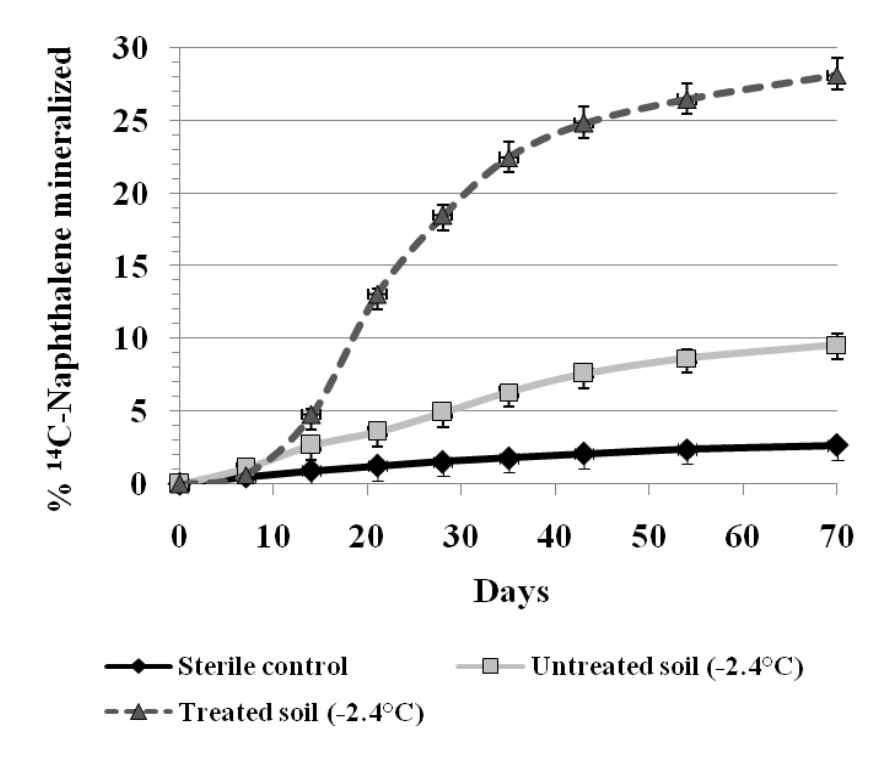


Figure 8.3. ¹⁴C-Naphthalene mineralization of top layer Day 39 mescosm soils at 5°C.

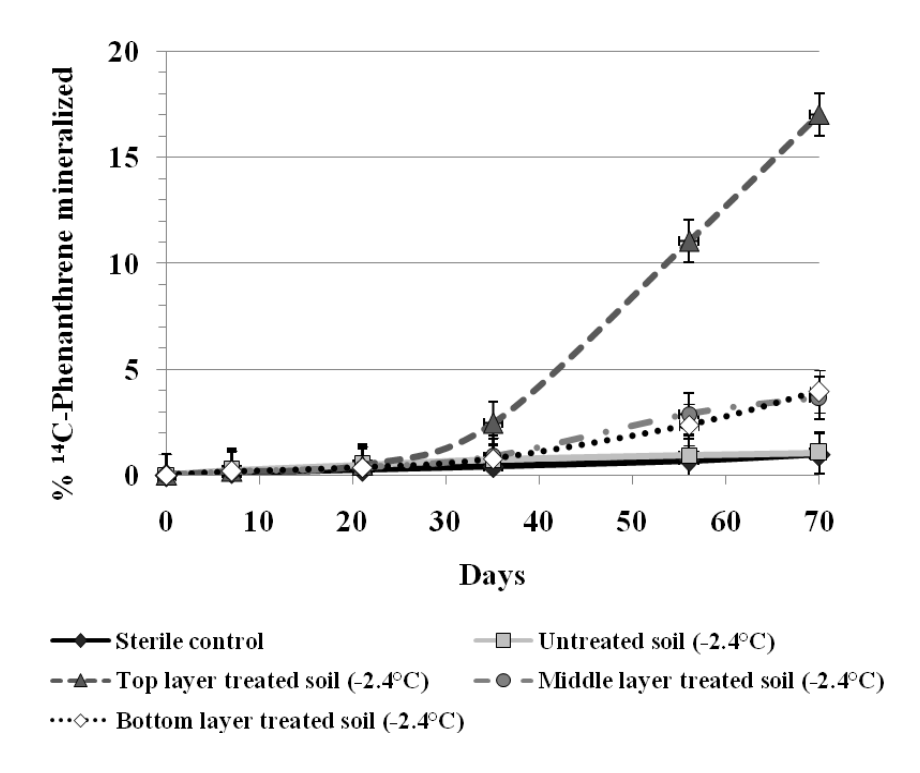


Figure 8.4. ¹⁴C-Phenanthrene mineralization of Day 39 mesocosm soils from at 5°C.

other timepoints were not measured. Treated top layer soils degraded substantially greater levels of ¹⁴C-naphthalene (28.1±1.2%) than corresponding untreated soils (9.6±0.8%); untreated soil ¹⁴C-naphthalene mineralization levels were significantly higher than ¹⁴C-hexadecane levels (Fig. 8.3). Unlike logarithmic ¹⁴C-hexadecane and ¹⁴C-naphthalene rate patterns, ¹⁴C-phenanthrene mineralizations exhibited exponential or linear patterns. Treated soils degraded greater levels of ¹⁴C-phenanthrene than untreated soils (0.3±<0.1%) (Fig. 8.4). Treated soil ¹⁴C-phenanthrene degradation was greatest in the top layer (17.1±1.2%), while middle and bottom layers were lower (3.7±0.6% and 4.0±0.1%, respectively) (Fig. 8.4).

8.3. Diazotrophic Community Structure in Hydrocarbon-Contaminated Soils during Simulated Seasonal Freezing

A DGGE profile of untreated mesocosm soils indicated that the *nifH* community remained constant throughout seasonal freezing (Fig. 8.5). Highest scoring BLASTN *nifH* matches in untreated soil included *Methylocystis rosea* (84% coverage/83% identity)

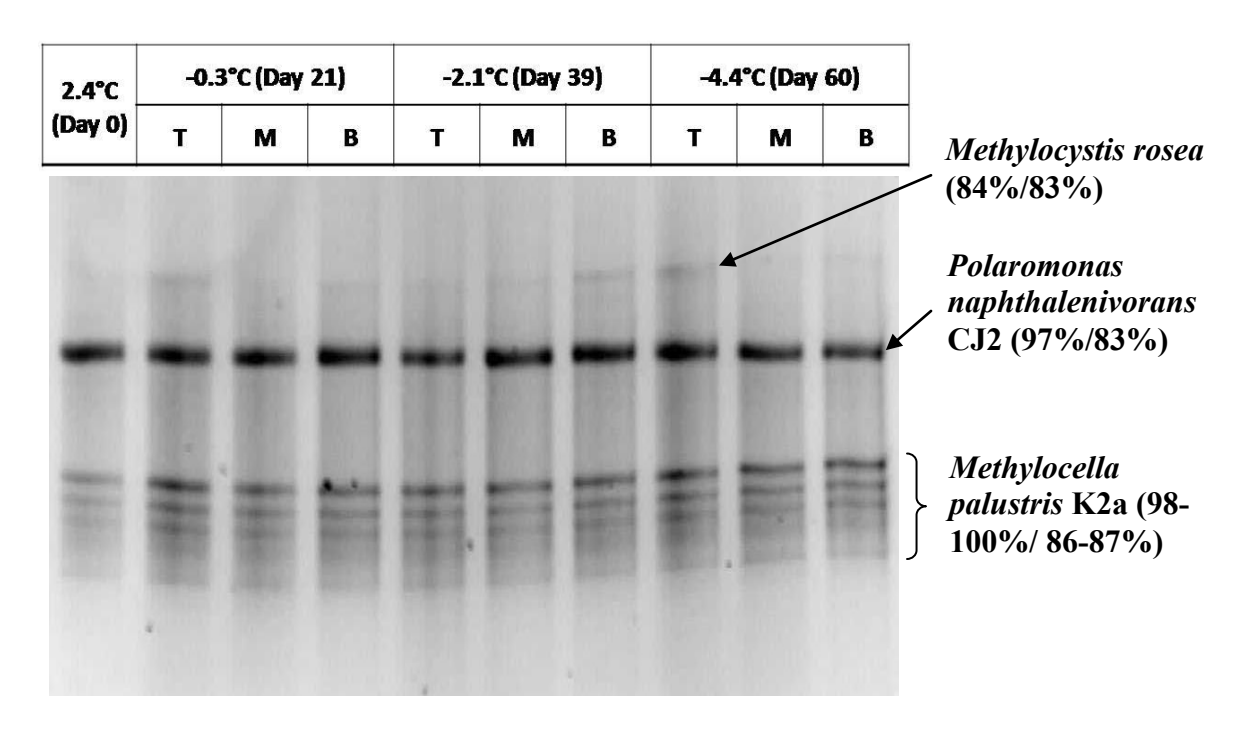


Figure 8.5. *nifH* DGGE of freezing phase untreated mesocosm soils.

(299), *Polaromonas naphthalenivorans* CJ2 (97% coverage/83% identity) (49) and *Methylocella palustris* K2a (98-100% coverage/86-87% identity) (260). The DGGE profile for treated mesocosm soils also remained constant, although the *Methylocystis rosea* homolog was not detected.

8.4. An Evaluation of Polycyclic Aromatic Hydrocarbon Biodegradation by Diazotrophic Burkholderia Strains Indigenous to Hydrocarbon-Contaminated Subarctic Soil

Preliminary genetic results indicated that two psychrotolerant *Burkholderia* strains SK35.3 and SK4.2 were involved in PAH biodegradation and nitrogen fixation. The *phnAc* genes from both strains were most closely related to *nahAc* genes from *Burkholderia phenazinium* and *B. glathei*. The *nifH* genes detected in strains SK35.3 and SK4.2 were homologous to *nifH* sequences from uncultured *Burkholderia* and *B. xenovorans*, respectively. As expected for *Burkholderia* species, *nodC* genes were not present in these free-living diazotrophs.

Both *Burkholderia* strains mineralized ¹⁴C-naphthalene at -5°C, with strain SK35.3 also capable of subzero ¹⁴C-phenanthrene mineralization. Linear biodegradation rates were low, but clearly distinguishable from sterile negative controls. *Rhodococcus* sp. strain Q15 degraded ¹⁴C-hydrocarbons at the lowest reported temperature 0°C (306), while corresponding PAH-degrading isolates remain undercharacterized (170). Although psychrotolerant *Sphingomonas* and *Pseudomonas* isolates mineralized ¹⁴C-naphthalene at 18-22°C (4), arctic and antarctic soils have demonstrated ¹⁴C-naphthalene mineralization at 7°C (73) and 8°C (5), respectively. As such, *Burkholderia* strains SK35.3 and SK4.2 are the first isolates to exhibit PAH biodegradation at subzero temperatures. Together with *Rhodococcus erythropolis* strain MD2, these microbes are also the first to demonstrate subzero hydrocarbon biodegradation. These results suggest a novel coldadapted monooxygenase and/or dioxygenase may be present. Nitrogen fixation will be investigated by Keomany Ker (NRS) using hydrocarbons as a sole carbon source. Compared to antarctic *Pseudomonas* isolates (67), any nitrogen fixation measured at subzero temperatures would also be a novel finding.

The phnAc genes found in treated soil were most closely related to B. phenazinium and B. glathei naphthalene dioxygenase (nahAc) genes. Because isolate and soil phnAc genes retrieved identical matches and shared 97-98% similarity, *Burkholderia* are likely the predominant PAH degraders in Resolution Island soil. ¹⁴C-Naphthalene and ¹⁴Cphenanthrene mineralizations revealed the potential for PAH biodegradation thirty-nine dates after soil treatments. Similar to logarithmic ¹⁴C-hexadecane rates from Day 39 soils, ¹⁴C-naphthalene was readily degraded by vegetative cells present at -2.1°C in treated mesocosm soils, indicating degradative potential by the microbial community. PAH concentrations present in the soil were determined to be negligible (less than 0.1 mg kg⁻¹ soil) (90). ¹⁴C-Naphthalene mineralization levels could have been enhanced by soil microbes containing nagAc genes, which were not detected in the Burkholderia isolates. Linear ¹⁴C-phenanthrene mineralization rates were delayed two weeks in comparison, suggesting low initial levels of phenanthrene degraders, slower mineralization rates due to an additional aromatic ring and/or limited bioavailability. Low PAH concentrations in contaminated Resolution Island soil also suggest the acclimation of dormant phenanthrene degraders to the sudden influx of utilizable carbon at elevated (5°C)

incubation temperatures. Similar to other studies (251, 309), the horizontal transfer of hydrocarbon-degradative genes could have increased the genetic capacity of existing *Burkholderia* populations. As indicated by significantly higher ¹⁴C-phenanthrene degradation levels, the top soil layer provided more favorable O₂ concentrations for an obligate aerobe such as *Burkholderia*.

Although hydrocarbon biodegradation has been associated with increased nitrogen fixation in previous studies (218, 275), *nifH* DGGE profiling indicated that *Burkholderia* were not prevalent in the soil diazotrophic community. Rather, the diazotrophic community included sequences distantly related to methanotrophic and naphthalene-degrading species and did not respond to soil treatments. Microbial nitrogen fixation has been suggested as a nutrient input (218) designed to prevent over-fertilization in coarse-textured soils (23, 79, 293, 295). Because PAHs are not readily available in the contaminated soil, *Burkholderia* strains probably survive in isolated niches proximal to the PAHs, but do not provide sufficient NH₄⁺ soil concentrations to sustain indigenous microbial activity. Although diazotrophs capable of utilizing atmospheric methane as a sole carbon and energy source have a competitive advantage over PAH-degrading strains, significant quantities of NH₄⁺ were not generated. Consequently, soil treatments are required for enhanced ¹⁴C-naphthalene and ¹⁴C-phenanthrene degradation. A *nifH* clone library of top layer untreated soil (-4.4°C) will be completed by Olga Onyshchenko (NRS) to quantify low *Burkholderia* levels in the soil diazotrophic community.

Chapter 9: Summary and Conclusions

Mesocosms containing greater soil quantities were subjected to a gradual freezing profile that realistically simulated ground soil conditions after summer landfarming on Resolution Island. The application of nutrient amendments and the liming of soil mesocosms significantly enhanced biodegradation rates of aliphatic nC10-nC16 hydrocarbon contaminants. Nutrient deficient soil conditions after hydrocarbon contamination probably induced dormancy in indigenous bacteria. Hydrocarbon degrading and heterotrophic populations grew in response to a more balanced C:N:P ratio from soil treatments. Metabolically active hydrocarbon degraders were acclimated by Day 21 at -0.3°C. Viable heterotrophs, however, were not acclimated until Day 39 at -2.1°C. Maximum ¹⁴C-hexadecane degradation rates and TPH F2 fraction reductions associated with population growth were also observed thirty-nine days after soil treatments. Decreasing temperatures began to induce dormancy in bacterial populations by -4.4°C.

A significant increase in *Actinomycetales* and *Rhodanobacter* populations corresponded to enhanced ¹⁴C-hexadecane degradation after soil treatments.

Actinomycetales populations probably represented psychrotolerant hydrocarbonoclastic K-strategists and were associated with increased hydrocarbon degrader growth by -0.3°C.

Rhodococcus erythropolis strain MD2 was related to represented **Actinomycetales** species* and degraded ¹⁴C-hexadecane at -5°C. **Rhodanobacter** populations likely represented psychrotolerant r-strategists that degraded hydrocarbon metabolites and were associated with increased heterotrophic growth at -2.1°C. Non-hydrocarbon-degrading **Rhodanobacter** strain SK35.1 was consistently isolated in association with PAH-degrading **Burkholderia** strains*, suggesting metabolite utilization. Abundant **Acidobacteriaceae** populations in represented K-strategists present treated and untreated soils.

Indigenous archaeal community clones formed two phylogenetically novel clades. Clade I also included alpine glacier, oil-based and/or acidic soil clones, and was most closely related to ammonia-oxidizing species from the recently characterized phylum *Thaumarchaeota*. A likely candidate for a novel phylum, Clade II included arctic lake clones and exhibited 71-73% identity to all other phyla.

Diazotrophic *Burkholderia* strains SK 35.3 and SK4.2 mineralized ¹⁴C-naphthalene and/or ¹⁴C-phenanthrene at -5°C. As such, *Burkholderia* and *Rhodococcus* strains described in this thesis are the first known isolates to degrade hydrocarbons at subzero temperatures. Since low PAH concentrations probably limited population levels in the soil, *Burkholderia* species were not represented in the *nifH* DGGE. Enhanced ¹⁴C-naphthalene and ¹⁴C-phenanthrene degradation after soil treatments indicated that indigenous diazotrophs do not input sufficient NH₄⁺ concentrations to balance the C:N:P ratio.

References

- 1. **Aghajari, N., van Petegem, F., Villeret, V., Chessa, J.-P., Gerday, C., Haser, R., and van Beeumen, J.** 2003. Crystal structures of a psychrophilic metalloprotease reveal new insights into catalysis by cold-adapted proteases. Proteins **50:** 636-647.
- 2. **Aitken, M.D., Stringfellow, W.T., Nagel, R.D., Kazunga, C., and Chen, S.H.** 1998. Characteristics of phenanthrene-degrading bacteria isolated from soils contaminated with polycyclic aromatic hydrocarbons. Can. J. Microbiol. **44(8):** 743-752.
- 3. **Aislabie, J., Balks, M.R., Foght, J.M., and Waterhouse, E.J.** 2004. Hydrocarbon spills on antarctic soils: effects and management. Environ. Sci. Technol. **38(5)**: 1265-1274.
- 4. **Aislabie, J., Foght, J., and Saul, D.** 2000. Aromatic hydrocarbon-degrading bacteria from soil near Scott Base, Antarctica. Polar Biol. **23:** 183-188.
- 5. **Aislabie, J., McLeod, M., and Fraser, R.** 1998. Potential of biodegradation of hydrocarbons in soil from the Ross Dependency, Antarctica. Appl. Microbiol. Biotechnol. **49:** 210-214.
- 6. **Aislabie, J., Ryburn, J., and Sarmah, A.** 2008. Hexadecane mineralization activity in ornithogenic soil from Seabee Hook, Cape Hallett, Antarctica. Polar Biol. **31:** 421-428.
- 7. **Aislabie, J., Saul, D.J., and Foght, J.M.** 2006. Bioremediation of hydrocarbon-contaminated polar soils. Extremophiles **10:** 171-179.
- 8. **Allison, D.G., and Sutherland, I.W.** 1987. The role of exopolysaccharides in adhesion of freshwater bacteria. J. Gen. Microbiol. **133:** 1319-1327.
- 9. **Al-Tahhan, R.A., Sandrin, T.R., Bodour, A.A., and Maier, R.M**. 2000. Rhamnolipid-induced removal of lipopolysaccharide from *Pseudomonas aeruginosa*: effect on cell surface properties and interaction with hydrophobic substrates. Appl. Environ. Microbiol. **66(8):** 3262-3268.
- 10. Altschul, S.F., Gish, W., Miller, W., Myers, E.W., and Lipman, D.J. 1990. Basic local alignment search tool. J. Mol. Biol. 215: 403-410.
- 11. **Ashelford, K.E., Chuzhanova, N.A., Fry, J.C., Jonas, A.J., and Weightman, A.J.** 2005. At least 1 in 20, 16S rRNA sequence records currently held in public repositories is estimated to contain substantial anomalies. Appl. Environ. Microbiol. **71:** 7724-7736.
- 12. **Ashelford, K.E., Chuzhanova, N.A., Fry, J.C., Jonas, A.J., and Weightman, A.J.** 2006. New screening software shows that most recent large 16S rRNA gene clone libraries contain chimeras. Appl. Environ. Microbiol. **72:** 5734-5741.
- 13. **Atlas, R.M.** 1986. Fate of petroleum pollutants in arctic ecosystems. Water Sci. Technol. **18:** 59-67.

- 14. **Baker, G.C., Smith, J.J., and Cowan, D.A**. 2003. Review and re-analysis of domain-specific 16S primers. J. Microbiol. Methods **55(3)**: 541-555.
- 15. **Balashova, N.V., Kosheleva, I.A., Golovchenko, N.P., and Boronin, A.M.** 1999. Phenanthrene metabolism by *Pseudomonas* and *Burkholderia* strains. Process Biochem. **35**: 291-296.
- 16. Balks, M.R., Paetzold, R.F., Kimble, J.M., Aislabie, J., and Campbell, I.B. 2002. Effects of hydrocarbon spills on the temperature and moisture regimes of Cryosols in the Ross Sea region. Antarct. Sci. 14(4): 319-326.
- 17. **Basta, T., Keck, A., Klein, J., and Stolz, A.** 2004. Detection and characterization of conjugative degradative plasmids in xenobiotic-degrading *Sphingomonas* strains. J. Bacteriol. **186(12):** 3862-3872.
- 18. **Bechmann, M.E., Kleinman, P.J.A., Sharpley, A.N., and Saporito, L.S.** 2005. Freeze-thaw effects of phosphorus loss in runoff from manured and catch-cropped soils. J. Environ. Qual. **34:** 2301-2309.
- 19. **Bell, K.S., Philp, J.C., Aw, D.W., and Christofi, N.** 1998. The genus *Rhodococcus*. J. Appl. Microbiol. **85(2)**: 195-210.
- 20. **Bertrand, J.C., Almallah, M., Acquaviva, M., and Mille, G.** 1990. Biodegradation of hydrocarbons by an extremely halophilic archaebacterium. Lett. Appl. Microbiol. **11:** 260-263.
- 21. **Bogan, B.W., Sullivan, W.R., Kayser, K.J., Derr, K., Aldrich, H.C., and Paterek, J.R.** 2003. *Alkanindiges illinoisensis* gen. nov., sp. nov., an obligately hydrocarbonoclastic, aerobic squalene-degrading bacterium isolated from oilfield soils. Int. J. Syst. Evol. Microbiol. **53(Pt 5):** 1389-1395.
- 22. **Bottos, E.M., Vincent, W.F., Greer, C.W., and Whyte, L.G.** 2008. Prokaryotic diversity of arctic ice shelf microbial mats. Environ. Microbiol. **10(4)**: 950-966.
- 23. **Braddock, J.F., Ruth, M.L., Catterall, P.H., Walworth, J.L., and McCarthy, K.A.** 1997. Enhancement and inhibition of microbial activity in hydrocarbon-contaminated arctic soils: implications for nutrient-amended bioremediation. Environ. Sci. Technol. **31:** 2078-2084.
- 24. **Braddock, J.F., Walworth, J.L., and McCarthy, K.A.** 1999. Biodegradation of aliphatic vs. aromatic hydrocarbons in fertilized arctic soils. Bioremediat. J. **3:** 105-116.
- 25. **Brandsdal, B.O., Smalas, A.O., and Aqvist, J.** 2001. Electrostatic effects play a central role in cold adaptation of trypsin. FEBS Lett. **499:** 171-175.
- 26. Brandt, A., Gooday, A.J., Brandão, S.N., Brix, S., Brökeland, W., Cedhagen, T., Choudhury, M., Cornelius, N., Danis, B., De Mesel, I., Diaz, R.J., Gillan, D.C., Ebbe, B., Howe, J.A., Janussen, D., Kaiser, S., Linse, K., Malyutina, M., Pawlowski, J., Raupach, M., and Vanreusel, A. 2007. First insights into the biodiversity and biogeography of the Southern Ocean deep sea. Nat. Lett. 447 (17): 307-311.

- 27. **Brezna, B., Khan, A.A., and Cerniglia, C.E.** 2003. Molecular characterization of dioxygenases from polycyclic aromatic hydrocarbon degrading *Mycobacterium* spp. FEMS Microbiol. Lett. **223(2):** 177-183.
- 28. **Brochier-Armanet, C., Boussau, B., Gribaldo, S., and Forterre, P.** 2008. Mesophilic *Crenarchaeota*: proposal for a third archaeal phylum, the *Thaumarchaeota*. Nat. Rev. Microbiol. **6:** 245-252.
- 29. **Brooks, P.D., and Williams, M.W.** 1999. Snowpack controls on nitrogen cycling and export in seasonally snow-covered catchments. Hydrol. Process. **13:** 2177-2190.
- 30. **Brooks, P.D., Williams, M.W., and Schmidt, S.K.** 1998. Inorganic nitrogen and microbial biomass dynamics before and during spring snowmelt. Biogeochemistry. **43:** 1-15.
- 31. **Bryant, F.O.** 1990. Improved method for the isolation of biosurfactant glycolipids from *Rhodococcus* sp. strain H13A. Appl. Environ. Microbiol. **56(5)**: 1494-1496.
- 32. **Bubier, J., Crill, P., and Mosedale, A.** 2002. Net ecosystem CO₂ exchange measured by autochambers during the snow-covered season at a temperate peatland. Hydrol. Process. **16**: 3667-3682.
- 33. **Bürgmann, H., Widmer, F., Sigler, W.V., and Zeyer, J.** 2004. New molecular screening tools for analysis of free-living diazotrophs in soil. Appl. Environ. Microbiol. **70(1):** 240-247.
- 34. **Busscher, H.J., Poortinga, A.T., and Bos, R.** 1998. Lateral and perpendicular interaction forces involved in mobile and immobile adhesion of microorganisms on model solid surfaces. Curr. Microbiol. **37:** 319-323.
- 35. Caballero-Mellado, J., Onofre-Lemus, J., Estrada-de Los Santos, P., and Martínez-Aguilar, L. 2007. The tomato rhizosphere, an environment rich in nitrogen-fixing *Burkholderia* species with capabilities of interest for agriculture and bioremediation. Appl. Environ. Microbiol. **73(16):** 5308-5319.
- 36. Cai, P., Huang, Q.-Y., and Zhang, X.-W. 2006. Interactions of DNA with clay minerals and soil colloidal particles and protection against degradation by DNase. Environ. Sci. Technol. 40: 2971-2976.
- 37. **Cavicchioli, R., Thomas, T., and Curmi, P.M.G.** 2000. Cold stress response in archaea. Extremophiles. **4:** 321-331.
- 38. Chain, P.S., Denef, V.J., Konstantinidis, K.T., Vergez, L.M., Agullo, L., Reves, V.L., Hauser, L., Córdova, M., Gómez, L., Gonzáles, M., Land, M., Lao, V., Larimer, F., LiPuma, J.J., Mahenthiralingam, E., Malfatti, S.A., Marx, C.J., Parnell, J.J., Ramette, A., Richardson, P., Seeger, M., Smith, D., Spilker, T., Sul, W.J., Tsoi, T.V., Ulrich, L.E., Zhulin, I.B., and Tiedje, J.M. 2006. *Burkholderia xenovorans* LB400 harbors a multi-replicon, 9.73Mbp genome shaped for versatility. Proc. Natl. Acad. Sci. U.S.A. 102(42): 15280-15287.
- 39. **Chang, M.K., Voice, T.C., and Criddle, C.S.** 1993. Kinetics of competitive inhibition and cometabolism in the biodegradation of benzene, toluene, and p-xylene by two *Pseudomonas* isolates. Biotechnol. Bioeng. **41:** 1057-1065.

- 40. Chang. W-J., Dyen, M. Spagnuolo, L., Simon, P., Flaherty, H., Whyte, L., Ghoshal, S. 2007. Pilot-scale Landfarming of Petroleum Hydrocarbon-Contaminated Soils from Resolution Island, Nunavut. Proceedings of the 5th Biannual Assessment and Remediation of Contaminated Soils in Arctic and Cold Climates Conference, Edmonton, Alberta, May 6-8, 2007, p. 199-208.
- 41. **Chao, A.** 1987. Estimating the population size for capture-recapture data data with unequal catchability. Biometrics. **43(4):** 783-791.
- 42. Chao, A., Ma, M.-C., and Yang, M.C.K. 1993. Stopping rules and estimation for recapture debugging with unequal failure rates. Biometrika. **80(1)**: 193-201.
- 43. **Chapman, H.D.** 1965. Cation exchange capacity. *In* A. Black (ed.), Methods of Soil Analysis. American Society of Agronomy, Madison, WI, USA.
- 44. **Chen, C.-I., and Taylor, R.T.** 1995. Thermophilic biodegradation of BTEX by two *Thermus* species. Biotechnol. Bioeng. **48(6)**: 614-624.
- 45. Chénier, M.R., Beaumier, D., Roy, R., Driscoll, B.T., Lawrence, J.R., and Greer, C.W. 2003. Impact of seasonal variations and nutrient inputs on nitrogen cycling and degradation of hexadecane by replicated river biofilms. Appl. Environ. Microbiol. 69(9): 5170-5177.
- 46. **Christensen, S., and Christensen, B.T.** 1991. Organic-matter available for denitrification in different soil fractions effect of freeze-thaw cycles and straw disposal. J. Soil Sci. **42**: 637-647.
- 47. Ciapina, E.M., Melo, W.C., Santa Anna, L.M., Santos, A.S., Freire, D.M., and Pereira Junior, N. 2006. Biosurfactant production by *Rhodococcus erythropolis* grown on glycerol as a sole carbon source. Appl. Biochem. Biotechnol. 129-132: 880-886.
- 48. Collins, T., Meuwis, M.A., Gerday, C., and Feller, G. 2003. Activity, stability and flexibility in glycosidases adapted to extreme thermal environments. J. Mol. Biol. 328: 419-428.
- 49. Copeland, A., Lucas, S., Lapidus, A., Barry, K., Detter, J.C., Glavina del Rio, T., Hammon, N., Israni, S., Dalin, E., Tice, H., Pitluck, S., Sims, D.R., Brettin, T., Bruce, D., Han, C., Tapia, R., Brainard, J., Schmutz, J., Larimer, F., Land, M., Hauser, L., Kyrpides, N., Kim, E., Madsen, E.L., and Richardson, P. 2006. Complete sequence of chromosome 1 of *Polaromonas naphthalenivorans* CJ2, Direct Submission. US DOE Joint Genome Institute.
- 50. Coulon, F., Pelletier, E., Gourhant, L., and Delille, D. 2005. Effects of nutrient and temperature on degradation of petroleum hydrocarbons in contaminated sub-antarctic soil. Chemosphere. **58(10)**: 1439-1448.
- 51. Coulon, F., Pelletier, E., St. Louis, R., Gourhant, L., and Delille, D. 2004. Degradation of petroleum hydrocarbons in two sub-antarctic soils: Influence of an oleophilic fertilizer. Environ. Toxicol. Chem. 23: 1893-1901.
- 52. **Cunliffe, M., and Kertesz, M.A.** 2006. The effect of *Sphingobium yanoikuyae* B1 inoculation on bacterial community dynamics and polycyclic aromatic hydrocarbon degradation in aged and freshly PAH-contaminated soils. Environ. Pollut. **144(1):** 228-237.

- 53. **D'Amico, S., Marx, J.C., Gerday, C., and Feller, G.** 2003. Activity-stability relationships in extremophilic enzymes. J. Biol. Chem. **278:** 7891-7896.
- 54. **DasSarma, S., and Fleischmann, E.F.** 1995. Archaea: A Laboratory Manual-Halophiles. Cold Spring Harbor Laboratory Press, Cold Spring Harbor, NY.
- 55. De Clercq, D., Van Trappen, S., Cleenwerck, I., Ceustermans, A., Swings, J., Coosemans, J., and Ryckeboer, J. 2006. *Rhodanobacter spathiphylli* sp. nov., a *Gammaproteobacterium* isolated from the roots of *Spathiphyllum* plants grown in a compost-amended potting mix. Int. J. Syst. Evol. Microbiol. **56(Pt 8):** 1755-1759.
- 56. **Debruyn, J.M., Chewning, C.S., and Sayler, G.S.** 2007. Comparative quantitative prevalence of *Mycobacteria* and functionally abundant *nidA*, *nahAc*, and *nagAc* dioxygenase genes in coal tar-contaminated sediments. Environ. Sci. Technol. **41:** 5426-5432.
- 57. Dedysh, S.N., Berestovskaya, Y.Y., Vasylieva, L.V., Belova, S.E., Khmelenina, V.N., Suzina, N.E., Trotsenko, Y.A., Liesack, W., and Zavarzin, G.A. 2004. *Methylocella tundrae* sp. nov., a novel methanotrophic bacterium from acidic tundra peatlands. Int. J.Syst. Evol. Microbiol. **54(Pt 1):** 151-156.
- 58. Dedysh, S.N., Liesack, W., Khmelenina, V.N., Suzina, N.E., Trotsenko, Y.A., Semrau, J.D., Bares, A.M., Panikov, N.S., and Tiedje, J.M. 2000. *Methylocella palustris* gen. nov., sp. nov., a new methane-oxidizing acidophilic bacterium from peat bogs, representing a novel subtype of serine-pathway methanotrophs. Int. J. Syst. Evol. Microbiol. 50(Pt 3): 955-969.
- 59. **Delille, D., and Coulon, F.** 2008. Comparative mesocosm study of biostimulation efficiency in two different oil-amended sub-antarctic soils. Microb. Ecol. **56(2)**: 243-252.
- 60. **Delille, D., Pelletier, E., Delille, B., and Coulon, F.** 2003. Effects of nutrient enrichments on the bacterial assemblage of Antarctic soils contaminated by diesel or crude oil. Polar Rec. **39:** 1-10.
- 61. **Deutscher, M.P.** 2006. Degradation of RNA in bacteria: comparison of mRNA and stable RNA. Nucleic Acids Res. **34:** 659-666.
- 62. **Dionisi, H.M., Chewning, C.S., Morgan, K.H., Menn, F.-M., Easter, J.P., and Sayler, G.S.** 2004. Abundance of dioxygenase genes similar to *Ralstonia* sp. strain U2 *nagAc* is correlated with naphthalene concentrations in coal tar-contaminated freshwater sediments. Appl. Environ. Microbiol. **70(7):** 3988-3995.
- 63. **Dontsova, K.M., Norton, L.D., Johnston, C.T., and Bigham, J.M**. 2004. Influence of exchangeable cations on water adsorption by soil clays. Soil Sci. Soc. Am. J. **68:** 1218-1227.
- 64. **Dröge, M., Pühler, A., and Selbitschka, W.** 1999. Horizontal gene transfer among bacteria in terrestrial and aquatic habitats as assessed by microcosm and field studies. Biol. Fertil. Soils **29(3)**: 221-245.

- 65. **Dyen, M.R.** 2007. Culture-dependent and -independent microbial analyses of petroleum hydrocarbon contaminated arctic soil in a mesocosm system. M.Sc. thesis. McGill University, Montréal, QC, Canada.
- 66. **Eady, R.** 1981. Current Perspectives in Nitrogen Fixation. Australian Academy of Science, Canberra, Australia.
- 67. Eckford, R., Cook, F.D., Saul, D., Aislabie, J., and Foght, J. 2002. Free-living hetrotrophic nitrogen-fixing bacteria isolated from fuel-contaminated antarctic soils. Appl. Environ. Microbiol. 68(10): 5181-5185.
- 68. **Environment Canada.** 2009, posting date. National Climate and Weather Data Archive. http://www.climate.weatheroffice.ec.gc.ca.
- 69. **Environment Canada.** 2004. Biological test method: Tests for toxicity of contaminated soil to earthworms (*Eisenia andrei*, *Eisenia fetida*, or *Lumbricus terrestris*). *In* Environmental Protection Series. Environment Canada, Fredericton, NB, Canada.
- 70. **Environmental Protection Agency.** 1994. Landfarming. *In* How to Evaluate Alternative Clean-Up Technologies for Underground Storage Tanks: A Guide for Corrective Action Plan Reviewers, EPA510-R-04-002. Environmental Protection Agency, Washington D.C., USA.
- 71. **Erickson, B.D., and Mondello, F.J.** 1992. Nucleotide sequencing and transcriptional mapping of the genes encoding a biphenyl dioxygenase, a multicomponent polychlorinated biophenyl-degrading-enzyme in *Pseudomonas* strain LB400. J.Bacteriol. **174:** 2903-2912.
- 72. **Eriksson, M., Ka, J.O., and Mohn, W.W.** 2001. Effects of low temperature and freeze-thaw cycles on hydrocarbon biodegradation in arctic tundra soil. Appl. Environ. Microbiol. **67(11):** 5107-5112.
- 73. Eriksson, M., Sodersten, E., Yu, Z., Dalhammar, G., and Mohn, W.W. 2003. Degradation of polycyclic aromatic hydrocarbons at low temperature and under aerobic and nitrate-reducing conditions in enrichment cultures from northern soils. Appl. Environ. Microbiol. 69(1): 275-284.
- 74. Fahy, A., Ball, A.S., Lethbridge, G., Timmis, K.N., and McGenity, K.J. 2008. Isolation of alkali-tolerant benzene-degrading bacteria from a contaminated aquifer. Lett. Appl. Microbiol. 47(1): 60-66.
- 75. **Farrar, D.M., and Cooleman, J.D.** 1967. The correlation of surface area with other properties of nineteen British clay soils. Eur. J. Soil Sci. **18(1):** 118-124.
- 76. **Feller, G., and Gerday, C.** 2003. Psychrophilic enzymes: hot topics in cold adaptation. Nat. Rev. Microbiol. **1:** 200-208.
- 77. Feller, G., Lonhienne, T., Deroanne, C., Libioulle, C., van Beeumen, J., and Gerday, C. 1992. Purification, characterization and nucleotide sequence of the thermolabile a-amylase from the antarctic psychrotroph *Alteromonas haloplanctis* A23. J. Biol. Chem. 267(8): 5217-5221.

- 78. **Felsenstein, J.** 2005. PHYLIP (Phylogeny Inference Package), Version 3.65. Department of Genome Sciences, University of Washington, Seattle, WA.
- 79. **Ferguson, S.H., Franzmann, P.D., Revill, A.T., Snape, I., and Rayner, J.L.** 2003. The effects of nitrogen and water on mineralisation of hydrocarbons in diesel-contaminated terrestrial antarctic soils. Cold Reg. Sci. Technol. **37:** 197-212.
- 80. **Fields, P.A., and Somero, G.N.** 1998. Hot spots in cold adaptation: Localized increases in conformational flexibility in lactate dehydrogenase A4 orthologs of antarctic notothenioid fishes. Proc. Natl. Acad. Sci. U.S.A. **95:** 11476-11481.
- 81. **Fierer, N., Bradford, M.A., and Jackson, R.B. 2007**. Toward an ecological classification of soil bacteria. Ecology. **88(6):** 1354-1364.
- 82. **Fitzhugh, R.D., Driscoll, C.T., Groffman, P.M., Tierney, G.L., Fahey, T.J., and Hardy, J.P.** 2001. Effects of soil freezing, disturbance on soil solution nitrogen, phosphorus and carbon chemistry in a northern hardwood ecosystem. Biogeochemistry **56:** 215-238.
- 83. Franklin, F.C., Lehrbach, P.R., Lurz, R., Rueckert, B., Bagdasarian, M., and Timmis, K.N. 1983. Localization and functional analysis of transposon mutations in regulatory genes of the TOL catabolic pathway. J. Bacteriol. **154(2):** 676-685.
- 84. **Fuenmayor, S.L., Wild, M., Boyes, A.L., and Williams, P.A.** 1998. A gene cluster encoding steps in conversion of naphthalene to gentisate in *Pseudomonas* sp. strain U2. J. Bacteriol. **180(9):** 2522-2530.
- 85. Galand, P.E., Lovejoy, C., Pouliot, J., Garneau, M.È., and Vincent, W.F. 2008. Microbial community diversity and heterotrophic production in a coastal arctic ecosystem: a stamukhi lake and its source waters. Limnol. Oceanogr. 53(2): 813-823.
- 86. Ganzert, L., Jurgens, G., Münster, U., and Wagner, D. 2007. Methanogenic communities in permafrost-affected soils of the Laptev Sea coast, Siberian Arctic, characterized by 16S rRNA gene fingerprints. FEMS Microbiol. Ecol. 59(2): 476-488.
- 87. **Gemmell, R.T., and Knowles, C.J.** 2000. Utilisation of aliphatic compounds by acidophilic heterotrophic bacteria: the potential for bioremediation of acidic wastewaters contaminated with toxic organic compounds and heavy metals. FEMS Microbiol. Lett. **192:** 185-190.
- 88. Gerday, C., Aittalab, M., Arpingy, J.L., Baise, E., Chessa, J.-P., Grasoux, G., Petrescu, I., and Feller, G. 1997. Psychrophilic enzymes: a thermodynamic challenge. Biochim. Biophys. Acta 1342: 119-131.
- 89. **Ghoshal, S., and Whyte, L.G.** 2007a. Bioremediation of petroleum hydrocarbon contaminated soils in arctic and subarctic conditions. Grant Proposal. McGill University, Montréal, QC, Canada.
- 90. **Ghoshal, S., and Whyte, L.G**. 2007b. Bioremediation of petroleum hydrocarbon contaminated soils in arctic and subarctic conditions. Annual Report. McGill University, Montréal, QC, Canada.

- 91. **Ghoshal, S., and Whyte, L.G.** 2009. Bioremediation of petroleum hydrocarbon contaminated soils in arctic and subarctic conditions. Annual Report. McGill University, Montréal, QC, Canada.
- 92. **Good, I.J. 1953.** The population frequencies of species and the estimation of population parameters. Biometrika **40**: 237-264.
- 93. **Greaves, M.P., and Wilson, M.J.** 1969. The adsorption of nucleic acids by montmorillonite. Soil Biol. Biochem. **1:** 317-323.
- 94. **Greaves, M.P., and Wilson, M.J.** 1970. The degradation of nucleic acids and montmorillonite nucleic acid complexes by soil microorganisms. Soil Biol. Biochem. **2:** 257-268.
- 95. **Greer, C.W., Masson, L., Comeau, Y., Brousseau, R., and Samson, R.** 1993. Application of molecular biology techniques for isolating and monitoring pollutant-degrading bacteria. Water Poll. Res. J. Can. **28:** 275-287.
- 96. **Grogan, P., Michelsen, A., Ambus, P., and Jonasson, S.** 2004. Freeze-thaw regime effects on carbon and nitrogen dynamics in sub-arctic heath tundra mesocosms. Soil Biol. Biochem. **36:** 641-654.
- 97. **Habe, H., and Omori, T.** 2003. Genetics of polycyclic aromatic hydrocarbon metabolism in diverse aerobic bacteria. Biosci. Biotechnol. Biochem. **67(2):** 225-243.
- 98. **Haemmerli, S.D., Leisola, M.S., Sanglard, D., and Fiechter, A**. 1986. Oxidation of benzo(a)pyrene by extracellular ligninases of *Phanerochaete chrysosporium*. Veratryl alcohol and the stability of ligninase. J. Biol. Chem. **261**: 6900-6903.
- 99. **Hageman, R.V., and Burris, R.H.** 1978. Nitrogenase and nitrogenase reductase associate and dissociate with each catalytic cycle. Proc. Natl. Acad. Sci. U.S.A. **75(6)**: 2699-2702.
- 100. **Hansel, C.M., Fendorf, S.M., Jardine, P.M., and Francis, C.A.** 2008. Changes in bacterial and archaeal community structure and functional diversity along a geochemically variable soil profile. Appl. Environ. Microbiol. 74(5): 1620-1633.
- 101. Hansen, A.A., Herbert, R.A., Mikkelsen, K., Jensen, L.L., Kristoffersen, T., Tiedje, J.M., Lomstain, B.A., and Finster, K.W. 2007. Viability, diversity and composition of the bacterial community in a high arctic permafrost soil from Spitsbergen, Northern Norway. Environ. Microbiol. 9(11): 2870-2884.
- 102. **Harayama, S., and Rekik, M.** 1993. Comparison of the nucleotide sequences of the metacleavage pathway genes of TOL plasmid pWW0 from *Pseudomonas putida* with other meta-cleavage genes suggests that both single and multiple nucleotide substitutions contribute to enzyme evolution. Mol. Gen. Genet. **239(1-2):** 81-89.
- 103. Hatzenpichler, R., Lebedeva, E.V., Spieck, E., Stoecker, K., Richter, A., Daims, H., and Wagner, M. 2008. A moderately thermophilic ammonia-oxidizing crenarchaeote from a hot spring. Proc. Natl. Acad. Sci. U.S.A. 105(6): 2134-2139.
- 104. **Head, I.M., Jones, D.M., and Röling, W.F.M.** 2006. Marine microorganisms make a meal of oil. Nat. Rev. Microbiol. **4:** 173-182.

- 105. **Heid, C.A., Stevens, J., Livak, K.J., and Williams, P.M.** 1996. Real-time quantitative PCR. Genome Res. **6(10)**: 986-994.
- 106. **Heitkamp, M.A., Freeman, J.P., Miller, D.W., and Cerniglia, C.E.** 1988. Pyrene degradation by a *Mycobacterium* sp.: identification of ring oxidation and ring fission products. Appl. Environ. Microbiol. **54:** 2556-2565.
- 107. **Helmke, E., and Weyland, H.** 2004. Psychrophilic versus psychrotolerant occurrence and significance in polar and temperate marine habitats. Cell Mol. Biol. **50(5):** 553-561.
- 108. **Henry, H.A.L.** 2007. Soil freeze-thaw experiments: trends, methodological weaknesses and suggested improvements. Soil Biol. Biochem. **39:** 977-986.
- 109. **Hermansson, M., Kjelleberg, S., Korhonen, T.K., and Stenström, T.-A.** 1982. Hydrophobic and electrostatic characterization of surface structures of bacteria and its relationship to adhesion to an air-water interface. Arch. Microbiol. **131:** 308-312.
- 110. **Herrmann, A., and Witter, E.** 2002. Sources of C and N contributing to the flush in mineralization upon freeze-thaw cycles in soils. Soil Biol. Biochem. **34:** 1495-1505.
- 111. **Hinchee, R.E., Wilson, J.T., and Downey, D.C.** 1995. Intrinsic Bioremediation. Battelle Press, Columbus, OH, USA.
- 112. **Hobbie, S.E., and Chapin, F.S.** 1996. Winter regulation of tundra litter carbon and nitrogen dynamics. Biogeochemistry **35:** 327-338.
- 113. **Hofer, B., Backhaus, S., and Timmis, K.N.** 1994. The biphenyl/polychlorinated biphenyl degradation locus (*bph*) of *Pseudomonas* sp. LB400 encodes four additional metabolic enzymes. Gene **144:** 9-16.
- 114. **Hofer, B., Eltis, L.D., Dowling, D.N., and Timmis, K.N.** 1993. Genetic analysis of a *Pseudomonas* locus encoding a pathway for biphenyl/polychlorinated biphenyl degradation. Gene **130**: 47-55.
- 115. **Høj, L., Olsen, R.A., and Torsvik, V.L.** 2005. Archaeal communities in high arctic wetlands at Spitsbergen, Norway (78 degrees N) as characterized by 16S rRNA gene fingerprinting. FEMS Microbiol. Ecol. **53(1):** 89-101.
- 116. **Høj, L., Olsen, R.A., and Torsvik, V.L.** 2008. Effects of temperature on the diversity of and community structure of known methanogenic groups and other archaea in high arctic peat. ISME J. **2(1)**: 37-48.
- 117. **Holmes, B., and Blanch, H.** 2007. Genus-specific associations of marine sponges with group I crenarchaeotes. Mar.Biol. **150:** 759-772.
- 118. **Huibers, P.D.T., and Katritzky, A.R.** 1998. Correlation of the aqueous solubility of hydrocarbons and halogenated hydrocarbons with molecular structure. J. Chem. Inform. Comput. Sci. **38(2)**: 283-292.
- 119. **Hyman, M.R., Murton, I.B., and Arp, D.J.** 1988. Interaction of ammonia monooxygenase from *Nitrosomonas-Europaea* with alkanes, alkenes, and alkynes. Appl. Environ. Microbiol. **54:** 3187-3190.

- 120. **INAC Contaminated Sites Program.** 2008, posting date. Resolution Island Remediation Project. http://www.ainc-inac.gc.ca/ai/scr/nu/lan/cts/zxca-eng.asp.
- 121. **Johnson, D.B.** 1995. Selective solid media for isolating and enumerating acidophilic bacteria. J. Microbiol. Methods **23**: 205-218.
- 122. **Junge, K., Eiken, H., and Deming, J.W.** 2004. Bacterial activity at -2 to -20 degrees C in Arctic wintertime sea ice. Appl. Environ. Microbiol. **70(1):** 550-557.
- 123. **Juottonen, H., Tuittila, E.S., Juutinen, S., Fritze, H., and Yrjälä, K**. 2008. Seasonality of rDNA- and rRNA-derived archaeal communities and methanogenic potential in a boreal mire. The ISME Journal **2(11)**: 1157-1168.
- 124. **Juteau, P., Larocque, R., Rho, D., and LeDuy, A.** 1999. Analysis of the relative abundance of different types of bacteria capable of toluene degradation in a compost biofilter. Appl. Microbiol. Biotechnol. **52(6):** 863-868.
- 125. **Ka, J.O., Yu, Z., and Mohn, W.W.** 2001. Monitoring the size and metabolic activity of the bacterial community during biostimulation of fuel-contaminated soil using competitive PCR and RT-PCR. Microb. Ecol. **42(3)**: 267-273.
- 126. **Kanabo, I.A.K., and Gilkes, R.J.** 1988. The effect of soil texture on the dissolution of North Carolina phosphate rock. J. Soil Sci. **39:** 191-198.
- 127. **Kanaly, R.A., Harayama, S., and Watanabe, K.** 2002. *Rhodanobacter* sp. strain BPC1 in a benzo[a]pyrene-mineralizing bacterial consortium. Appl. Environ. Microbiol. **68(12):** 5826-5833.
- 128. Kang, H., Hwang, S.Y., Kim, Y.M., Kim, E., Kim, Y.S., Kim, S.K., Kim, S.W., Cerniglia, C.E., Shuttleworth, K.L., and Zylstra, G.J. 2003. Degradation by phenanthrene and naphthalene by a *Burkholderia* species strain. Can. J. Microbiol. 49(2): 139-144.
- 129. **Kaprelyants, A.S., Gottschal, J.C., and Kell, D.B.** 1993. Dormancy in non-sporulating bacteria. FEMS Microbiol. Rev. **10(3-4):** 271-285.
- 130. **Kato, T., Hirota, M., Tang, Y., Cui, X., Li, Y., Zhao, X., and Oikawa, T.** 2005. Strong temperature dependence and no moss photosynthesis in winter CO₂ flux for a *Kobresia* meadow on the Qinghai-Tibetan plateau. Soil Biol. Biochem. **37:** 1966-1969.
- 131. **Keener, W.K., and Arp, D.J.** 1993. Kinetic studies of ammonia monooxygenase inhibition in *Nitrosomonas-Europaea* by hydrocarbons and halogenated hydrocarbons in an optimized whole-cell assay. Appl. Environ. Microbiol. **59:** 2501-2510.
- 132. **Kell, D.B., and Young, M.** 2000. Bacterial dormancy and culturability: the role of autocrine growth factors. Curr. Opin. Microbiol. **3:** 238-243.
- 133. **Kelley, I., Freeman, J.P., Evans, F.E., and Cerniglia, C.E.** 1993. Identification of metabolites from the degradation of fluoranthene by *Mycobacterium* sp. strain PYR-1. Appl. Environ. Microbiol. 59: 800-806.

- 134. **Kemnitz, D., Kolb, S., and Conrad, R**. 2007. High abundance of *Crenarchaeota* in a temperate acidic forest soil. FEMS Microbiol. Ecol. **60:** 442-448.
- 135. Kim, S.-J., Kweon, O., Jones, R.C., Freeman, J.P., Edmonson, R.D., and Cerniglia, C.E. 2007. Complete and integrated pyrene degradation pathway in *Mycobacterium vanbaalenii* PYR-1 based on systems biology. J. Bacteriol. **189(2)**: 464-472.
- 136. Kim, S.Y., Hwang, K.Y., Kim, S.H., Sung, H.C., Han, Y.S., and Cho, Y. 1999. Sequence, biochemical properties, and crystal structure of malate dehydrogenase from a psychrophile *Aquaspirillium arcticum*. J. Biol. Chem. **274**: 11761-11767.
- 137. **Kiyohara, H., Torigoe, S., Kaida, N., Asaki, T., Iida, T., Hayashi, H., and Takizawa, N.** 1994. Cloning and characterization of a chromosomal gene cluster, *pah*, that encodes the upper pathway for phenanthrene and naphthalene utilization by *Pseudomonas putida* OUS82. J. Bacteriol. **176(8):** 2439-2443.
- 138. Klatte, S., Jahnke, K.D., Kroppenstedt, R.M., Rainey, F.A., and Stackebrandt, E. 1994. *Rhodococcus luteus* is a later subjective synonym of *Rhodococcus fascians*. Int. J. Syst. Evol. Microbiol. **44:** 627-630.
- 139. **Kodres, C.A.** 1998. Coupled water and air flows through a bioremediation soil pile. Environ. Model. Softw. **14:** 37-47.
- 140. Könnecke, M., Bernhard, A.E., de la Torre, J., Walker, C.B., Waterbusy, J.B., and Stahl, D.A. 2005. Isolation of an autotrophic ammonia-oxidizing marine archaeon. Nature. 437: 543-546.
- Kulichevskaya, I.S., Milekhina, E.I., Borzenkov, I.A., Zvyagintseva, I.S., and Belyaev,
 S.S. 1992. Oxidation of petroleum hydrocarbons by extremely halophilic archaebacteria.
 Microbiology 60: 596-601.
- 142. **Kuzenetsov, V.D., Zaitseva, T.A., Vakulenko, L.V., and Filippova, S.N**. 1992. *Streptomyces albaxialis* sp. nov.: a new petroleum hydrocarbon-degrading species of thermo- and halotolerant *Streptomyces*. Microbiology **61:** 62-67.
- 143. Labbé, D., Margesin, R., Schinner, F., Whyte, L.G., and Greer, C.W. 2007. Comparative phylogenetic analysis of microbial communities in pristine and hydrocarbon-contaminated alpine soils. FEMS Microbiol. Ecol. **59:** 466-475.
- 144. Lam, P., Jensen, M.M., Lavik, G., McGinnis, D.F., Müller, B., Schubert, C.J., Amann, R., Thamdrup, B., and Kuypers, M.M. 2007. Linking crenarchaeal and bacterial nitrification to anammox in the Black Sea. Proc. Natl. Acad. Sci. U.S.A. 104(17): 7104-7109
- 145. Lamarche, J., Bradley, R.L., Hooper, E., Shipley, B., Simao Beaunoir, A.M., and Beaulieu, C. 2007. Forest floor bacterial community composition and catabolic profiles in relation to landscape features in Quebec's southern boreal forest. Microb. Ecol. 54(1): 10-20
- 146. **Lane, D.J.** 1991. 16S/23S rRNA sequencing, pp. 115-176. *In* E. Stackebrandt, and M. Goodfellow (ed.), Nucleic Acid Techniques in Bacterial Systematics. John Wiley & Sons, Chichester, United Kingdom

- 147. **Lang, S., and Wagner, F.** 1987. Structure and properties of biosurfactants, pp. 21-45. *In* N. Kosaric, W.L. Cairns, and N.C.C. Gray (ed.), Biosurfactants and Biotechnology. Marcel Dekker, New York, NY, USA.
- 148. Larsen, K.S., Jonasson, S., and Michelsen, A. 2002. Repeated freeze-thaw cycles and their effects on biological processes in two arctic ecosystem types. Appl. Soil Ecol. 21: 187-195.
- 149. **Laurie, A.D., and Lloyd-Jones, G.** 1999. The *phn* genes of *Burkholderia* sp. strain RP007 constitute a divergent gene cluster for polycyclic aromatic hydrocarbon catabolism. J. Bacteriol. **181(2):** 531-540.
- 150. Le Borgne, S., Paniagua, D., and Vazquez-Duhalt, R. 2008. Biodegradation of organic pollutants by halophilic bacteria and archaea. J. Mol. Microbiol. Biotechnol. 15: 74-92.
- 151. **Leahy, J.G., and Colwell, R.R.** 1990. Microbial degradation of hydrocarbons in the environment. Microbiol. Mol. Biol. Rev. **54(3)**: 305-315.
- 152. Lee, S., Malone, C., and Kemp, P.F. 1993. Use of multiple 16S rRNA-targeted fluorescent probes to increase signal strength and measure cellular RNA from natural planktonic bacteria. Mar. Ecol. Prog. Ser. 101: 193-201.
- 153. **Lehmicke, L.G., Williams, R.T., and Crawford, R.L.** 1979. ¹⁴C-Most-probable-number method for enumeration of active heterotrophic microorganisms in natural waters. Appl. Environ. Microbiol. **38(4):** 644-649.
- 154. **Lipson, D.A., and Monson, R.K.** 1998. Plant-microbe competition for soil amino acids in the alpine tundra: effects of freeze-thaw and dry-rewet events. Oecologia **113**: 406-414.
- 155. **Lipson, D.A., and Schmidt, S.K.** 2004. Seasonal changes in an alpine soil bacterial community in the Colorado Rocky Mountains. Appl. Environ. Microbiol. **70:** 2867-2879.
- 156. **Lipson, D.A., Schmidt, S.K., and Monson, R.K**. 2000. Carbon availability and temperature control the post-snowmelt decline in alpine soil microbial biomass. Soil Biol. Biochem. **32:** 441-448.
- 157. **Ludwig, B., Wolf, I., and Teepe, R.** 2004. Contribution of nitrification and denitrification to the emission of N₂O in a freeze-thaw event in an agricultural soil. J. Plant Nutr. Soil Sci. **167:** 678-684.
- 158. Luz, A.P., Pellizari, V.H., Whyte, L.G., and Greer, C.W. 2004. A survey of indigenous microbial hydrocarbon degradation genes in soils from Antarctica and Brazil. Can. J. Microbiol. **50**: 323-333.
- 159. **MacLeod, C.T., and Daugulis, A.J.** 2003. Biodegradation of polycylic aromatic hydrocarbons in a two-phase partitioning bioreactor in the presence of a bioavailable solvent. Appl. Microbiol. Biotechnol. **62:** 291-296.
- 160. **Madigan, M.T., Martinko, J.M., and Parker, J.** 2003. Brock Biology of Microorganisms, 10th ed. Pearson Education, Upper Saddle River, NJ, USA.

- 161. **Maier, R.M., Pepper, I.L., and Gerba, C.P.** Environmental Microbiology, 2nd ed. Academic Press, Burlington, MA, USA.
- 162. **Männistö, M.K., and Häggblom, M.M**. 2006. Characterization of psychrotolerant heterotrophic bacteria from Finnish Lapland. Syst. Appl. Microbiol. **29(3):** 229-243.
- 163. **Männistö, M.K., Tiirola, M., and Häggblom, M.M.** 2009. Effect of freeze-thaw cycles on bacterial communities of arctic tundra soil. Microb. Ecol. **58:** 621-631.
- 164. Mardanov, A.V., Ravin, N.V., Svetlitchnyi, V.A., Beletsky, A.V., Miroshnichenko, M.L., Bonch-Osmolovskaya, E.A., and Skyrabin, K.G. 2009. Metabolic versatility and indigenous origin of the archaeon *Thermococcus sibiricus*, isolated from a Siberian oil reservoir, as revealed by genome analysis. Appl. Environ. Microbiol. 75(13): 4580-4588.
- 165. **Margesin, R.** 2007. Alpine microorganisms: useful tools for low temperature bioremediation. J. Microbiol. **45(4):** 281-285.
- 166. Margesin, R., Labbé, D., Schinner, F., Greer, C.W., and Whyte, L.G. 2003. Characterization of hydrocarbon-degrading microbial populations in contaminated and pristine alpine soils. Appl. Environ. Microbiol. 69: 3085-3092.
- 167. **Margesin, R., and Schinner, F**. 1997a. Efficiency of indigenous and inoculated cold-adapted soil microorganisms for biodegradation of diesel oil in alpine soils. Appl. Environ. Microbiol. **63(7)**: 2660-2664.
- 168. **Margesin, R., and Schinner, F.** 1997b. Bioremediation of diesel-oil contaminated alpine soils at low temperatures. Appl. Microbiol. Biotechnol. **47:** 462-468.
- 169. **Margesin, R., and Schinner, F**. 1999a. A feasibility study for the *in situ* remediation of a former tank farm. World J. Microbiol. Biotechnol. **15:** 615-622.
- 170. **Margesin, R., and Schinner, F.** 2001a. Biodegradation and bioremediation of hydrocarbons in extreme environments. Appl. Microbiol. Biotechnol. **56:** 650-663.
- 171. **Margesin, R., and Schinner, F**. 2001b. Bioremediation (natural attentuation and biostimulation) of diesel-oil-contaminated soil in an alpine glacier skiing area. Appl. Environ. Microbiol. **67:** 3127-3133.
- 172. Marshall, K.C., Stout, R., and Mitchell, R. 1971. Mechanism of the initial events in the sorption of marine bacteria to surfaces. J. Gen. Microbiol. 68: 337-348.
- 173. Martinez-Aguilar, L., Díaz, R., Pena-Cabriales, J.J., Estrada-de Los Santa, P., Dunn, M.F., and Caballero-Mellado, J. 2008. Multichromosomal genome structure and confirmation of diazotrophy in novel plant-associated *Burkholderia* species. Appl. Environ. Microbiol. 74(14): 4574-4579.
- 174. Master, E.R., Agar, N.Y., Gómez-Gil, Y., Powlowski, J.B., Mohn, W.W., and Eltis, L.D. 2008. Biphenyl dioxygenase from an arctic isolate is not cold-adapted. Appl. Environ. Microbiol. 74(12): 3908-3911.

- 175. McCarthy, K.A., Walker, L., Vigoren, L., and Bartel, J. 2004. Remediation of spilled petroleum hydrocarbons by *in situ* landfarming at an arctic site. Cold Reg. Sci. Technol. 40(1-2): 31-39.
- 176. **Mendez, M.O., Neilson, J.W., and Maier, R.M.** 2008. Characterization of a bacterial community in an abandoned semiarid lead-zinc mine tailing site. Appl. Environ. Microbiol. **74(12):** 3899-3907.
- 177. **Metje, M., and Frenzel, P.** 2007. Methanogenesis and methogenic pathways in a peat from subarctic permafrost. Environ. Microbiol. **9(4):** 954-964.
- 178. **Meyer, O.** 1994. Functional groups of microorganisms, pp. 67-96. *In* E. Schulze, and H. Mooney (ed.), Biodiversity and Ecosystem Function. Springer-Verlag, New York, NY, USA.
- 179. **Michel, V., Lehoux, I., Depret, G., Anglade, P., Labadie, J., and Hebraud, M.** 1997. The cold shock response of the psychrotrophic bacterium *Pseudomonas fragi* involves four low-molecular-mass nucleic acid-binding proteins. J. Bacteriol. **179(23):** 7331-7342.
- 180. **Mikan, C.J., Schimel, J.P., and Doyle, A.P.** 2002. Temperature controls of microbial respiration in arctic tundra soils above and below freezing. Soil Biol. Biochem. **34:** 1785-1795.
- 181. **Mills, S.A., and Frankenberger Jr., W.T.** 1994. Evaluation of phosphorus sources promoting bioremediation of diesel fuel in soil. Environ. Contam. Toxicol. **53:** 280-284.
- 182. **Mohn, W.W., Radziminski, C.Z., Fortin, M.-C., and Reimer, K.J.** 2001. On site bioremediation of hydrocarbon-contaminated arctic tundra soils in inoculated biopiles. Appl. Microbiol. Biotechnol. **57:** 424-427.
- 183. **Mohn, W.W., and Stewart, G.R.** 2000. Limiting factors for hydrocarbon degradation at low temperature in arctic soils. Soil Biol. Biochem. **32:** 1161-1172.
- 184. **Moody, J.D., Doerge, D.R., Freeman, J.P., and Cerniglia, C.E.** 2002. Degradation of biphenyl by *Mycobacterium* sp. strain PYR-1. Appl. Microbiol. Biotechnol. **58:** 364-369.
- 185. **Moody, J.D., Freeman, J.P., Doerge, D.R., and Cerniglia, C.E.** 2001. Degradation of phenanthrene and anthracene by cell suspensions of *Mycobacterium* sp. strain PYR-1. Appl. Environ. Microbiol. **67:** 1476-1483.
- 186. **Moody, J.D., Freeman, J.P., Fu, P.P., and Cerniglia, C.E.** 2004. Degradation of benzo[a]pyrene by *Mycobacterium vanbaalenii* sp. strain PYR-1. Appl. Environ. Microbiol. **70:** 340-345.
- 187. **Morgan, P., and Watkinson, R.J.** 1989. Hydrocarbon degradation in soils and methods for soil biotreatment. Crit. Rev. Biotechnol. **8:** 305-333.
- 188. Morrison, T.B., Weis, J.J., and Wittwer, C.T. 1998. Quantification of low-copy transcripts by continuous SYBR Green I monitoring during amplification. Biotechniques **24(6)**: 954-958.

- 189. **Mulligan, C.N.** 2004. Environmental applications for biosurfactants. Environ. Pollut. 133(2): 183-198.
- 190. Mullis, K., Faloona, F., Scharf, S., Saiki, R., Horn, G., and Erlich, H. 1986. Specific enzymatic amplification of DNA in vitro: The polymerase chain reaction. Cold Spring Harbor Symposium in Quantitative Biology 51: 263-273.
- 191. Mutalik, S.R., Vaidya, B.K., Joshi, R.M., Desai, K.M., and Nene, S.N. 2008. Use of response surface optimization for the production of biosurfactant from *Rhodococcus* spp. MTCC 2574. Bioresour. Technol. **99(16):** 7875-7880.
- 192. **Muyzer, G., and De Waal, E.C.** 1994. Determination of the genetic diversity of microbial communities using DGGE analysis of PCR-amplified 16S rDNA, pp. 207-214. *In* L.J. Stal, and P. Caumette (ed.), Microbial Mats, Structure, Development and Environmental Significance. Springer-Verlag, Berlin, Germany.
- 193. Muyzer, G., De Waal, E.C., and Uitterlinden, A.G. 1993. Profiling of complex microbial populations by denaturing gradient gel electrophoresis analysis of polymerase chain reaction-amplified genes coding for 16S rRNA. Appl. Environ. Microbiol. **59:** 695-700.
- 194. **Muyzer, G., Hottentrager, S., Teske, A., and Wawer, C.** 1996. Denaturing gradient gel electrophoresis of PCR-amplified 16S rDNA. A new molecular approach to analyze the genetic diversity of mixed microbial communities, pp. 3.4.4.1-3.4.4.22. *In* A.D.L. Akkermans, J.D. van Elsas and F.J. de Bruijn (ed.), Molecular Microbial Ecology Manual. Kluwer Academic Publishing, Dordrecht, the Netherlands.
- 195. Nemergut, D.R., Costello, E.K., Meyer, A.F., Pescador, M.Y., Weintraub, M.N., and Schmidt, S.K. 2005. Structure and function of alpine and arctic soil microbial communities. Res. Microbiol. **156**: 775-784.
- 196. Nemergut, D.R., Townsend, A.R., Sattin, S.R., Freeman, K.R., Fierer, N., Neff, J.C., Bowman, W.D., Schadt, C.W., Weintraub, M.N., and Schmidt, S.K. 2008. The effects of chronic nitrogen fertilization on alpine tundra soil microbial communities: implications for carbon and nitrogen cycling. Environ. Microbiol. 10(11): 3093-3105.
- 197. **Neufeld, J.D., and Mohn, W.W.** 2005. Unexpectedly high bacterial diversity in arctic tundra relative to boreal forest soils, revealed by serial analysis of ribosomal sequence tags. Appl. Environ. Microbiol. **71(10):** 5710-5718.
- 198. Nicol, G.W., Tscherko, D., Chang, L., Hammesfahr, U., and Prosser, J.I. 2006. Crenarchaeal community assembly and microdiversity in developing soils at two sites associated with deglaciation. Environ. Microbiol. **8(8):** 1382-1393.
- 199. **Ogram, A.V., Mathot, M.L., Harsh, J.B., Boyle, J., and Pettigrew Jr., C.A.** 1994. Effects of DNA polymer length on its adsorption to soils. Appl. Environ. Microbiol. **60**: 393-396.
- 200. **Oh, Y.S., Shareefdeen, Z., Baltzis, B.C., and Bartha, R**. 1994. Interactions between benzene, toluene, and p-xylene (BTX) during their biodegradation. Biotechnol. Bioeng. **44:** 533-538.

- 201. **Ohhata, N., Yoshida, N., Egami, H., Katsuraqi, T., Tani, Y., and Takagi, H.** 2007. An extremely oligotrophic bacterium, *Rhodococcus erythropolis* N9T-4, isolated from crude oil. J. Bacteriol. 189(19): 6824-6831.
- 202. Olsen, G.J., Lane, D.J., Giovannoni, S.J., Pace, N.R., and Stahl, D.A. 1986. Microbial ecology and evolution: a ribosomal RNA approach. Annu. Rev. Microbiol. 40: 337-365.
- 203. **O'Reilly, K.** 1998. US APO 432 New York Resolution Island, NWT. http://www.pinetreeline.org/other/other8/other8e.html.
- 204. **O'Toole, G., Kaplan, H.B., and Kolter, R.** 2000. Biofilm formation as microbial development. Annu. Rev. Microbiol. **54:** 49-79.
- 205. Oztas, T., and Fayetorbay, F. 2003. Effect of freezing and thawing processes on soil aggregate stability. Catena. 52: 1-8.
- 206. Pace, N.R., Stahl, D.A., Lane, D.J., and Olsen, G.J. 1986. The analysis of natural microbial populations by ribosomal RNA sequences. Adv. Microb. Ecol. 9: 1-56.
- 207. **Park, J.W. and Crowley, D.E.** 2005. Normalization of soil DNA extraction for accurate quantification of target genes by real-time PCR and DGGE. Biotechniques. **38(4):** 579-586.
- 208. **Paudyn, K., Rutter, A., Rowe, R.K., and Poland, J.S.** Remediation of hydrocarbon contaminated soils in the Canadian Arctic by landfarming. Cold Reg. Sci. Technol. **53:** 102-114.
- 209. **Peltovuori, T., and Soinne, H.** 2005. Phosphorus solubility and sorption in frozen, airdried and field-moist soil. Eur. J. Soil Sci. **56:** 821-826.
- 210. **Peng, F., Liu, Z., Wang, L., and Shao, Z.** 2007. An oil-degrading bacterium: *Rhodococcus erythropolis* strain 3C-9 and its biosurfactants. J. Appl. Microbiol. **102(6)**: 1603-1611.
- 211. **Peng, F., Wang, Y., Sun, F., Liu, Z., Lai, Q., and Shao, Z.** 2008. A novel lipopeptide produced by a Pacific Ocean deep-sea bacterium, *Rhodococcus* sp. TW53. J. Appl. Microbiol. **105(3):** 698-705.
- 212. **Pepi, M., Cesaro, A., Liut, G., and Baldi, F.** 2005. An Antarctic psychrotrophic bacterium *Halomonas* sp. ANT-3b, growing on n-hexadecane, produces a new emulsyfying glycolipid. FEMS Microbiol. Ecol. **53:** 157-166.
- 213. **Peterson, L.W., Moldrup, P., Jacobsen, O.H., and Rolsten, D.E.** 1996. Relations between specific surface area and soil physical and chemical properties. Soil Sci. **161(1):** 9-21.
- 214. **Philp, J.C., and Atlas, R.M.** 2005. Bioremediation of Contaminated Soils and Aquifers, pp. 139-165. *In* R.M. Atlas, and J.C. Philp (ed.), Bioremediation: Applied Microbial Solutions for Real-World Environmental Cleanup. ASM Press, Washington, D.C.

- 215. **Philp, J.C., Bamforth, S.M., Singleton, I., and Atlas, R.M.** 2005. Environmental pollution and restoration: A role for bioremediation, pp. 1-48. *In* R.M. Atlas, and J.C. Philp (ed.), Bioremediation: Applied Microbial Solutions for Real-World Environmental Cleanup. ASM Press, Washington, D.C., USA
- 216. Philp, J.C., Kuyukina, M.S., Ivshina, I.B., Dunbar, S.A., Christofi, N., Lang, S., and Wray, V. 2002. Alkanotrophic *Rhodococcus ruber* as a biosurfactant producer. Appl. Microbiol. Biotechnol. **59(2-3):** 318-324.
- 217. **Pianka, E.R.** 1970. On r and K selection. Am. Nat. **104**: 592-597.
- 218. **Piehler, M.F., Swistak, J.G., Pinckney, J.L., and Paerl, H.W**. 1999. Stimulation of diesel fuel biodegradation by indigenous nitrogen fixing bacterial consortia. Microb. Ecol. **38:** 69-78.
- 219. **Pouliot, J., Galand, P.E., Lovejoy, C., and Vincent, W.F.** 2009. Vertical structure of archaeal communities and the distribution of ammonia monooxygenase A gene variants in two meromictic high arctic lakes. Environ. Microbiol. **11(3):** 687-699.
- 220. **Powell, S.M., Ferguson, S.H., Bowman, J.P., and Snape, I**. 2006. Using real-time PCR to assess changes in the hydrocarbon-degrading microbial community in antarctic soil during bioremediation. Microb. Ecol. **52:** 523-532.
- 221. **Prieme, A., and Christensen, S.** 2001. Natural perturbations, drying-rewetting and freeze-thawing cycles, and the emission of nitrous oxide, carbon dioxide and methane from farmed organic soils. Soil Biol. Biochem. **33:** 2083-2091.
- 222. Rainey, F.A., Klatte, S., Kroppenstedt, R., and Stackebrandt, E. 1995. *Dietzia*, a new genus containing *Dietzia maris*, comb. nov., formerly *Rhodococcus maris*. Int. J. Syst. Evol. Microbiol. **45(1):** 32-36.
- 223. **Ranjard, L., and Richaume, A.** 2001. Quantitative and qualitative microscale distribution of bacteria in soil. Res. Microbiol. **152:** 707-716.
- 224. **Rike, A.G., Haugen, K.B., and Engene, B.** 2005. *In situ* biodegradation of hydrocarbons in arctic soil at sub-zero temperatures field monitoring and theoretical simulation of the microbial activation temperature at a Spitsbergen contaminated site. Cold Reg. Sci. Technol. **41:** 189-209.
- 225. **Rinnan, R., and Baath, E.** 2009. Differential utilization of carbon substrates by bacteria and fungi in tundra soil. Appl. Environ. Microbiol. **75(11)**: 3611-3620.
- 226. Rivkina, E., Shcherbakova, V., Laurinavichius, K., Petrovskaya, L., Krivushin, K., Kraev, G., S., P., and Gilichinsky, D. 2007. Biogeochemistry of methane and methanogenic archaea in permafrost. FEMS Microbiol. Ecol. 61(1): 1-15.
- 227. **Romanowski, G., Lorenz, M.G., and Wackernagel, W.** 1991. Adsorption of plasmid DNA to mineral surfaces and protection against DNase I. Appl. Environ. Microbiol. **57(4)**: 1057-1061.

- 228. **Rosenberg, E.** 2006. Hydrocarbon-oxidizing bacteria, pp. 564-577. *In* M. Dworkin, S. Falkow, E. Rosenburg, K.-H. Schleifer, and E. Stackebrandt (ed.), Prokaryotes. Springer, New York.
- 229. Rosenberg, E., Legmann, R., Kushmaro, A., Taube, R., Adler, E., and Ron, E.Z. 1992. Petroleum bioremediation a multiphase problem. Biodegradation 3: 337-350.
- 230. **Rosenberg, M., Bayer, E.A., Delarea, J., and Rosenberg, E.** 1982. The role of thin fimbriae in adherence and growth of *Acinetobacter calcoaceticus* RAG-1 on hexadecane. Appl. Environ. Microbiol. **44(4):** 929-937.
- 231. **Rothenstein, C.** 2003. Memorandum: FY 2003 semi-annual (mid-year) activity report. Office of Solid Waste and Emergency Response, Environmental Protection Agency, Washington, D.C., USA.
- 232. Roussel, E.G., Sauvadet, A.L., Chaduteau C., Fouquet, Y., Charlou, J.L., Prieur, D., and Cabon Bonavita, M.A. 2009. Archaeal communities associated with shallow to deep subseafloor sediments of the New Caledonia Basin. Environ. Microbiol. 11(9): 2446-2462.
- 233. Ruberto, L., Dias, R., Lo Balbo, A., Vazquez, S.C., Hernandez, E.A., and Mac Cormack, W.P. 2009. Influence of nutrients addition and bioaugmentation on the hydrocarbon biodegradation of a chronically contaminated antarctic soil. J. Appl. Microbiol. 106(4): 1101-1110.
- 234. Russell, R.J., Gericke, U., Danson, M.J., Hough, D.W., and Taylor, G.L. 2003. Structural adaptations of the cold-active citrate synthase from an antarctic bacterium. Structure 6: 351-361.
- 235. **Sambrooke, J., and Russell, D.W.** 2001. Molecular Cloning. Cold Spring Harbor Laboratory Press, Cold Spring Harbor, NY, USA.
- 236. Sanscartier, D., Laing, T., Reimer, K., and Zeeb, B. 2009. Bioremediation of weathered petroleum hydrocarbon contamination in the Canadian High Arctic: laboratory and field studies. Chemosphere. 77(8): 1121-1126.
- 237. Sarita, S., Sharma, P.K., Priefer, U.B., and Prell, J. 2005. Direct amplification of rhizobial *nodC* sequences from soil total DNA and comparison to *nodC* diversity of root nodule isolates. FEMS Microbiol. Ecol. **54(1):** 1-11.
- 238. Schadt, C.W., Martin, A.P., Lipson, D.A., and Schmidt, S.K. 2003. Seasonal dynamics of previously unknown fungal lineages in tundra soils. Science. 301: 1359-1361.
- 239. Schafer, A., Harms, H., and Zehnder, A.J.B. 1998. Bacterial accumulation at the airwater interface. Environ. Sci. Technol. 32: 3704-3712.
- 240. **Schafer, A.N., Snape, I., and Siciliano, S.D.** 2007. Soil biogeochemical toxicity end points for sub-antarctic islands contaminated with petroleum hydrocarbons. Environ. Toxicol. Chem. **26(5):** 890-897.
- 241. **Schafer, A.N., Snape, I., and Siciliano, S.D.** 2009. Influence of liquid water and soil temperature on petroleum hydrocarbon toxicity in antarctic soil. Environ. Toxicol. Chem. **28(7):** 1409-1415.

- 242. **Schimel, J.P., and Clein, J.S.** 1996. Microbial response to freeze-thaw cycles in tundra and taiga soils. Soil Biol. Biochem. **29:** 1061-1066.
- 243. **Schimel, J.P., Kielland, K., and Chapin, F.S**. 1996. Nutrient availability and uptake by tundra plants, pp. 203-221. *In* J.F. Reynolds, and J.D. Tenhunen (ed.), Landscape Function: Implications for Ecosystem Response to Disturbance. A Case Study of Arctic Tundra. Springer, Berlin, Germany.
- 244. **Schloss, P.D., and Handelsman, J.** 2005. Introducing DOTUR, a computer program for defining operational taxonomic units and estimating species richness. Appl. Environ. Microbiol. **71(3):** 1501-1506.
- 245. **Scott, K.F., Rolfe, B.G., and Shine, J. 1981**. Biological nitrogen fixation: primary structure of the *Klebsiella pneumoniae nifH* and *nifD* genes. J. Appl. Mol. Genet. **1(1):** 71-81.
- 246. **Sehy, U., Dyckmans, J., Ruser, R., and Munch, J.C.** 2004. Adding dissolved organic carbon to simulate freeze-thaw related N₂O emissions from soil. J. Plant Nutr. Soil Sci. **167**: 471-478.
- 247. **Semple, K.T., Reid, B.J., and Fermor, T.R**. 2001. Impact of composting strategies on the treatment of soils contaminated with organic pollutants. Environ. Pollut. **112:** 269-283.
- 248. **Seo, J.S., Keum, Y.S., Hu, Y., Lee, S.E., and Li, Q.X.** 2007. Degradation of phenanthrene by *Burkholderia* sp. C3: initial 1,2- and 3,4-dioxygenation and meta- and ortho-cleavage of naphthalene-1,2-diol. Biodegradation. **18(1):** 123-131.
- 249. **Shannon, C.E., and Weaver, W.** 1949. The Mathematical Theory of Communication. Illinois Press, Urbana, IL, USA.
- 250. **Sharma, S., Szele, Z., Schilling, R., Munch, J.C., and Schloter, M.** 2006. Influence of freeze-thaw stress on the structure and function of microbial communities and denitrifying populations in soil. Appl. Environ. Microbiol. **72:** 2148-2154.
- 251. **Shields, M.S., Reagin, M.J., Gerger, R.R., Campbell, R., and Somerville, C.** 1995. TOM, a new aromatic degradative plasmid from *Burkholderia (Pseudomonas) cepacia G4*. Appl. Environ. Microbiol. **61(4):** 1352-1356.
- 252. Shintani, M., Fukushima, N., Tezuka, M., Yamane, H., and Nojiri, H. 2008. Conjugative transfer of the IncP-7 carbazole degradative plasmid, pCAR1, in river water samples. Biotechnol. Lett. **30(1)**: 117-122.
- 253. **Shreve, G.S., Inguva, S., and Gunnam, S. 1995**. Rhamnolipid biosurfactant enhancement of hexadecane biodegradation by *Pseudomonas aeruginosa*. Mol. Mar. Biol. Biotechnol. **4:** 331-337.
- 254. **Sikkema, J., de Bont, J.A., and Poolman, B.** 1995. Mechanisms of membrane toxicity of hydrocarbons. Microbiol. Rev. **59(2)**: 201-222.
- 255. Simpson, E.H. 1949. Measurement of diversity. Nature 163: 688.

- 256. **Singleton, D.R., Furlong, M.A., Rathbun, S.L., and Whitman, W.B. 2001**. Quantitative comparisons of 16S rRNA gene sequence libraries from environmental samples. Appl. Environ. Microbiol. **67(9):** 4374-7376.
- 257. **Six, J., Bossuyt, H., Degryse, S., and Denef, K.** 2004. A history of research on the link between (micro)aggregates, soil biota, and soil organic matter dynamics. Soil Till. Res. **79:** 7-31.
- 258. **Sjursen, H., Michelsen, A., and Holmstrup, M.** 2005. Effects of freeze-thaw cycles on microarthropods and nutrient availability in a sub-arctic soil. Appl. Soil Ecol. **28:** 79-93.
- 259. **Skogland, T., Lomeland, S., and Goksøyr, J.** 1988. Respiratory burst after freezing and thawing of soil: experiments with soil bacteria. Soil Biol. Biochem. **20:** 851-856.
- 260. Slobodova, N.V., Kolganova, T.V., Boulygina, E.S., Kuzenetsov, B.B., Tourova, T.P., and Kravchenko, I.K. 2006. Comparative characterization of methanotrophic enrichments by serological and molecular methods. Microbiology **75(3)**: 336-342.
- 261. Smalas, A.O., Leiros, H.K., Os, V., and Willassen, N.P. 2000. Cold-adapted enzymes. Biotechnol. Annu. Rev. 6: 1-57.
- 262. **Soinne, H., and Peltovuori, T**. 2005. Extractability of slurry and fertilizer phosphorus in soil after repeated freezing. Agric. Food Sci. **14:** 181-188.
- 263. **Stallwood, B., Shears, J., Williams, P.A., and Hughes, K.A.** 2005. Low temperature bioremediation of oil-contaminated soil using biostimulation and bioaugmentation with a *Pseudomonas* sp. from maritime Antarctica. J. Appl. Microbiol. **99(4):** 794-802.
- 264. **Stephenson, G.L., Solomon, K.T., Hale, B., Greenberg, B.M., and Scroggins, B.M.** 1997. Development of suitable test methods for evaluating the toxicity of contaminated soils to a battery of plant species relevant to soil environments in Canada. *In F.J. Dwyer, T.R. Doane, and M.L. Hinman (ed.), Environmental Toxicology and Risk Assessment: Modeling and Risk Assessment. American Society for Testing and Materials, Philadelphia, USA.*
- 265. **Steven, B., Briggs, G., McKay, C.P., Pollard, W.H., Greer, C.W., and Whyte, L.G.** 2007a. Characterization of the microbial diversity in a permafrost sample from the Canadian High Arctic using culture-dependent and culture-independent methods. FEMS Microbiol. Ecol. **59:** 513-523.
- 266. **Steven, B., Niederberger, T.D., Bottos, E.M., Dyen, M.R., and Whyte, L.G.** 2007b. Development of a sensitive radiorespiration method for detecting microbial activity at subzero temperatures. J. Microbiol. Methods **71(3)**: 275-280.
- 267. **Steven, B., Pollard, W.H., Greer, C.W., and Whyte, L.G.** 2008. Microbial diversity and activity through a permafrost/ground ice core profile from the Canadian High Arctic. Environ. Microbiol. **10(12):** 3388-3403.
- 268. **Stingley, R.L., Khan, A.A., and Cerniglia, C.E.** 2004. Molecular characterization of a phenanthrene degradation pathway in *Mycobacterium vanbaalenii* PYR-1 Biochem. Biophys. Res. Commun. **322(1):** 133-146.

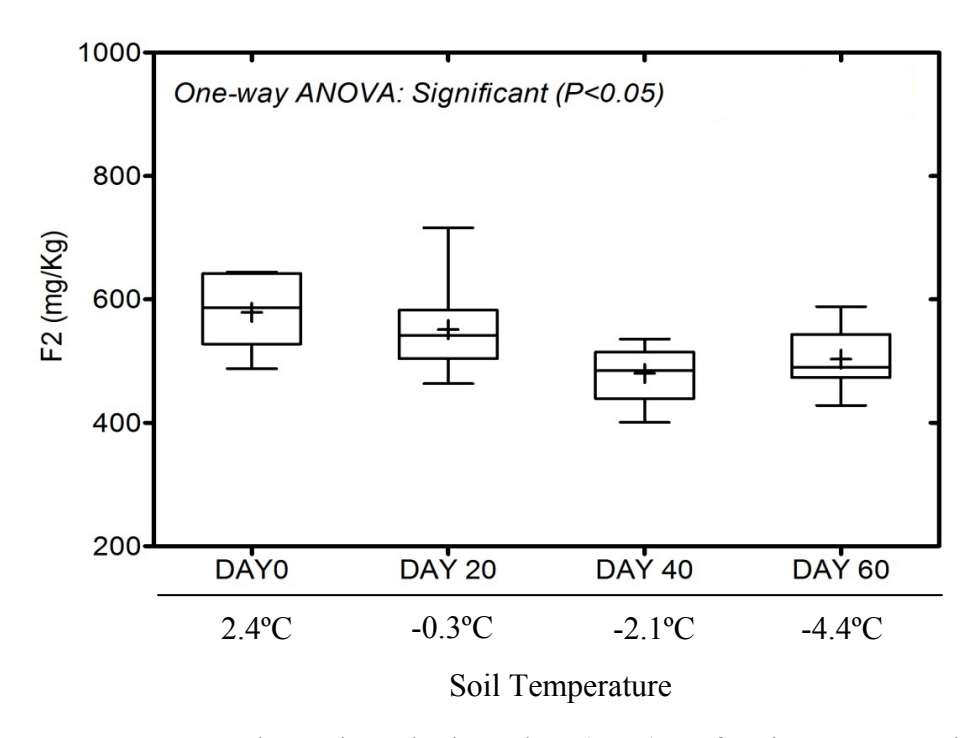
- 269. **Sulkava, P., and Huhta, V.** 2003. Effects of hard frost and freeze-thaw cycles on decomposer communities and N mineralization in boreal forest soil. Appl. Soil Ecol. **22**: 225-239.
- 270. **Tarnocai, C., and Campbell, I.B.** 2002. Soils of the polar regions, pp. 1018-1021. *In* R. Lal (ed.), Encyclopedia of Soil Science. Marcel Dekker, New York.
- 271. Tate, R. 2000. Soil Microbiology, 2nd ed. John Wiley and Sons, New York.
- 272. Tendeng, C., Krin, E., Soutoutrina, O.A., Marin, A., Danchin, A., and Bertin, P.N. 2003. A novel H-NS-like protein from an antarctic psychrophilic bacterium reveals a crucial role for the N-terminal domain in thermal stability. J. Biol. Chem. 278: 18754-18760.
- 273. **Thomassin-Lacroix, E.J., Eriksson, M., Reimer, K.J., and Mohn, W.W.** 2002. Biostimulation and bioaugmentation for on-site treatment of weathered diesel fuel in arctic soil. Appl. Microbiol. Biotechnol. **59(4-5):** 551-556.
- 274. **Thompson, L.M., Black, C.A., and Zoellner, J.A**. 1954. Occurrence and mineralization of organic phosphorus in soils, with particular references and associations with nitrogen, carbon, and pH. Soil Sci. **77**: 185-196.
- 275. **Toccalino, P.L., Johnson, R.L., and Boone, D.R.** 1993. Nitrogen limitation and nitrogen fixation during alkane biodegradation in a sandy soil. Appl. Environ. Microbiol. **59(9)**: 2977-2983.
- 276. **Tsao, C.-W., Song, H.-G., and Bartha, R.** 1998. Metabolism of benzene, toluene, and xylene hydrocarbons in soil. Appl. Environ. Microbiol. **64(12):** 4924-4929.
- 277. **Tsuneda, S., Aikawa, H., Hayashi, H., Yuasa, A., and Hirata, A.** 2003. Extracellular polymeric substances responsible for bacterial adhesion onto solid surface. FEMS Microbiol. Lett. **223(2)**: 287-292.
- 278. **Tuleva, B., Christova, N., Cohen, R., Stoev, G., and Stoineva, I.** 2008. Production and structural elucidation of trehalose tetraesters (biosurfactants) from a novel alkanthrotrophic *Rhodococcus wratislaviensis* strain. J. Appl. Microbiol. **104(4):** 1703-1710.
- 279. Turle, R., Nason, T., Malle, H., and Fowlie, P. 2007. Development and implementation of the CCME reference method for the Canada-wide standard for petroleum hydrocarbons (PHC) in soil: a case study. Anal. Bioanal. Chem. 387(3): 957-964.
- 280. Vacca, D.J., Bleam, W.F., and Hickey W.J. 2005. Isolation of soil bacteria adapted to degrade humic acid-sorbed phenanthrene. Appl. Environ. Microbiol. 71(7): 3797-3805.
- 281. van Beilen, J., Li, Z., Duetz, W.A., Smits, T.H.M., and Witholt, B. 2003. Diversity of alkane hydroxylase systems in the environment. Oil Gas Sci. Technol. **58(4)**: 427-440.
- 282. van Beilen, J., Panke, S., Lucchini, S., Franchini, A., Rothlisberger, M., and Witholt, B. 2001. Analysis of *Pseudomonas putida* alkane-degradation gene clusters and flanking insertion sequences: evolution and regulation of the *alk* genes. Microbiology 147: 1621-1630.

- 283. **van Beilen, J., Wubbolts, M.G., and Witholt, B.** 1994. Genetics of alkane degradation by *Pseudomonas oleovorans*. Biodegradation **5:** 161-174.
- 284. van Beilen, J.B., and Funhoff, E.G. 2007. Alkane hydroxylases involved in microbial alkane degradation. Appl. Microbiol. Biotechnol. 74(1): 13-21.
- 285. van Beilen, J.B., Funhoff, E.G., van Loon, A., Just, A., Kaysser, L., Bouza, M., and Holtackers, R. 2006. Cytochrome P450 alkane hydroxylases of the CYP153 family are common in alkane-degrading eubacteria lacking integral membrane alkane hydroxylases. Appl. Environ. Microbiol. 72(1): 59-65.
- 286. **van der Mei, H.C., Weerkamp, A.H., and Busscher, H.J**. 1987. Physico-chemical surface characteristics and adhesive properties of *Streptococcus salivarius* strains with defined cell surface structures. FEMS Microbiology Letters **40(1)**: 15-19.
- 287. van Loosdrecht, M.C.M., Norde, W., Lyklema, J., and Zehnder, A.J.B. 1990. Hydrophobic and electrostatic parameters in bacterial adhesion. Aquat. Sci. **52(1)**: 103-114.
- 288. Vandamme, P., Opelt, K., Knöchel, N., Berg, C., Schönmann, S., De Brandt, E., Eberl, L., Falsen, E., and Berg, G. 2007. *Burkholderia bryophila* sp. nov. and *Burkholderia megapolitana* sp. nov., moss-associated species with antifungal and plant-growth-promoting properties. Int. J. Syst. Evol. Microbiol. **57(Pt 10):** 2228-2235.
- 289. Vandevivere, P., and Kirchman, D.L. 1993. Attachment stimulates exopolysaccharide synthesis by a bacterium. Appl. Environ. Microbiol. **59(10)**: 3280-3286.
- 290. Vaz, M.D.R., Edwards, A.C., Shand, C.A., and Cresser, M.S. 1994. Changes in the chemistry of soil solution and acetic-acid extractable-P following different types of freeze-thaw episodes. Eur. J. Soil Sci. 45: 353-359.
- 291. Vázquez, S., Nogales, B., Ruberto, L., Hernandez, E., Christie-Oleza, J., Lo Balbo, A., Bosch, R., Lalucat, J., and Mac Cormack, J. 2009. Bacterial community dynamics during bioremediation of diesel oil-contaminated antarctic soil. Microb. Ecol. 57(4): 598-610.
- 292. von Fahnestocke, F.M., Smith, L.A., Wickramanayake, G.B., Place, M.C., Kratzke, R.J., Major, W.R., Walker, A.M., Wollenberg, J.P., Carlsey, M.J., Dinh, P.V., and Ta, N.T. 1996. Biopile design and construction manual.
- 293. Walecka-Hutchinson, C.M., and Walworth, J.L. 2007. Evaluating the effects of gross nitrogen mineralization, immobilization and nitrification on nitrogen fertilizer availability in soil experimentally contaminated with diesel. Biodegradation 18: 133-144.
- 294. Walker, V.K., Palmer, G.R., and Voordouw, G. 2006. Freeze-thaw tolerance and clues to the winter survival of a soil community. Appl. Environ. Microbiol. 72: 1784-1792.
- 295. Walworth, J.L., Woolard, C.R., Braddock, J.F., and Reynolds, C.M. 1997. Enhancement and inhibition of soil petroleum biodegradation through the use of fertilizer nitrogen: an approach in determining optimum levels. J. Soil Contam. 6(5): 465-480.
- 296. Walworth, J.L., Woolard, C.R., and Harris, K.C. 2003. Nutrient amendments for contaminated peri-glacial soils: use of an organic controlled release nutrient source. Cold Reg. Sci. Technol. 37: 81-88.

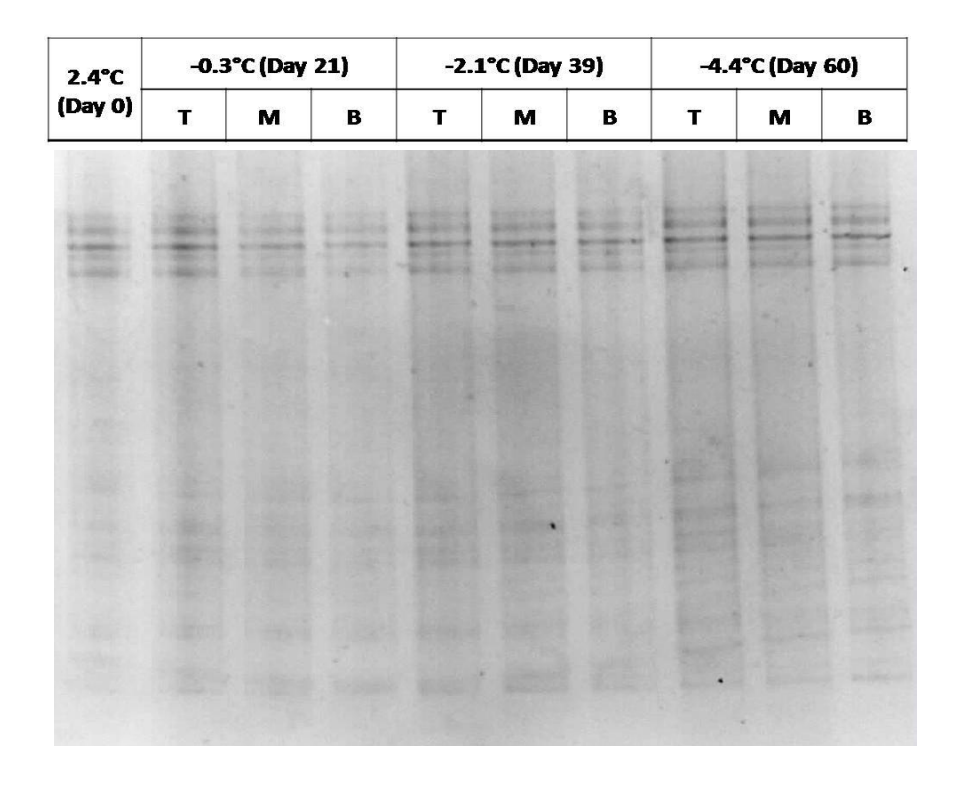
- 297. **Wang, F.L., and Bettany, J.R.** 1994. Organic and inorganic nitrogen leaching from incubated soils subjected to freeze-thaw and flooding. Can. J. Soil Sci. 74: 201-206.
- 298. Wang, Q., Garrity, G.M., Tiedje, J.M., and Cole, J.R. 2007. Naive Bayesian classifier for rapid assessment of rRNA sequences into the new bacterial taxonomy. Appl. Environ. Microbiol. 73(16): 5261-5267.
- 299. Wartiainen, I., Hestnes, A.G., McDonald, I.R., and Scenning, M.M. 2006. *Methylocystis rosea* sp. nov., a novel methanotrophic bacterium from arctic wetland soil, Svalbard, Norway (78 degrees N). Int. J. Syst. Evol. Microbiol. **56(Pt 3):** 541-547.
- 300. Wendisch, V.F., Zimmer, D.P., Khodursky, A., Peter, B., Cozzarelli, N., and Kustu, S. 2001. Isolation of *Escherichia coli* mRNA and comparison of expression using mRNA and total RNA on DNA microarrays. Anal. Biochem. **290(2)**: 205-213.
- 301. Weon, H.Y., Kim, B.Y., Hong, S.B., Jeon, Y.A., Kwon, S.W., Go, S.J., and Koo, B.S. 2007. *Rhodanobacter ginsengisoli* sp. nov. and *Rhodanobacter terrae* sp. nov., isolated from soil cultivated with Korean ginseng International Journal of Systematic and Evolutionary Microbiology **57(Pt 12)**: 2810-2813.
- 302. **Whitehead, T.R., and Cotta, M.A.** 1999. Phylogenetic diversity of methogenic archaea in swine waste storage pits. FEMS Microbiol. Lett. **179**: 223-226.
- 303. Whyte, L.G., Bourbonnière, L., Bellerose, C., and Greer, C.W. 1999a. Bioremediation assessment of hydrocarbon-contaminated soils from the High Arctic. Bioremediat. J. 3: 69-79.
- 304. Whyte, L.G., Goalen, B., Hawari, J., Labbé, D., Greer, C.W., and Nahir, M. 2001. Bioremediation treatability assessment of hydrocarbon-contaminated soils from Eureka, Nunavut. Cold Reg. Sci. Technol. 32: 121-132.
- 305. Whyte, L.G., Greer, C.W., and Inniss, W.E. 1996. Assessment of the biodegradation potential of psychrotrophic microorganisms. Can. J. Microbiol. 42: 99-106.
- 306. Whyte, L.G., Hawari, J., Zhou, E., Bourbonniere, L., Inniss, W.E., and Greer, C.W. 1998. Biodegradation of variable-chain-length alkanes at low temperatures by a psychrotrophic *Rhodococcus* sp. Appl. Environ. Microbiol. **64(7)**: 2578-2584.
- 307. Whyte, L.G., Slagman, S.J., Pietrantonio, F., Bourbonnière, L., Koval, S.F., Lawrence, J.R., Inniss, W.E., and Greer, C.W. 1999b. Physiological adaptations involved in alkane assimilation at a low temperature by *Rhodococcus* sp. strain Q15. J. Appl. Microbiol. 65(7): 2961-2968.
- 308. Widmer, F., Shaffer, B.T., Porteous, L.A., and Seidler, R.J. 1999. Analysis of *nifH* gene pool complexity in soil and litter at a Douglas fir soil site in the Oregon Cascade Mountain range. Appl. Environ. Microbiol. **65(2):** 374-380.
- 309. Wilson, M.S., Herrick, J.B., Jeon, C.O., Hinman, D.E., and Madsen, E.L. 2003. Horizontal transfer of *phnAc* diooxygenase genes within one of two phenotypically and genotypically distinctive naphthalene-degrading guilds from adjacent soil environments. Appl. Environ. Microbiol. **69(4)**: 2172-2181.

- 310. Winter, H.C., and Burris, R.H. 1976. Nitrogenase. Annu. Rev. Biochem. 45: 409-426.
- 311. Winter, J.P., Zhang, Z.Y., Tenuta, M., and Voroney, R.P. 1994. Measurement of microbial biomass by fumigation-extraction in soil stored frozen. Soil Sci. Soc. Am. J. 58: 1645-1651.
- 312. Woese, C.R. 1987. Bacterial evolution. Microbiol. Rev. 51: 221-271.
- 313. Wu, L., Vomocil, J.A., and Childs, S.W. 1990. Pore size, particles size, aggregate size, and water retention. Soil Sci. Soc. Am. J. 54: 952-956.
- 314. Yakimov, M.M., Lunsdorf, H., and Golyshin, P.N. 2003. *Thermoleophilum albans* and *Thermoleophilum minutum* are culturable representatives of group 2 of the *Rubrobacteridae* (*Actinobacteria*). Int. J. Syst. Evol. Microbiol. **53:** 377-380.
- 315. Yakimov, M.M., Timmis, K.N., and Golyshin, P.N. 2007. Obligate oil-degrading marine bacteria. Curr. Opin. Biotechnol. **18(3)**: 257-266.
- 316. Yanai, Y., Toyota, K., and Okazaki, M. 2004. Effects of successive soil freeze-thaw cycles on soil microbial biomass and organic matter decomposition potential of soils. Soil Sci. Plant Nutr. 50: 831-837.
- 317. **Yarwood, S.A., Myrold, D.D., and Hogberg, M.N.** 2009. Termination of belowground C allocation by trees alters soil fungal and bacterial communities in a boreal forest. FEMS Microbiol. Ecol. **70(1)**: 151-162.
- 318. Yen, K.M., Serdar, C.M., and Gunsalus, I.C. 1988. Genetics of naphthalene catabolism in *Pseudonomads*. Crit. Rev. Microbiol. **15(3)**: 247-268.
- 319. You, J., Das, A., Dolan, E.M., and Hu, Z. 2009. Ammonia-oxidizing archaea involved in nitrogen removal. Water Res. 43(7): 1801-1809.
- 320. **Zhang, Y., and Miller, R.M.** 1994. Effect of a *Pseudomonas* rhamnolipid biosurfactant on cell hydrophobicity and biodegradation of octadecane. Appl. Environ. Microbiol. **60:** 2101-2106.
- 321. **Zhou, N.Y., Fuenmayor, S.L., and Williams, P.A.** 2001. *nag* genes of *Ralstonia* (formerly *Pseudomonas*) sp. strain U2 encoding enzymes for gentisate catabolism. J. Bacteriol. **183(2):** 700-708.
- 322. **Zita, A., and Hermansson, M.** 1994. Effects of ionic strength on bacterial adhesion and stability of flocs in a wastewater activated sludge system. Appl. Environ. Microbiol. **60(9)**: 3041-3048.
- 323. **Zvyagintseva, I.S., Poglazova, M.N., Gotoeva, M.T., and Belyaev, S.S.** 2001. Effect of the medium salinity on oil degradation by *Nocardioform* bacteria. Microbiology **70(6):** 759-764.

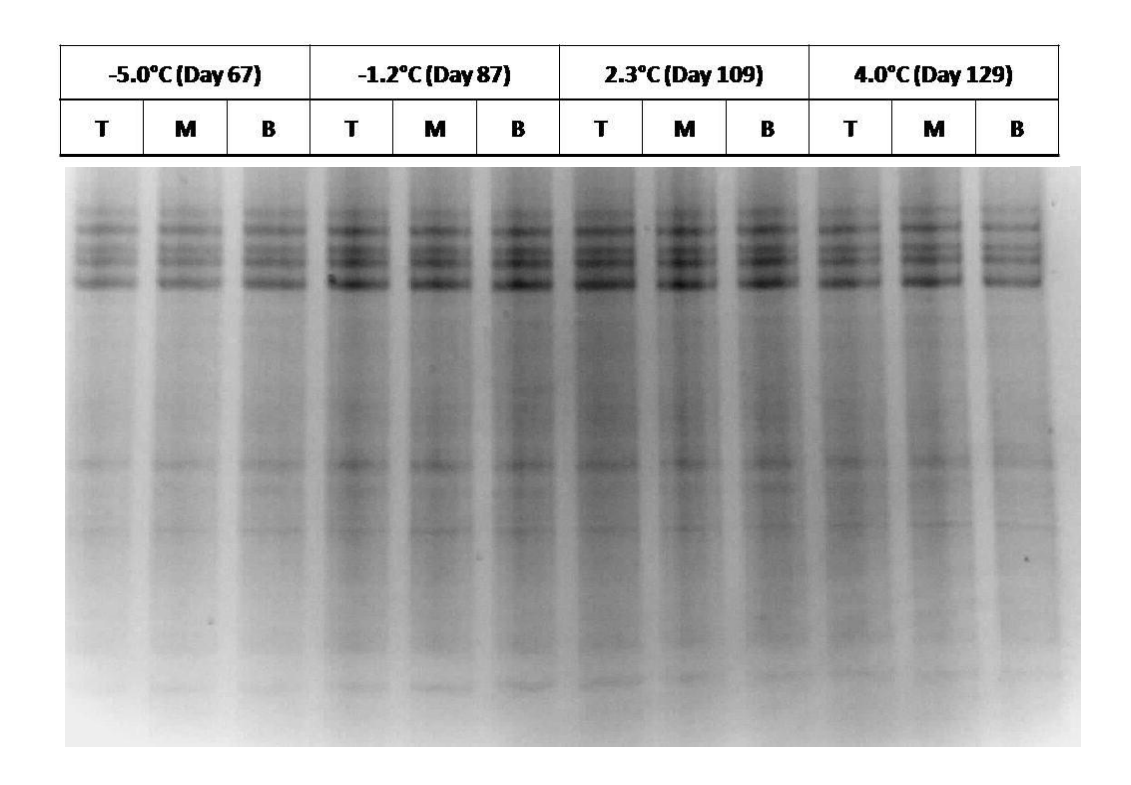
Appendices



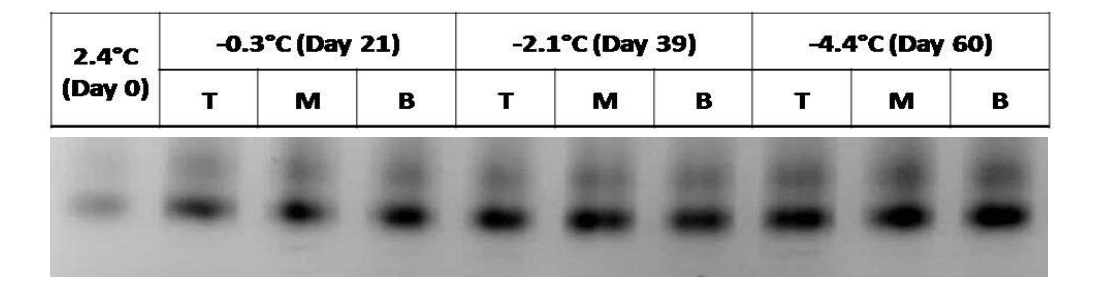
Appendix A. Total petroleum hydrocarbon (TPH) F2 fraction concentrations (contributed by WonJae Chang).



Appendix B. Bacterial DGGE of freezing phase untreated mesocosm soils.



Appendix C. Bacterial DGGE of thawing phase untreated mesocosm soils.



Appendix D. *phnAc* DGGE of freezing phase treated mesocosm soils.